Summer 8-2021

Host Cell Responses to Zika Virus Infection

Bikash R. Sahoo
University of Nebraska-Lincoln, bsahoo@huskers.unl.edu

HOST CELL RESPONSES TO ZIKA VIRUS INFECTION

by

Bikash Ranjan Sahoo

A DISSERTATION

Presented to the Faculty of

The Graduate College at the University of Nebraska

In Partial Fulfillments of Requirements

For the Degree of Doctor of Philosophy

Major: Integrative Biomedical Sciences

Under the Supervision of Professor Asit K. Pattnaik and Professor Rodrigo Franco Cruz

Lincoln, Nebraska

August, 2021

HOST CELL RESPONSES TO ZIKA VIRUS INFECTION

Bikash Ranjan Sahoo, Ph.D.

University of Nebraska, 2021

Advisors: Asit K. Pattnaik and Rodrigo Franco Cruz

The re-emergence of Zika virus (ZIKV) in 2015 as a significant human pathogen causing neurological diseases in infants as well as adults is a serious global health concern. A clear understanding of the mechanisms involved in ZIKV replication in infected host cells as well as the host responses to virus infection are keys to the development of therapeutic strategies against ZIKV. Studies conducted in this dissertation demonstrate that ZIKV infection induces the activation of mTOR signaling cascade that promotes viral protein accumulation and infectious progeny production. While both mTORC1 and mTORC2 are essential for ZIKV replication, the observation that depletion of Raptor, the unique component of mTORC1, imposes a robust negative effect on ZIKV protein expression and progeny production also suggests a mTOR-independent role played by Raptor. Additionally, the activation of autophagy at early times of infection indicates an antiviral role for autophagy in ZIKV infection. The observation that pharmacological inhibition of autophagy led to increased accumulation of ZIKV proteins further strengthens this contention. Since infection-induced oxidative stress contributes to ZIKV pathogenesis, studies reported in this dissertation also show that ZIKV infection alters the redox homeostasis in infected cells and triggers Nrf2-mediated antioxidant response. Depletion of Nrf2 downregulates the cellular pool of GSH

and NADPH leading to enhanced ZIKV replication thereby underscores a role for cellular antioxidants in the suppression of ZIKV replication. The dependency of ZIKV replication on host cell glycolysis is highlighted by significant reduction in viral protein expression and virus yield due to pharmacologic inhibition. When glycolysis is inhibited, gluconeogenesis was found to facilitate ZIKV replication by compensating carbon input via oxidative mitochondrial metabolism. Further experimentation comparing the metabolic profiles of mock- and ZIKV-infected cells may provide important information in understanding the role of cellular metabolism in virus replication.

ACKNOWLEDGMENTS

I would like to express my deep gratitude to my advisor, Dr. Asit K. Pattnaik. Working under his guidance, has been a very educative experience for me. I sincerely thank him for bearing with my inexperience and naiveness and never giving up on me. He has been a constant source of support and it was a priviledge working with him.

I would like to thank Dr. Rodrigo Franco Cruz, my co-advisor, for allowing me to share with his knowledge and experience. From designing experiments to analysing the results, he has been immensely helpful in putting together this work. Apart from that, he has also been very supportive and I will definitely miss his constant words of encouragment.

I also thank the members of my graduate committee: Dr. Fernando A. Osorio for for teaching me humility, Dr. Jay Reddy for his valuable suggestions and critically corrrecting my dissertation and Dr. Quingsheng Li for providing insightful advice throughout my Ph.D. program.

I take this oppurtunity to thank Dr. You (Joe) Zhou and Jaydeep Kolape at the microscopy core facility of University of Nebraska-Lincoln (UNL) for their help in getting the confocal images. I sincerely appreciate the help of Dirk Anderson of the flowcytometry core facility at UNL for helping me with my studies.

I would like to thank my colleage, Arun Saravanakumar Annamalai, who taught me perseverance and has greatly inspired me. I am grateful to Aryamav Pattnaik and Prakash Kumar Sahoo for supporting me and walking me through my tryst with depression. Both of them have given me innumerable joyous moments that I will cherish

for life. I am thankful to Jayesh, Ninaad, Rajkumar, Alondra, Carla, Veronica, and Mercedes for their help and for reminding me to have fun. I am thankful to Dr. Bhopal Mohapatra and Dr. Prasanta Dash for providing an atmosphere of positivity and joy.

I am grateful to Rebecca Richardson-Carlson for her help in the lab, to the faculty and staff at School of Veterinary Medicine and Biomedical Sciences and Nebraska Center for Virology; Jan Edwards, Mark Garett, Donna Bode and Jennifer Lottman for making life at UNL hassle-free.

This dissertation would not have been possible without the support and sacrifices of my parents, siblings and other family members. Last but not least, I am thankful to my beautiful wife, Susmita, for her love, support and motivation.

Bikash Ranjan Sahoo, Ph.D.

University of Nebraska-Lincoln

August, 2021

TABLE OF CONTENTS

LIST OF FIGURES

LIST OF ABBREVIATIONS

2-DG	2-deoxyglucose
3-MA	3-methyladenosine
4EBP1	Eukaryotic initiation factor 4E (eIF4E)-binding protein 1
6-AN	6-aminonicotinamide
6PGD	6-Phosphogluconate dehydrogenase
aa	Amino acid
ARE	Antioxidant response element
BPTES	Bis-2-(5-phenylacetamido-1,3,4-thiadiazol-2-yl)ethyl sulfide
BSO	Buthionine sulfoximine
CPE	Cytopathic effect
CQ	Chloroquine
CZS	Congenital zika syndrome
DENV	Dengue virus
DMEM	Dulbecco's Modified Eagle's Medium
ER	Endoplasmic reticulum
FACS	Fluorescence Activated Cell Sorting
FAO	Fatty acid oxidation
fNSC	Fetal neural stem cell
G6PD	Glucose 6-phosphate dehydrogenase
GBS	Guillain-Barre syndrome
GCLC	Glutamate-Cysteine Ligase Catalytic Subunit
GCLM	Glutamate-Cysteine Ligase Modifier Subunit
GSH	Glutathione
hpi	Hours post infection
hpt	Hours post transfection
HRP	Horseradish peroxidase
IFN-β	Interferon-β
kDa	Kilodalton
LUHMES	Lund university human mesecephalic
mBCl	Monochlorobimane

MOI	Multiplicity of infection
mRNA	Messenger RNA
MTase	Methyltransferase
mTOR	Mechanistic target of rapamycin
mTORC	mTOR complex
NAC	N-acetylcysteine
NAD	Nicotinamide adenine dinucleotide
NADPH	Nicotinamide adenine dinucleotide phosphate
NPC	Neuronal progenitor cell
Nrf2	Nuclear factor E2-related factor 2
NS	Non-structural
NT	Non-targeting
PBS	Phosphate buffered saline
pfu	Plaque forming units
PI	Propidium iodide
PI3K	Phsophatidylinositol-3-kinase
PKB	Protein kinase B
PKC	Protein kinase C
PPP	Pentose phosphate pathway
PS	Penicillin streptomycin
RC	Replication compartment
RIPA	Radio-immunoprecipitation assay
ROS	Reactive oxygen species
ROT	Rotenone
SDS-PAGE	Sodium dodecyl sulfate polyacrylamide gel electrophoresis
SGK	Serum and glucocorticoid induced kinases
siRNA	Short-interfering RNA
ss	Single stranded
TBEV	Tick-borne encephalitis virus
TBS	Tris-buffered saline
TGN	Trans-golgi network

ULK1	Unc-like kinase 1
UTR	Untranslated region
VGM	Virus growth medium
YFV	Yellow fever virus
ZIKV	Zika virus

CHAPTER 1: INTRODUCTION

1.1 Zika virus (ZIKV): Discovery, history, and re-emergence

In 1947, scientists isolated a filterable and previously unrecorded virus from the serum of a pyrexial rhesus monkey in the Zika forest of Kampala, Uganda (Dick et al., 1952). The following year, in 1948, a second isolation of the same virus was made from *Aedes africanus* mosquitoes (Dick et al., 1952). Cross neutralization tests showed evidence of a novel virus that was not identical to yellow fever virus (YFV) or Theiler's mouse encephalomyelitis virus that were prevalent in that region. Owing to the location of its discovery, this novel virus was named Zika virus (ZIKV) (Dick et al., 1952; Musso and Gubler, 2016). While seropositivity in humans was reported in Tanzania and Uganda in 1952, the first case of human infection with ZIKV was reported in 1954 in Nigeria (Macnamara, 1954; Musso and Gubler, 2016). The virus was isolated from *Aedes aegypti* mosquitos in Malaysia in 1969 and the first case of human infection outside of the African continent was reported in Central Java, Indonesia (Musso and Gubler, 2016). Since its discovery, only about 14 cases of human infection were reported in Asia and Africa (Kindhauser et al., 2016; Musso and Gubler, 2016; Sharma et al., 2017) (Fig. 1.1). After almost 60 years, in 2007, the virus re-merged and about 72.6% of the population was infected causing a major epidemic in the Yap Island of Federated States of Micronesia (Kindhauser et al., 2016). A second outbreak affecting about 11.5% of the population occurred in 2013 in French Polynesia. Additional smaller outbreaks also occurred in other Pacific Islands such as New Caledonia, Cook Islands, and Easter Island in 2013-14 (Cao-Lormeau et al., 2014; Musso and Gubler, 2016; Musso et al., 2014). In 2015, ZIKV caused an outbreak of epidemic proportion in Brazil and rapidly

A

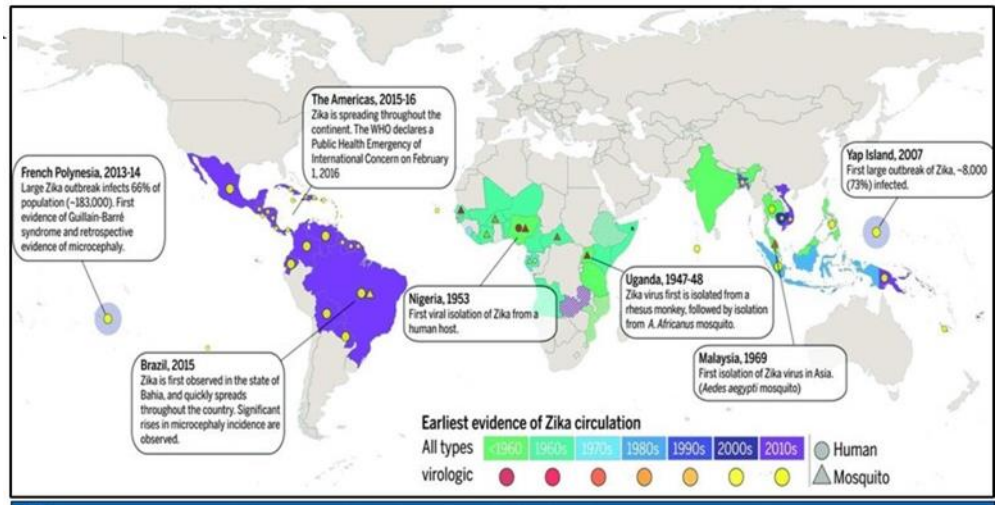
The Americas, 2015-16
Zika is spreading throughout the continent. The WHO declares a Public Health Emergency of International Concern on February 1, 2016
French Polynesia, 2013-14
Large Zika outbreak infects 66% of population (~183,000). First evidence of Guillain-Barré syndrome and retrospective evidence of microcephaly.
Yap Island, 2007
First large outbreak of Zika, ~8,000 (73%) infected.
Nigeria, 1953
First viral isolation of Zika from a human host.
Uganda, 1947-48
Zika virus first is isolated from a rhesus monkey, followed by isolation from A. Africanus mosquito.
Malaysia, 1969
First isolation of Zika virus in Asia. (Aedes aegypti mosquito)
Brazil, 2015
Zika is first observed in the state of Bahia, and quickly spreads throughout the country. Significant rises in microcephaly incidence are observed.
Earliest evidence of Zika circulation
All types
virologic
<1960
1960s
1970s
1980s
1990s
2000s
2010s
Human
Mosquito

B

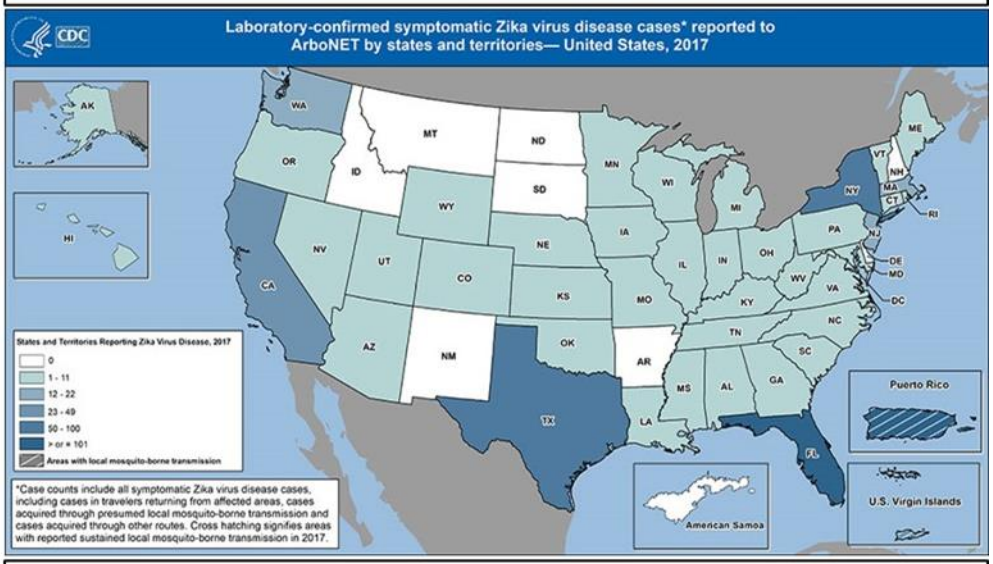
CDC
Laboratory-confirmed symptomatic Zika virus disease cases* reported to ArboNET by states and territories— United States, 2017
States and Territories Reporting Zika Virus Disease, 2017
0
1 - 11
12 - 22
23 - 49
50 - 100
> or = 101
Areas with local mosquito-borne transmission
*Case counts include all symptomatic Zika virus disease cases, including cases in travelers returning from affected areas, cases acquired through presumed local mosquito-borne transmission and cases acquired through other routes. Cross hatching signifies areas with reported sustained local mosquito-borne transmission in 2017.
Puerto Rico
U.S. Virgin Islands
American Samoa

C

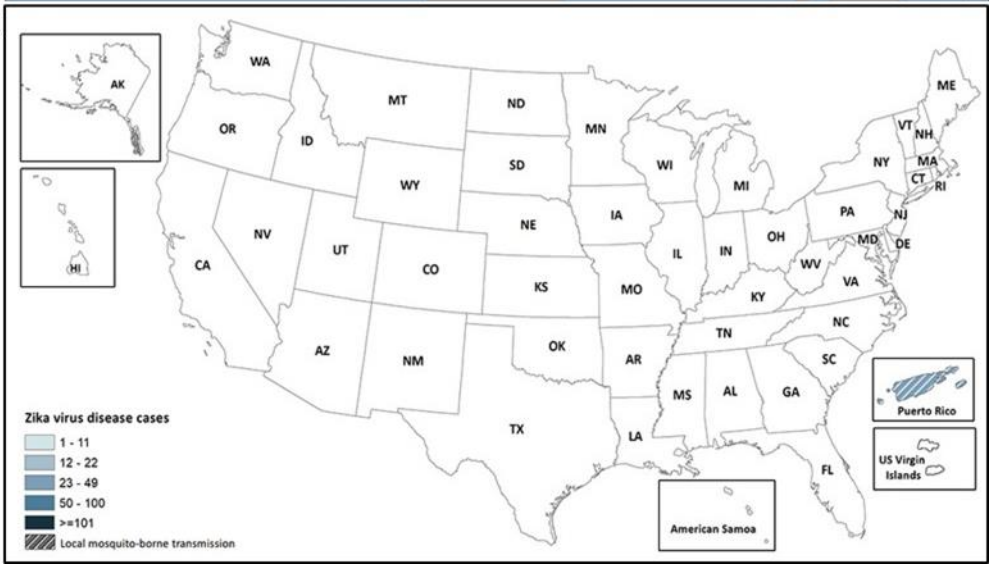
Zika virus disease cases
1 - 11
12 - 22
23 - 49
50 - 100
>=101
Local mosquito-borne transmission
Puerto Rico
US Virgin Islands
American Samoa

Figure 1.1: Global presence of ZIKV. **A** Worldwide spread of ZIKV from 1947 to 2016 (Image sourced from Lessler et al, 2016). **B** ZIKV in the USA and its territories: Numbers of laboratory-confirmed symptomatic Zika virus infections reported to ArboNET by US states and territories as of 2017 and **C** 2021. ZIKV infections in the US and its territories have significantly declined in the past three years [Image sourced from the Centers for Disease Control and Prevention (CDC), National Center for Emerging and Zoonotic Infectious Diseases (NCEZID), Division of Vector-Borne Diseases (DVBD)].

spread the Americas and other parts of the world (Kazmi et al., 2020; Zanluca et al., 2015). In the United States of America, the Center for Disease Control and Prevention (CDC) reported about 5,746 symptomatic infections till 2019 with most of them associated with travelling to places where ZIKV was actively spreading. The CDC also reported about 37,000 cases in US territories (Fig. 1.1). Globally, the virus has been reported in more than 84 countries and the recent outbreaks in the Americas have been associated with increased instances of Guillain-Barré Syndrome (GBS) in adults and microcephaly in neonates (Maslow and Roberts, 2020). Although only a few cases of transmission of ZIKV have been reported since 2017, it has the potential to cause major outbreaks in the future (Musso et al., 2019).

1.2 ZIKV: Classification

ZIKV belongs to the family *Flaviviridae* and genus flavivirus. The *Flaviviridae* family consists of four genera: Flavivirus, Pestivirus, Hepacivirus and Pegivirus (2017). The genus Flavivirus comprises of over 70 arthropod-borne viruses. Further classification of flaviviruses is based on the arthropod vector utilized by them. Viruses like ZIKV, Dengue virus (DENV), Yellow Fever Virus (YFV), Japanese Encephalitis (JEV) and West Nile virus (WNV) are transmitted by mosquitoes (Kuno et al., 1998). Viruses like Kyasanur Forest Disease virus (KFDV), Tick-borne Encephalitis virus (TBEV), Omsk Hemorrhagic Fever Virus (OHFV) and Alkhurma virus (ALKV), which are responsible for encephalitis and hemorrhagic diseases, are transmitted by ticks.

1.3 ZIKV: Virion structure

The cryo-EM structure at near atomic resolution (3.8Å and 3.7Å) of ZIKV was solved by two independent groups and was found to be consistent with other closely related flaviviruses such as DENV and WNV (Kostyuchenko et al., 2016; Sirohi et al., 2016). As depicted in Fig. 1.2, the immature virion is ~60nm in diameter while a mature ZIKV particle is ~50nm in diameter (Kostyuchenko et al., 2016; Prasad et al., 2017; Sirohi et al., 2016; Sirohi and Kuhn, 2017). The viral genome is a single-stranded, positive-sense and non-segmented RNA of about 11 kilobases and is encapsulated by the viral capsid protein and the host derived lipid bilayer (Boyer et al., 2018) (Fig. 1.2).

A mature ZIKV virion contains 180 copies of the viral E and M proteins that are embedded in the host derived lipid membrane (Sirohi and Kuhn, 2017). The E protein consists of 4 domains, namely, ectodomains I, II and III (DI, DII, DIII) and a stem-transmembrane domain. The surface of the virion is covered by the E protein while the M protein resides beneath the E protein and is attached by a small extra-cellular region (Sirohi and Kuhn, 2017). The E protein is organized as a dimer and 3 such dimers are arranged in parallel to form a raft configuration. There are 30 rafts in a single ZIKV particle (Sirohi and Kuhn, 2017). ZIKV does not exhibit the usual T=3 quasi-equivalence even with 180 units of E and M proteins arranged in a raft configuration. This is because of the unusual arrangement of the E protein (Sirohi and Kuhn, 2017).

1.4 ZIKV: Genome organization

The infectious genome of ZIKV is a single-stranded, positive-sense RNA of about 11 kb in length and is arranged in the following order: 5’ untranslated region (UTR), a single open reading frame (ORF) and the 3’ UTR (van Hemert and Berkhout, 2016). The

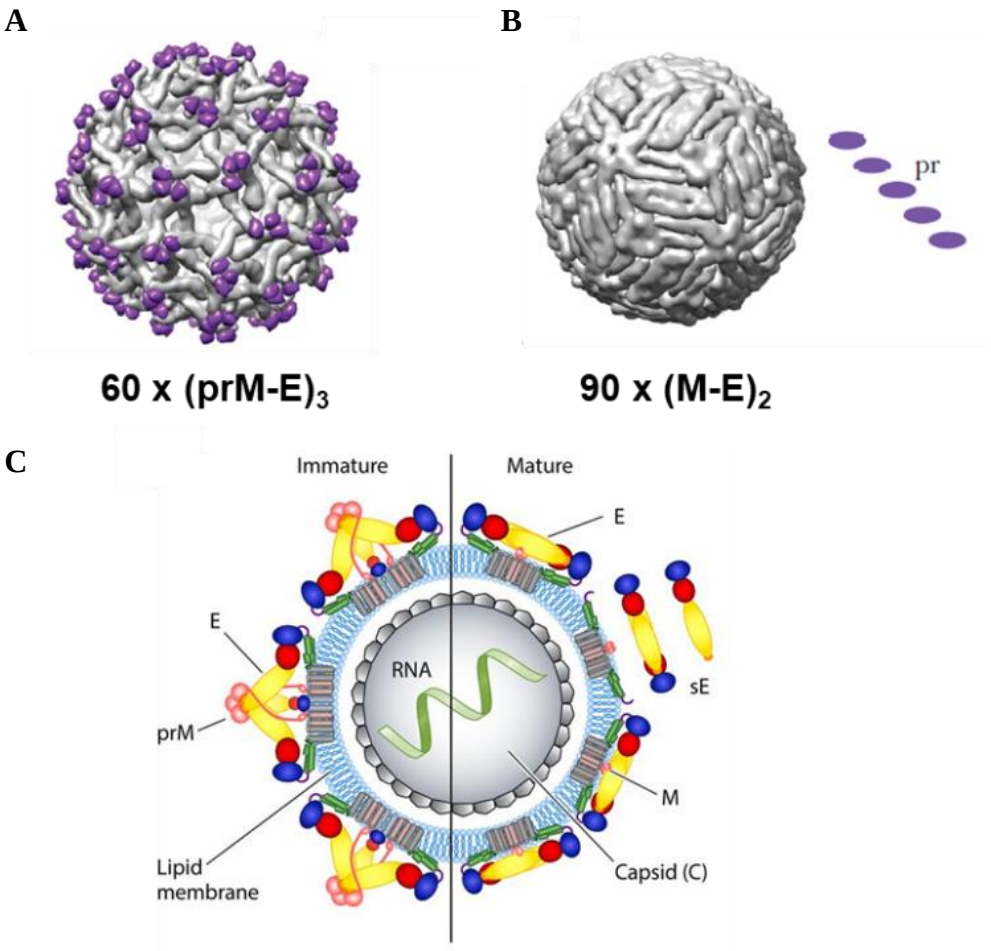

Figure 1.2: Structure of Zika virus particles. Immature and mature ZIKV particles. Proteolytic processing of prM protein, by host protease furin, in the immature non-infectious virion **A** results in the generation of mature, smooth-surfaced, infectious particle **B**. The immature particle contains 60 trimers of prM-E heterodimers, while the mature particle contains 90 conformationally rearranged heterodimers of M-E (Images were adapted from Sirohi, D. and Kuhn, R.J. (2017)). **C** Schematic representation of a prototypical flavivirus (including Zika virus) immature and mature particle showing a cross-sectional organization of viral proteins and RNA. sE, soluble E protein [Image sourced from Heinz, F.X. and Stiansy, K. (2017)].

5’ UTR is ~106 nucleotides long and has a type I cap (m7GpppAmp) structure at the 5’ terminus and is followed by conserved AG dinucleotide (Brinton and Dispoto, 1988). The 3’ UTR comprises of ~430 nucleotides and does not have a poly A tail but ends with consists of conserved CU_{OH} at the 3 ’-terminus (Brinton et al., 1986) (Fig. 1.3).

The ORF is ~10.2 kilobases and is translated into a single polypeptide of ~3400 amino acids in the cytoplasm of an infected cell (Chambers et al., 1990). The single polypeptide is processed and cleaved by proteases of host as well as viral origin and results in three amino-terminal structural (capsid, C; pre-membrane, prM; and envelope, E) proteins and seven carboxy-terminal non-structural (NS1, NS2A, NS2B, NS3, NS4A, NS4B, and NS5) proteins (Kuno and Chang, 2007) (Fig. 1.3). As in other flaviviruses like DENV, WNV, YFV and JEV, the structural proteins are responsible for virus attachment and entry into host cells, and virion formation while the non-structural proteins aid in genome replication, polypeptide processing, evasion of host antiviral defenses and virion assembly (Diamond and Pierson, 2015; Kumar et al., 2016).

1.5 ZIKV: Structural proteins

1.5.1 Capsid (C) protein

The C protein is 104 aa in length and has a molecular weight of ~14 kDa (Shang et al., 2018). Following translation, the protein relocates to the cytoplasmic side of the ER and helps in the translocation of the viral prM protein into the ER lumen (Byk and Gamarnik, 2016; Tan et al., 2020). It has an overall positive charge and associates with the negatively charged genomic RNA forming the nucleocapsid core which gets incorporated into new virions (Shang et al., 2018; Tan et al., 2020). It has been shown to

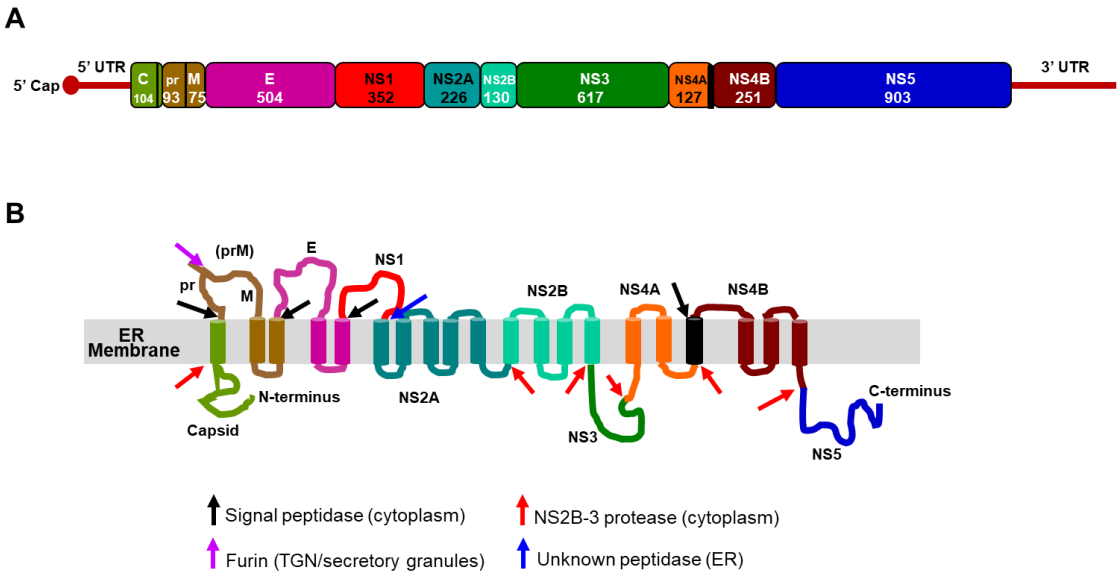

Figure 1.3: ZIKV genome organization, encoded proteins, and their topology. A The viral genome is shown as a red line with a cap structure at the 5' end, followed by an untranslated region (5'UTR), various proteins (with amino acid residue length) generated from a single ORF that is translated from the genome, and the 3' UTR. **B** Topology of the viral proteins. Arrows show various protease cleavage sites for generation of the mature proteins. A small protein (2K) present between NS4A and NS4B is membrane-associated. The cylindrical structures represent membrane-associated domains of the proteins (Image redrawn from Tan *et al*, 2020)

play a vital role in the process of virus assembly and is responsible for the overall icosahedral structure of the virus particle (Tan et al., 2020). Additionally, the capsid protein is known to translocate into the nucleus of the infected cells and interfere with ribosome biogenesis and alter host transcriptome (Sotcheff and Routh, 2020).

1.5.2 Precursor membrane (prM) and membrane (M) proteins

The prM protein is a glycosylated protein of 168 aa in length (Kuno and Chang, 2007). Post synthesis, the prM protein relocates into the ER where, and in association with the viral envelope protein, forms immature virions and acts a chaperone for efficient and proper folding of the envelope protein (Lorenz et al., 2002; Nambala and Su, 2018; Nambala et al., 2020). The prM protein is cleaved by cellular furin protease in the trans-golgi network and results in pr peptide and the M protein (Hsieh et al., 2011). The pr peptide associates with the envelope protein and helps in egress of mature virus particles (Oliveira et al., 2017). Recent studies suggest that the prM protein plays a significant role in increased neurovirulence and the development of microcephaly in mice (Yuan et al., 2017). The study also found that a serine to asparagine aa substitution (S139N) in the prM protein of ZIKV resulted in a more infectious phenotype while a reverse mutation (N139S) produced a less infectious virus (Yuan et al., 2017).

1.5.3 Envelope (E) protein

The envelope protein is the outermost covering of a ZIKV particle, 504 aa in length and has a molecular weight of ~53 kDa (Dai et al., 2016). It has a single glycosylation site at position 154 (N154) (Annamalai et al., 2017; Carbaugh et al., 2019;

Routhu et al., 2019). Flaviviral E protein plays a significant role in recognition of host cell receptor, membrane fusion, viral entry into the host cell and assembly of progeny virions (Cruz-Oliveira et al., 2015; Valente and Moraes, 2019). It is cleaved by host signal peptidase from the translated polyprotein in the ER lumen following which hetero-dimerization of E and prM occurs (Dai et al., 2016). The E protein consists of three major domains: DI, DII, and DIII out of which EDIII is a major target for potent flavivirus type-specific neutralizing antibodies (mAb) (Beltramello et al., 2010; Dai et al., 2016). The highly conserved fusion loop epitope (FLE) in DII is also a target for less potent cross-neutralizing mAbs (Beltramello et al., 2010; Costin et al., 2013).

1.6 ZIKV: Nonstructural (NS) proteins

1.6.1 Non-structural protein 1 (NS1)

The non-structural protein 1 (NS1) of ZIKV is a 352 aa long glycoprotein. As with most mosquito-borne flaviviruses, ZIKV NS1 has 2 conserved glycosylation sites (Pryor and Wright, 1994). Depending on the glycosylation pattern, its molecular weight ranges between 46 to 54 kDa (Muller and Young, 2013; Rastogi et al., 2016). Zika virus NS1 protein shares structural similarity to related flaviviruses like DENV2 and WNV (Muller and Young, 2013; Xu et al., 2016). NS1 exists in multiple locations in a cell. It is found to be associated with intracellular vesicular compartments induced by virus infection, on the surface of the infected cell and as a soluble lipoparticle that is secreted (Muller and Young, 2013). Intracellular NS1 exists as a dimer and is associated with vesicular compartments (Winkler et al., 1988). It functions as an essential cofactor in virus replication and is found to co-localize with double-stranded RNA (dsRNA)

(Mackenzie et al., 1996). The secreted form of NS1 forms a hexamer and is known to be highly immunogenic. It has also been shown to interact with host factors and contributes to disease pathogenesis (Avirutnan et al., 2006; Muller and Young, 2013). Studies with several flaviviruses have suggested that NS1 protein glycosylation plays a critical role in viral genome replication and pathogeneis (Annamalai et al., 2019; Pletnev et al., 1993; Pryor et al., 1998; Pryor and Wright, 1994).

1.6.2 Non-structural protein 2 (NS2)

Proteolytic cleavage of ZIKV NS2 from the single polypeptide results in 2 proteins: NS2A and NS2B. While NS2A is 226 aa in length, NS2B is 130 aa long (Sirohi and Kuhn, 2017). Following proteolytic cleavage, NS2A relocates to the endoplasmic reticulum (ER) where it is an essential component of viral replication complex (Xie et al., 2013). Additionally, it also helps in progeny virion assembly and downregulation of host immune response (Xie et al., 2013). NS2B is a critical component of a so called 'two-component protease' and is essential to the proper functioning of the NS3 protein (Gupta et al., 2015).

1.6.3 Non-structural protein 3 (NS3)

Flaviviral NS3 protein is one of the largest proteins and is ~617 aa in length (Brecher et al., 2013). It has 2 domains: i) N-terminal serine protease (NS3Pro) domain, and ii) C-terminal RNA helicase (NS3Hel) and triphosphatase (NS3RTPase) domain (Brecher et al., 2013; Li et al., 1999; Warrener et al., 1993). It has been shown that the association of NS2B with NS3 results in the proteolytic cleavage of NS3 and the

formation of an active serine protease complex which serves a critical role in flavivirus replication and progeny virion assembly (Arias et al., 1993; Chambers et al., 1991; Chambers et al., 1993). The flaviviral NS2B-NS3 protease complex is highly conserved and is a potential target for the development of inhibitors against flaviviruses (Li et al., 2017b; Li et al., 2018).

1.6.4 Non-structural protein 4 (NS4)

Like NS2, flavivirus NS4 is processed to generate NS4A and NS4B, with an additional highly hydrophobic 2K peptide that is located between them (Sirohi and Kuhn, 2017). NS4A is 127 aa long and is an important viral protein that remains associated with cellular membranes and is involved in membrane rearrangements and the formation of viral replication complexes (Miller et al., 2007; Roosendaal et al., 2006). Additionally, it has also been demonstrated that ZIKV NS4A inhibits the interaction of RLR-MAVS and impairs antiviral immune responses (Ma et al., 2018). NS4B is 251 aa in length and has been shown to interfere with host type-I interferon response by blocking the activation of STAT1 (Gerold et al., 2017; Munoz-Jordan et al., 2005). Both ZIKV NS4A and NS4B have been shown to interfere with the Akt-mTOR axis of signaling and induce autophagy in human neural stem cells (Liang et al., 2016). Addittionaly, inhibition of the Akt-mTOR axis, a key signaling pathway involved in neuronal development, along with the activation of autophagy can be a potential mechanism by which ZIKV induces microcephaly (Liang et al., 2016).

1.6.5 Non-structural protein 5 (NS5)

Flaviviral NS5 is 903 aa in length and is the largest and the most conserved of all the proteins (Song et al., 2021). It has two domains: i) a C-terminal RNA-dependent RNA polymerase (RdRp) domain, and ii) a N-terminal methyltransferase (MTase) domain (Elshahawi et al., 2019; Song et al., 2021). While the RdRp domain aides in *de novo* viral RNA synthesis, the MTase domain contributes to methylation of the RNA cap to form N-7-methyl-guanosine and 2'-O-methyl-adenosine using S-adenosyl-L-methionine (SAM) as the methyl donor (Godoy et al., 2017; Zhang et al., 2017). In addition to viral genome replication, NS5 also contributes to immune evasion. A recent report demonstrated that ZIKV NS5 interacts with host retinoic acid-inducible gene I (RIG-I) and prevents the nuclear translocation of interferon regulatory factor 3 (IRF3) resulting in inhibition of interferon-β (IFN-β) production and signaling (Li et al., 2020).

1.7 Life cycle of ZIKV

ZIKV reservoir is maintained in mosquitoes and is transmitted to humans by infected female *Aedes* mosquitoes while feeding for blood. Following this, the virus interacts with several cell surface receptors like dendritic-cell-specific intercellular adhesion molecule-3-grabbing non-integrin (DC-SIGN) (Pierson and Diamond, 2020; Tassaneetrithep et al., 2003), Tyro3, Axl and Mertk (TAM) family of phosphatidylserine receptors (Meertens et al., 2012; Perera-Lecoin et al., 2013) and/or T-cell immunoglobulin domain and mucin domain (TIM) (Meertens et al., 2012; Pierson and Diamond, 2020) and infects skin cells such as dermal epidermal keratinocytes, fibroblasts, and immature dendritic cells (Hamel et al., 2015). The virus then infects monocytes and macrophages in the draining lymph nodes leading to the spread of ZIKV

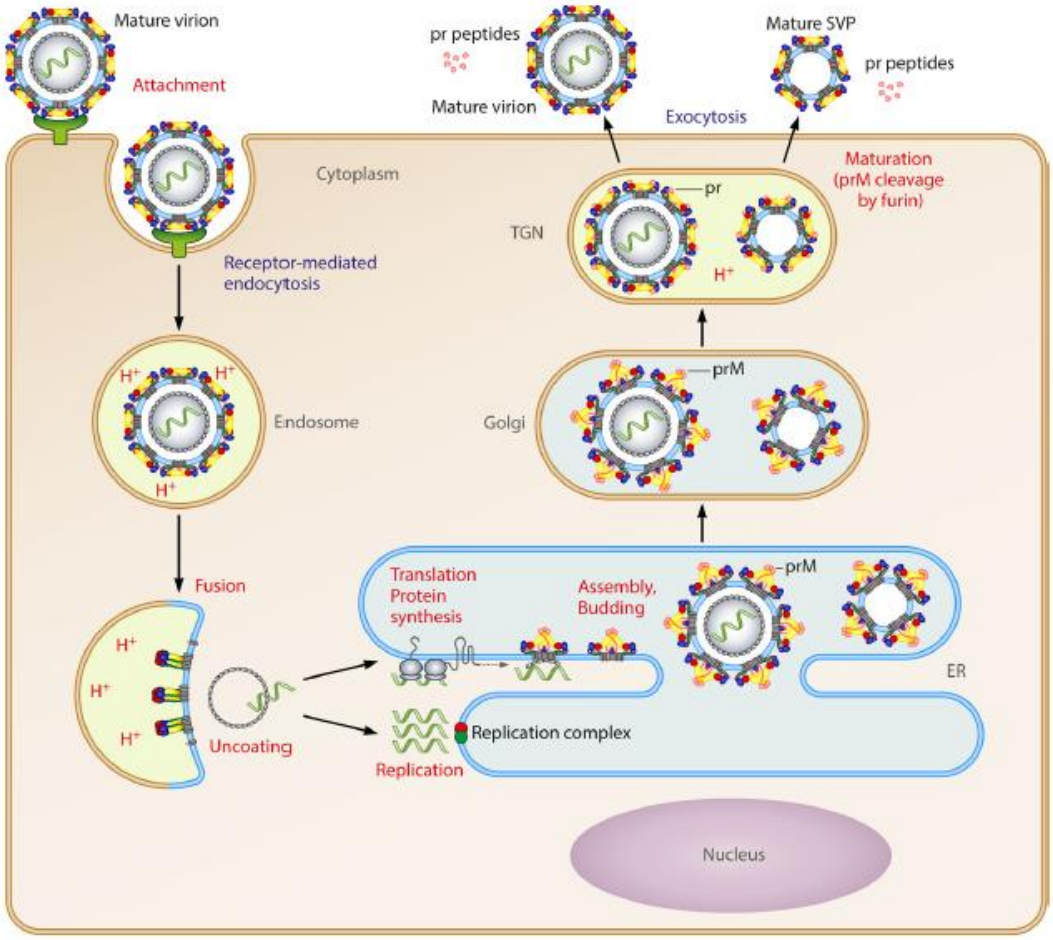

Figure 1.4: Replication of ZIKV in host cells. The virus enters host cells by receptor-mediated endocytosis and fuses its membrane by an acidic-pH-triggered mechanism in the endosome to release the viral RNA. The positive-stranded genomic RNA serves as the only viral mRNA and leads to the synthesis of a polyprotein that is co- and post translationally processed into three structural and seven nonstructural proteins. Virus assembly takes place at the ER membrane and leads to the formation of immature virions, which are further transported through the TGN that causes structural changes allowing the cleavage of prM by the cellular protease, furin. The mature virions are transported to the cell membrane and released by budding (Image sourced from Heinz *et al*, 2017).

to other organs in the body such as the reproductive organs, the placenta, the brain and spinal cord (Miner and Diamond, 2017).

Following interaction of the virus with cell surface receptor(s), clathrin-mediated endocytosis internalizes the virion (Hackett and Cherry, 2018) and delivers to an early endosome where the viral E protein undergoes structural modifications due to an acidic environment (Perera-Lecoin et al., 2013). This is followed by the fusion of the endosomal membrane with the viral envelope and release of the viral genomic RNA into the cytosol (Pierson and Diamond, 2020) (Fig. 1.4).

Once inside a cell, ZIKV follows a similar chain of events as other members of the *Flaviviridae* family. The genomic RNA serves as an mRNA template for cap dependent translation which is initiated as soon as the genomic RNA is released into the cytosol (Barrows et al., 2018). It encodes a single open reading frame that is flanked by a 5’ and 3’ UTR (Pierson and Diamond, 2020). The presence of the ER-localization signal at the carboxy-terminal end of the C protein promotes its translocation to the ER membrane where it rapidly associates with the ribosomes leading to co-translation and insertion of the polyprotein into the ER lumen where the synthesis of nascent viral proteins occurs. The nascent proteins are then cleaved by host and viral proteases to generate the mature structural and non-structural proteins (Sager et al., 2018). The flanking UTRs aide in translation of the viral RNA, replication, and subversion of host immune response (Gebhard et al., 2011). The translation of viral proteins primes the host environment for viral genomic RNA replication which occurs in endoplasmic reticulum (ER) derived membrane-bound structures called replication compartments (RCs) (Aktepe and Mackenzie, 2018; Barrows et al., 2018). The ultrastructure of such RCs has

been solved using cryo-EM tomography which shows spherical structures budding from the cytosolic face of the ER and containing all the components necessary for viral RNA replication and progeny virion assembly (Aktepe and Mackenzie, 2018; Pierson and Diamond, 2020; Welsch et al., 2009). Apart from serving as the template for the synthesis of viral proteins, the genomic RNA also serves as a template for RNA synthesis. The first step involves the synthesis of a negative-sense RNA resulting in the formation of dsRNA intermediate from which the positive-sense viral genome is produced (Lindenbach and Rice, 2003). Along with the newly synthesized viral proteins, the positive-strand RNA is packaged into progeny virus particles at the surface of the ER. These immature progeny virions then bud from the ER surface and are transported into the TGN where the prM protein is cleaved by furin-like proteases (Tomar et al., 2017; Wang et al., 2017). This is followed by the homodimerization of the E protein resulting in mature virions which are then released from the cell by exocytosis (Nambala et al., 2020) (Fig. 1.4).

1.8 ZIKV: Clinical Disease

In general, the clinical presentation of flavivirus infection in humans ranges from mild illness that includes asymptomatic infection or episodes of self-limiting fevers to severe and life-threating conditions including shock syndrome, haemorrhagic fever, encephalitis, congenital defects, and hepatitis (Pierson and Diamond, 2020). While majority of flavivirus, including ZIKV, infections do not present with any symptoms (Musso et al., 2018; Musso and Gubler, 2016), a fraction of infected individuals may present with symptoms including but not limited to conjunctivitis, myalgia, headache, arthralgia and a rash that do not have any long-term consequences (Antoniou et al., 2020;

Burger-Calderon et al., 2018; Pierson and Diamond, 2020). However, in 2015, the ZIKV outbreak in Brazil caused major concern because of its association with microcephaly, fetal growth retardation, brain malformations, and other neurological disorders, collectively termed as congenital Zika syndrome (CZS) in infants and Guillain-Barré syndrome in adults (Cao-Lormeau et al., 2016; Coyne and Lazear, 2016; Heukelbach et al., 2016; Miner and Diamond, 2017; Rawal et al., 2016; Wheeler, 2018).

Microcephaly is a congenital abnormality in which the size of the head of the fetus is smaller than the average head size of infants in the same age and sex group (Antoniou et al., 2020) and such a condition is associated with reduced brain size and developmental disabilities (Heukelbach et al., 2016) (Fig. 1.5). Microcephaly can occur because of i) failure of the brain to grow appropriately during pregnancy due to reduced neuron production, called congenital microcephaly, or ii) failure to develop post-partum due to loss of dendritic connections, called secondary or postnatal microcephaly (Barbelanne and Tsang, 2014; Faizan et al., 2016). The 2015 outbreak in Brazil saw an increased incidence of infants born with congenital microcephaly where pregnant women were diagnosed positive for ZIKV infection (Antoniou et al., 2020; Heukelbach et al., 2016). Apart from that, ZIKV infection have also been associated, albeit infrequently, with organ failures, subcutaneous bleeding and thrombocytopenia, encephalitis, and meningitis (Carteaux et al., 2016; Karimi et al., 2016; Pierson and Diamond, 2018; Swaminathan et al., 2016). Additionally, very few cases of death have been reported in children with sickle cell anemia who were infected with ZIKV (Pierson and Diamond, 2018) and in adults with cancer (Pierson and Diamond, 2018; Swaminathan et al., 2016).

Figure 1.5: Association of ZIKV infection and microcephaly. The circumference of the head is compared between a healthy infant and an infant suffering from microcephaly. Severe reduction in the size of the head along with developmental deficits is seen newborn children suffering from congenital microcephaly. The 2015-16 ZIKV outbreak in Brazil has been associated with an increased incidence of children born with microcephaly (Image source: https://www.cdc.gov/pregnancy/zika/testing-follow-up/zika-syndrome-birth-defects.html).

1.8.1 Association of ZIKV with microcephaly

The reemergence of ZIKV in 2015 as a potential pathogen that caused serious developmental disorders redirected the scientific community to focus on investigating its causal role in microcephaly. This was borne out of the observation that ZIKV was found in the brain tissues of the fetuses suffering from microcephaly in women who, during the first trimester of pregnancy, were infected with the virus (Driggers et al., 2016; Mlakar et al., 2016). While, initially, it was unclear whether ZIKV targeted mature neurons or progenitor cells that would eventually proliferate and differentiate into mature neurons, several studies revealed that ZIKV directly targeted the cortical neural progenitor cells leading to cell death (Li et al., 2016b; Tang et al., 2016). These findings provided evidence for the Centers for Disease Control and Prevention (CDC) to declare that ZIKV can cause microcephaly (Rasmussen et al., 2016). Additionally, the findings that not only can ZIKV be transmitted via mosquitoes but can also be transmitted sexually between individuals as well as vertically, from mother to the fetus, led to increased public concerns (Christian et al., 2019; D'Ortenzio et al., 2016).

Although a direct understanding of the molecular mechanisms of ZIKV-induced microcephaly is yet to be established, a number of reports have described several probable mechanisms that may contribute to neurological deficits in developing brains. One of the probable mechanisms is the accumulation of several nucleotide mutations in key viral proteins that are involved in immune evasion (Mlakar et al., 2016). When compared with the French Polynesian strain, the Brazilian strain contains three mutations in the NS1 protein at sites K940E, T1027A, and M1143V which are implicated in immune evasion (Mlakar et al., 2016; Wen et al., 2017). Additionally, a mutation in

NS4B at T2509I, implicated in the inhibition of type I interferon signaling and in NS5 at M2634V, implicated in the masking of the viral RNAs from recognition by the host, also tend to contribute to the development of microcephaly (Mlakar et al., 2016). Another report demonstrated that a single nucleotide mutation in the prM protein (S139N) lead to increased virulence in mice and human neural progenitor cells (NPCs) and resulted in more severe microcephaly and fetal demise in neonatal mice (Yuan et al., 2017). Furthermore, the failure of host exonucleases to degrade subgenomic flaviviral RNAs (sfRNAs) produced in the 3' UTRs results in their accumulation in the cytosol and are known to contribute to pathologic effects (Akiyama et al., 2016). Such observations can explain the unprecedented emergence of ZIKV and its association with neurological complications in the recent times.

Another potential mechanism for ZIKV-induced microcephaly can be attributed to tissue tropism, i.e., the ability of the virus to infect specific types of cells and tissues. ZIKV has been shown to preferentially infect neural progenitor cells and induce apoptosis resulting in their depletion (Dang et al., 2016; Tang et al., 2016). Mature neurons are also infected by the virus albeit to a lesser extent (Tang et al., 2016). This phenomenon can very likely cause neurodevelopmental deficits. Indeed, when developing wild type mice fetuses were infected with ZIKV by intra-ventricular injections, differentiation of neural progenitor cells was significantly inhibited and this resulted in the development of microcephaly (Li et al., 2016a). Additionally, with direct intracranial inoculation of ZIKV in early post-natal wild-type mice pups depleted proliferating cells in the stem cell compartment of the ventricular zone (Huang et al., 2016).

While mouse models played a significant role in the initial studies needed to establish the causal role of ZIKV for microcephaly, later studies in human brain organoid cultures provided a much better understanding of the effect ZIKV infection in a more relevant model system. Several groups have reprogrammed human pluripotent stem cells (hPSCs) that can be induced and developed into three dimensional (3-D) organoids which can be used as a more relevant model system to study specific aspects of brain development and ZIKV pathogenesis (Lancaster et al., 2013; Qian et al., 2016). In corroboration with the findings from mouse models, ZIKV infection of human neurosphere organoid cultures *in vitro* was shown to induce cell death (Garcez et al., 2016). Using such models, it has been shown that ZIKV infection induces pre-mature differentiation of neural progenitor cells, leads to cell death, and can produce phenotypes of microcephaly (Dang et al., 2016; Gabriel et al., 2017). ZIKV infection in the first trimester of pregnancy has been shown to result in developmental deficits in the brain and microcephaly in the fetus (Driggers et al., 2016; Mlakar et al., 2016; Olagnier et al., 2016). Hofbauer cells (placental macrophages) and to a lesser extent, cytotrophoblasts, in the placenta are the main targets of ZIKV and this leads to vertical transmission of ZIKV from mother to the developing fetus (Quicke et al., 2016).

In addition to cell-autonomous effects of ZIKV infection on hNPCs, bystander effect is also seen and may contribute to ZIKV induced pathogenesis (Christian et al., 2019). In a 20-week old fetus with intra-uterine ZIKV infection, cell death by apoptosis was seen in infected as well as uninfected bystander cortical neurons which was likely due to neurotoxic factors including interleukin 1 β (IL1-β), and tumor necrosis factor α (TNFα) secreted by the infected cells (Olmo et al., 2017). Additionally, glial cells and

microglia (resident macrophages) act as viral reservoirs and also play a bystander role in ZIKV induced disease. Microglia have been reported to be direct targets of ZIKV infection as shown in the examination of brain tissue from aborted fetuses (Lum et al., 2017). The proliferation of NPCs was found to be inhibited when they were grown in conditioned media taken from infected primary microglia (Wang et al., 2018). Furthermore, co-culturing of ZIKV-infected microglia and NPCs resulted in the spread of infection to the NPCs resulting in cell death (Mesci et al., 2018). In human induced pleuripotent stem cells (hiPSCs) derived populations, ZIKV successfully infected a variety of cells like astrocytes, microglia-like cells and hNPCs but cell death by apoptosis was only seen hNPCs (Muffat et al., 2018). Another study reported that infection of human fetal neural stem cells (fNSCs) induces autophagy and subsequent cell death by impairing the Akt/mTOR signaling cascade (Liang et al., 2016).

1.9 mTOR signaling cascade

Virus replication in host cells requires modulation of host cell pathways such as energy metabolism and macromolecule synthesis as well as inhibiting antiviral responses leading to production of viral progeny by the host cell machinery. The mechanistic (formerly, called mammalian) target of rapamycin (mTOR) signaling cascade is critical to the regulation of various cellular and metabolic processes including gene expression, protein translation, cell proliferation, cell survival, autophagy, etc. (Foster and Fingar, 2010; Saxton and Sabatini, 2017b) (Fig. 1.6). The mTOR kinase is an evolutionarily conserved serine/threonine kinase and exists as two functionally unique complexes,

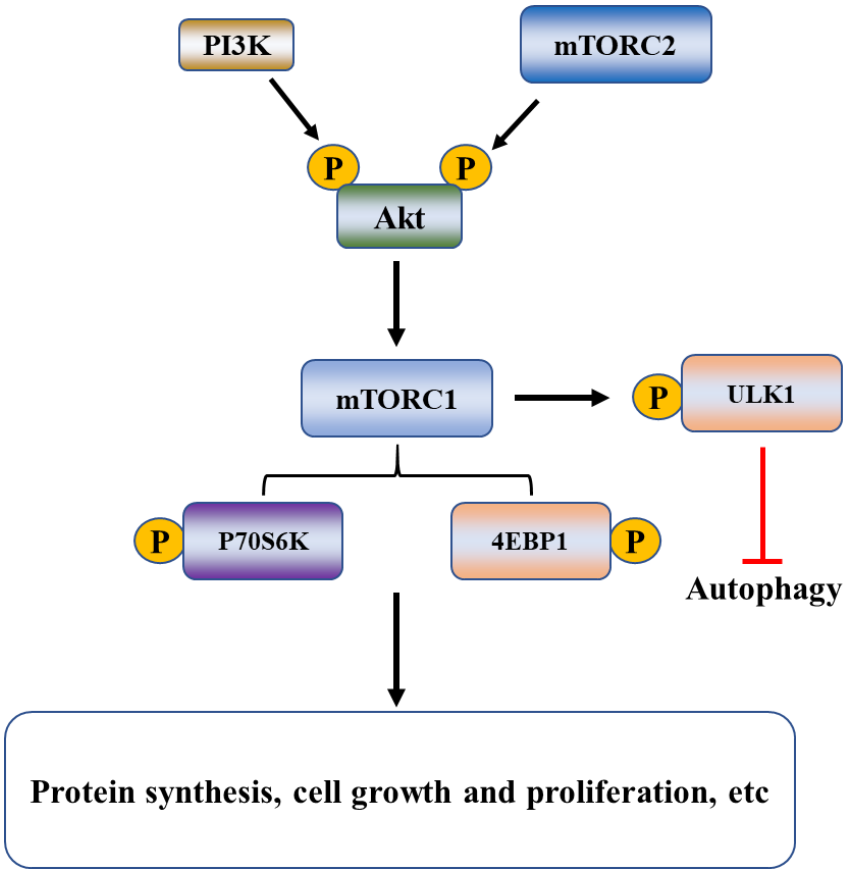

Figure 1.6: The mTOR cascade. Schematic showing the activation of mTORC1 leading to protein synthesis, cell growth and proliferation and the inhibition of autophagy. The phosphorylation of Akt at Ser 473 and Thr 308 by mTORC2 and PI3K activates it which in turn phosphorylates and activates mTORC1. This leads to the phosphorylation of P70S6K at Thr389, that regulates cell growth and cell cycle progression, and 4EBP1 at multiple sites, that regulates the translation of mRNAs and cell proliferation. Activated mTORC1 also phosphorylates ULK1 at Ser 757 resulting in the inhibition of ULK 1 function. Dephosphorylated ULK1 induces autophagy.

mTOR complex (mTORC) 1 and mTORC2 (Foster and Fingar, 2010; Saxton and Sabatini, 2017b). Each complex responds to different environmental stressors and has unique regulatory properties, as well as cellular activities. The regulatory associated protein of mTOR (Raptor) and the rapamycin insensitive companion of mTOR (Rictor) are essential and distinguishing subunits of the mTORC1 and mTORC2, respectively and act as scaffold proteins to assemble and stabilize respective complexes (Saxton and Sabatini, 2017b; Yang et al., 2013). The phosphorylation and activation of downstream effectors of mTORC1, the p70 ribosomal S6 kinase 1 (p70S6K), the eukaryotic initiation factor 4E (eIF4E)-binding protein 1 (4EBP1), and Unc-51 like autophagy activating kinase 1 (ULK1) regulate cap-dependent mRNA translation, metabolism, and protein/organelle quality control mechanisms via autophagy (Saxton and Sabatini, 2017b; Yang et al., 2013). In conditions of abundant nutrients, mTORC1 triggers ribosome assembly and translation of mRNA leading to cellular growth and proliferation, and inhibition of autophagy (Le Sage et al., 2016). On the other hand, the regulation of mTORC2 is not fully understood, but is known to associate with the ribosomes and that this association is triggered primarily by insulin-stimulated phosphatidylinositol 3-kinase (PI3K) signaling (Zinzalla et al., 2011). mTORC2 phosphorylates several proteins of the AGC family of kinases such as protein kinase C (PKC), protein kinase B (PKB/Akt), and the serum and glucocorticoid induced kinases (SGK) regulating various aspects of cytoskeletal structure modelling and cellular survival (Saxton and Sabatini, 2017b).

The mTOR cascade can be activated by multiple extracellular stressors that bind to cell surface receptors which transduce the signal to PI3K (Le Sage et al., 2016). This

results in the phosphorylation of the growth factor-activated kinase, Akt, at threonine308 (Thr308) and subsequently at serine 473 (Ser473) by mTORC2 resulting in its activation (Le Sage et al., 2016; Sarbassov et al., 2005). An activated Akt phosphorylates tuberous sclerosis protein 2 (TSC2) leading to the conversion of Rheb-GDP to Rheb-GTP resulting in the activation of mTORC1 (Inoki et al., 2002; Menon et al., 2014) (Fig. 1.6). In contrast, several intracellular and extracellular stimuli such as energy deficit, generation of reactive oxygen species (ROS) and growth factor deficiency can inhibit the mTOR cascade (Huang and Manning, 2009; Wang and Proud, 2011). Viruses including ZIKV are also known to manipulate the mTOR signaling cascade to support their optimal replication and pathogenic potential.

1.9.1 mTOR and microcephaly

mTOR signaling plays a very important role the proper development and functioning of the brain and is key to phenomena such as neural stem cells proliferation, spatio-temporal organization, migration and differentiation of neurons, assembly and maintenance of neural circuits as well as regulation of complex behaviors such as sleeping, feeding, and maintenance of circadian rhythms (Lipton and Sahin, 2014). The mTOR signaling cascade is tightly regulated in proper brain development and any abnormality or impairment has been implicated in several neurodegenerative diseases (Lipton and Sahin, 2014). It has been observed that while early loss of mTOR function in brain development leads to death and exhaustion of progenitor cells that are necessary for proper brain development, over-activation may also be catastrophic and lead to rapid exhaustion of stem cell niches resulting in serious pathological consequences (Lipton and

Sahin, 2014). Studies done with a conditional mutant of mTOR demonstrated that while early activation of the cascade induced microcephaly, delayed activation in post-mitotic neurons lead to cortical hypertrophy, neuro-degeneration, and early death in mice (Kassai et al., 2014). Attempts to dissect the roles of mTORC1 and mTORC2 by Rictor and Raptor specific knockouts demonstrated that while Rictor knockouts that were specific to the brain led to reduced neuronal size, shorter dendritic processes and smaller brains, brain-specific Raptor knockouts resulted in reduced cell size and death, inhibition of gliogenesis, and post-natal fetal demise (Cloetta et al., 2013; Thomanetz et al., 2013).

1.9.2 mTOR and autophagy

Apart from regulating cell proliferation, cellular metabolism, energy metabolism and macromolecule synthesis, the mTOR signaling cascade also tightly regulates autophagy, a cellular survival response that is known to sequester and degrade damaged cell organelles, proteins and/or invading pathogens, by regulating the phosphorylation of ULK1 at serine 757 (S757) (Khandia et al., 2019; Le Sage et al., 2016; Nazio et al., 2013; Schmeisser and Parker, 2019). In the event of nutrient depletion, autophagy is activated due to inactivation of mTORC1 and resulting dephosphorylation and activation of ULK1 (Schmeisser and Parker, 2019) (Fig. 1.6). In the context of virus replication, autophagy can be pro-viral or anti-viral. Several viruses including coxsackievirus B3, hepatitis C virus, coronaviruses and DENV are known to activate autophagy that enhances viral protein synthesis and replication in infected cells (Ke, 2018; Ke and Chen, 2011; Lee et al., 2008; Reggiori et al., 2010; Sir et al., 2008; Wong et al., 2008). Furthermore, influenza A virus (IAV) has been shown to induce autophagosome formation at early

time points of infection and at later time points inhibit the fusion of autophagosomes with lysosomes thereby leading to accumulation of autophagosomes in the infected cells (Gannage et al., 2009). In contrast, viruses like herpes simplex virus (HSV-1), human immunodeficiency virus (HIV), and influenza virus subvert the activation of autophagy to enhance their replication (Brand et al., 1997; Lu et al., 1995; Poppers et al., 2000).

1.10 Redox regulation and oxidative stress in virus infection

1.10.1 Nrf2 signaling cascade

Nuclear factor E2-related factor 2 (Nrf2) is a modular transcription factor that belongs to the cap'n'collar family of transcription factors. It consists of a highly conserved leucine-zipper (b-ZIP) structure and seven Neh (Neh 1-7) domains and is known to counter oxidative stress (Ramezani et al., 2018; Tonelli et al., 2018). Normally, Nrf2 remains associated with Kelch-like erythroid cell-derived protein with CNC homology [ECH]-associated protein 1 (Keap1) in the cytoplasm which drives its interaction with cullin-3-based E3ubiquitin ligase (Cul3) (Itoh et al., 1999; Kobayashi et al., 2004). This association results in poly-ubiquitination of Nrf2, and subsequent proteasome mediated degradation resulting in very low basal levels of Nrf2 in cells (Itoh et al., 1999; Kobayashi et al., 2004; Taguchi et al., 2011; Tonelli et al., 2018). When a cell undergoes oxidative stress, an imbalance in the generation and neutralization of reactive oxygen species (ROS) occurs and the association of Keap1 with Nrf2 is impaired leading to free Nrf2 which then translocates to the nucleus and induces the expression of antioxidant response elements (AREs) (Baird et al., 2014; Itoh et al., 1997; Ramezani et al., 2018). AREs are a cluster of multiple genes associated with antioxidant defense, ROS

detoxification enzymes, NADPH regeneration and regulation of metabolism that protect the cell from the damaging effects of ROS (Baird et al., 2014; Hayes and Dinkova-Kostova, 2014; Ramezani et al., 2018). The restoration of redox balance is sensed by Keap1 which translocates into the nucleus and binds to Nrf2, thereby dissociating Nrf2 from the AREs. The Keap1/Nrf2 complex translocates back to the cytoplasm where Nrf2 is poly-ubiquitinated and degraded (Ramezani et al., 2018; Sun et al., 2007).

1.10.2 Nrf2 regulates cellular antioxidant defense system and pentose phosphate pathway (PPP)

Generally, ROS are formed as a byproduct of normal cellular metabolism by various cellular enzymes in the mitochondria, endoplasmic reticulum (ER) and peroxisomes and are needed to maintain cellular homeostasis and serve as critical components of cellular signaling (Arfin et al., 2021; Halliwell, 2007). Cellular antioxidant system plays an important role in maintaining a balance between the production and scavenging of ROS thereby protecting the cell against damage and subsequent death (Dandekar et al., 2015; Pizzino et al., 2017). Oxidative stress is a condition in which the generation and scavenging of the ROS is impaired and the balance shifts more towards the generation (Sies, 2015; Zhang et al., 2019). Studies done in flaviviruses have demonstrated that viruses such as DENV, JEV, and HCV. induce glucose uptake, increase expression of key glycolytic and PPP enzymes, enhance lipid biosynthesis as well as induce unfolded protein response (UPR) and oxidative stress in infected cells (Fontaine et al., 2015; Zhang et al., 2019). The oxidative stress induced by

the infection of flaviviruses has been implicated in the virus-induced pathogenesis (Valadao et al., 2016).

DENV infection has been shown to alter intracellular GSH levels, induce oxidative stress and cell death in infected cells (Seet et al., 2009; Tian et al., 2010; Wang et al., 2013). Recent studies have revealed that in DENV-infected cells, the viral NS2B3 complex interacts physically with and induces degradation of Nrf2 in a proteolysis-independent manner, likely through lysosomal degradation/autophagy (Ferrari et al., 2020; Zevini et al., 2020). Degradation of Nrf2 leads to suppression of antioxidant response genes resulting in ROS-associated inflammatory responses and cell death (Ferrari et al., 2020; Zevini et al., 2020). Glutathione (GSH) is key player in the antioxidant defense system of a cell and Nrf2 is known to control the critical components of the GSH antioxidant system (Tonelli et al., 2018). The regulation of GSH levels by Nrf2 in a cell is directly controlled by the expression of the glutamate-cysteine ligase (GCL) complex that consists of two subunits: the catalytic subunit (GCLC) and the modifier subunit (GCLM) (Moinova and Mulcahy, 1999; Wild et al., 1999).

In addition to regulating the levels of GSH, Nrf2 also regulates the expression of enzymes that are key to the conversion of nicotinamide adenine dinucleotide phosphate (NADP) to its reduced form NADPH, thereby playing an essential role in maintaining cellular redox homeostasis (Gorrini et al., 2013; Tonelli et al., 2018). NADPH is central to providing reducing power for the majority of ROS-detoxifying enzymes (Fernandez-Marcos and Nobrega-Pereira, 2016). Nrf2 induces the production of NADPH by positively regulating principal NADPH-generating enzymes glucose-6-phosphate dehydrogenase (G6PD), and 6-phosphogluconatedehydrogenase (6PGD), key enzymes

involved in the oxidative branch of the pentose phosphate pathway (PPP) as well as other enzymes like malic enzyme 1 (ME1) and isocitrate dehydrogenase 1 (IDH1) (DeBlasi and DeNicola, 2020; Lee et al., 2003; Mitsuishi et al., 2012; Wu et al., 2011). The PPP branches out from the glycolysis pathway and serves two major functions: i) generation of ribose-5-phosphate from glucose-6-phosphate for the synthesis of nucleotides and ii) generation of NADPH that is used by the cellular oxidative defense mechanism (Patra and Hay, 2014). Both of the above mentioned processes are carried out by the oxidative part of PPP (Patra and Hay, 2014). Under oxidative stress condition, the non-oxidative part of PPP utilizes transketolase and transaldolase enzymes to convert ribose-5-phosphate into glucose-6-phosphate that can feed into the oxidative part of PPP to generate more NADPH while also being shunted into glycolysis (Patra and Hay, 2014).

1.11 Modulation of cellular metabolism by virus infection

Virus infection modulates and reprograms cellular metabolism to aid in replication and optimal viral progeny production (Thaker et al., 2019a). Metabolic changes in virus infected cells closely resemble cancer cells and are characterized by increased glycolytic metabolism and anabolic processes to enhance synthesis of macromolecules such as nucleotides and lipids (Delgado et al., 2012; Pavlova and Thompson, 2016; Thaker et al., 2019a). Several metabolic profiling studies show that infection of host cells with viruses such as adenovirus, human cytomegalovirus (hCMV) and influenza A virus lead to a significant increase in the rate of glycolysis of the host cells (Thaker et al., 2019a). Furthermore, the infection of cells with adenovirus leads to increased glutaminolysis, the process in which glutamine is metabolized to glutamate and

aspartate resulting in the production of pyruvate, lactate, and citrate (Thai et al., 2015). Infection with hCMV has also been reported to increase the translocation of glucose transporter, GLUT 4, to the cell surface and increase glucose uptake by the infected cells (Yu et al., 2011). Infection with prototypic flaviviruses like DENV and ZIKV have also been shown to enhance glycolysis and fatty acid biosynthesis in infected cells (Fontaine et al., 2015; Thaker et al., 2019b)

1.12 Overall hypothesis and objectives

Determining the effect of ZIKV infection on critical host cell signaling pathways like the mTOR cascade is essential to achieve a holistic understanding of the molecular basis of ZIKV induced pathogenesis. Additionally, a detailed understanding of ZIKV induced modulations of host cell pathways can aid in the development of antiviral strategies that target the host cell. The association of ZIKV infection with increased incidence of microcephaly in neonates together with the findings that both inhibition and hyperactivation of the mTOR signaling cascade can lead to defective brain development and death of neural progenitor cells led me to ***hypothesize that ZIKV infection and pathogenesis involves the dysregulation of the mTOR signaling pathway***. Host metabolic adaptations are required for viral replication. We ***hypothesize that ZIKV virus infection hijacks the host cell metabolic machinery for optimal virus propagation, and this might lead to increased rate of glucose metabolism and oxidative stress.*** These hypotheses formed the basis to investigate the role of cellular processes such as the mTOR signaling pathway, cell metabolism and antioxidant response in ZIKV replication. The following objectives were addressed in this dissertation:

1.12.1 Do mTOR signaling cascade and autophagy regulate ZIKV infection?

The experimental approach and the results of the studies in this objective are described in chapter 3.

1.12.2 How does host antioxidant defense regulate ZIKV replication?

The experimental approach and the results of the studies in this objective are described in chapter 4.

1.12.3 Does ZIKV infection depend on cellular glycolysis and gluconeogenesis?

The experimental approach and the results of the studies in this objective are described in chapter 5.

CHAPTER 2: MATERIALS AND METHODS

2.1 Cell culture

The Lund Human Mesencephalic (LUHMES) cells (ATCC CRL-2927), a subclone of tetracycline-controlled, v-myc-overexpressing human mesencephalic-derived cell line, MESC2.10 (Scholz *et al,* 2011), obtained from the American Type Culture Collection Biosource Center, were cultured as described previously (Scholz *et al.*, 2011). Briefly, cell culture flasks and dishes were pre-coated overnight with 50 µg/ml poly-L-ornithine (Sigma-Aldrich, Cat. # P2533-10G) followed by washing with sterile distilled water. Subsequently, they were coated with 1 µg/ml fibronectin (BD Biosciences, Cat. # 354008), washed with sterile water, air-dried, and stored at 4º C before use. The cells were cultured in Dulbecco's Modified Eagle's Medium/F12 (DMEM/F12, Hyclone, Cat. # SH30023.02), supplemented with Neuroplex N-2 (Gemini, Cat. # 400-163), 2 mM L-glutamine (Hyclone, Cat. # SH3003401) and 40 ng/ml recombinant basic fibroblast growth factor, (Peprotech, Cat. #100-18C). A172 cells (Glioblastoma, *Homo sapiens*, ATCC CRL-1620) were grown in DMEM supplemented with 10% heat inactivated fetal bovine serum (FBS) and 1x antibiotics solution (100 U/ml penicillin, 20 U/ml streptomycin, PS). The human neuroblastoma SK-N-SH (Neuroblastoma, *Homo sapiens*) cells stably expressing EGFP-LC3 (Garcia-Garcia *et al*, 2013) were grown in DMEM containing 10% FBS and PS. Vero E6 (Epithelial, *Cercopithecus aethiops*, ATCC CRL-1586) cells were grown in DMEM supplemented with 10% FBS and PS. All cells were maintained at 37°C, 5% CO_2 atmosphere in a humidified incubator.

2.2 Preparation and concentration of recombinant ZIKV (rMR) stock

Stocks of the infectious clone-derived MR766 ZIKV (rMR) were prepared in Vero cells as described previously (Annamalai *et al*, 2017). Briefly, Vero cells were infected with rMR virus at a multiplicity of infection (MOI) of 0.1 plaque forming unit per cell (PFU/cell). The virus was allowed to adsorp at 37º C for 1 hr following which the inoculum was removed and virus growth medium (VGM) [DMEM containing 2%FBS, PS, 20 mM hydroxyethyl piperazine ethane sulfonic acid (HEPES), 1 mM sodium pyruvate, and non-essential amino acids] was added to the cells. The infected cells were incubated at 37º C for 4-5 days until cytopathic effect (CPE) was evident. The culture supernatant was collected and clarified at 10,000xg for 30 mins at 4º C. Following clarification, the stock virus was stored in small aliquots at -80ºC. In some experiments where higher MOI was used, high titer virus stocks were prepared by ultracentrifugation. Briefly, ~10 ml of clarified culture media containing the virus was taken in an ultracentrifuge tube and underlaid with ~2 ml of 20% sucrose in PBS. This was followed by centrifugation at 100,000xg for 4 h at 4ºC. The virus pellet was resuspended in 200 µl of PBS and stored at -80ºC.

2.3 Plaque assay

Plaque assay for virus quantification was done as described in Annamalai *et al*, 2017. Briefly, Vero E6 cells were plated in 12 well plate 24 hr prior to the assay. The required monolayer confluency was 90-100%. Ten-fold serial dilutions of virus stock or culture supernatants for titration were made in cold VGM. One hundred microliters of each dilution of the virus were plated in duplicates onto Vero E6 cell monolayers. Cells

were incubated at 37°C for 1 h with intermittent rocking every 10 min intervals to prevent the cell monolayer from drying and to ensure uniform exposure of the virus suspension to the cell monolayer. Following virus adsorption, the inoculum was removed, and the cell monolayer was washed once with phosphate buffered saline (PBS) to remove any unbound virus. A 1:1 mixture of 2% low gelling temperature (LGT) agarose dissolved in sterile distilled water and 2X VGM was added to the cells. The overlay was allowed to solidify for 15 min at room temperature and the cells were incubated for 5 days at 37°C in a humidified cell culture incubator for plaques to develop. Following incubation, the cells were fixed with fixing solution containing 10% formaldehyde in PBS for at least 60 min. The agarose plugs were removed, and the cell monolayers were stained for 30 minutes with staining solution containing 0.1% crystal violet and 30% methanol in PBS. The staining solution was removed, and the cells were washed with distilled water. The number of plaques was manually counted for each dilution and the titer of the virus in the supernatant was determined by multiplying the average number of plaques with the dilution factor and was expressed as plaque forming units per ml (PFU/ml).

2.4 Antibodies and other reagents

Anti-phosphorylated (p)-p70S6K (T389)/(p)-p85S6K (T412) (Cat. # 9234S), anti-p70S6K (Cat. # 2708S), anti-p-Akt (S473) (Cat #. 9018B), anti-Akt (Cat. # 2938P), anti-mTOR (Cat. # 2983), anti-Rictor (Cat. #2114), anti-Raptor (Cat #2280), and anti-Nrf2 (Cat #12721T) antibodies were obtained from Cell Signaling Technologies. Anti-p62 (Cat. # ab109012), anti-G6PD (Cat # ab993), and anti-6PDG (Cat. # 129199) were

obtained from Abcam. Anti-ZIKV E antibody was obtained from Genetex (Cat. # GTX1333325). Anti-flavivirus group antigen antibody was obtained from Millipore (4G2, Cat # MAB10216-I-100UG). Anti-β-actin (Cat. # A2228), goat anti-rabbit immunoglobulin (IgG)-horseradish peroxidase (HRP)-conjugated (Cat. # A6154), and goat anti-mouse IgG–HRP conjugated (Cat. # A4416) antibodies were obtained from Sigma-Aldrich. Choloroquin (CQ) (Cat. # C6628) was obtained from Sigma-Aldrich and dissolved in water. 3-Methyladenine (3-MA) was obtained from Tokyo Chemical Industry (Cat. # M2518) and was prepared fresh by dissolving in warm water (37-50^{o}C) prior to treating cells. Rapamycin was obtained from LC Laboratories (Cat. # R-5000) and dissolved in dimethyl sulfoxide (DMSO). Torin1 was obtained from Apex Bio (Cat. # A8312-5) and dissolved in ethanol. MRT68921 (Cat. # S7949) were obtained from Selleck Chemical and dissolved in water. 6-aminonicotinamide (6-AN) (Cat # AAL0669203) was obtained from Thermo Fisher Scientific and dissolved in DMSO. N-acetyl L-cysteine (NAC) (Cat # AC160280250), Ascorbic acid (Cat # AC352680050), and 2-Deoxy-D-glucose (2DG) (Cat # AC111980050) were obtained from Acros Organics and dissolved in water. Etomoxir (sodium salt) (Cat # 11969) was obtained from Caymen Chemical and dissolved in water. Buthionine sulfoximine (BSO) was obtained from Caymen Chemical (Cat # 14484) and dissolved in water. BPTES (Cat # 19284), UK5099 (UK) (Cat # 16980) and Rotenone (Cat # 13995) were obtained from Caymen Chemical and were dissolved in DMSO.

2.5 Immunofluorescence

For detection of ZIKV E protein in infected cells, cells were mock-infected or infected with ZIKV at indicated MOIs. After 24 h, cells were washed with cold 1X PBS and fixed with 1:1 mixture of methanol and acetone at -20ºC for 10 mins. The fixed cells were washed with PBS and stained with 4G2 (anti-flavivirus group) antibody (1:1000 in PBS). After incubation for 1 h on a shaking platform, excess unbound antibody was washed with PBS. The cells were stained with Alexa 488 conjugated anti-mouse IgG secondary antibody (1:1000 in PBS) for 1 h. Following washing of unbound antibody with PBS, images were acquired using a Nikon Eclipse Ts2R fluorescence microscope.

2.6 Pharmacological inhibition

For pharmacological inhibition of mTOR kinase, cells were either left untreated or were pre-treated with 250 nM torin1 or 1 µM rapamycin for 1 h prior to being mock-infected or infected with ZIKV at a MOI of 1 with or without the inhibitors and incubated in media with or without the inhibitors. Similarly, for inhibition of autophagy, cells were either left untreated or treated with 3-MA (5 mM) or MRT68921 (1 µM) for 1 h prior to infection with ZIKV with or without the inhibitors and further incubated in media with or without the inhibitors till the indicated time points. For the inhibition of autophagic flux, cells were treated with CQ (50 µM) 4 h prior to the termination of the experiment. For inhibition of *de novo* synthesis of GSH, cells were incubated with culture medium without or with BSO (500 µM) following virus adsorption, for 48 hpi. Similarly, PPP inhibition was achieved by treating cells with 6-AN following virus adsorption, for 48 hpi. For inhibition of glycolysis, following infection with ZIKV, cells were either left

untreated or were treated with 2DG (10 mM) for the indicated time points post infection. For virus yield under conditions of various drug treatments, 100 µl of culture supernatant was collected at the indicated hours post-infection (hpi) and infectious virus titers were determined by plaque assay as mentioned above.

2.7 siRNA-mediated protein depletion

For the depletion of endogenous mTOR, Rictor, Raptor, Nrf2, G6PD and 6PDG proteins in A172 cells, we used human small interfering RNA (siRNA) pools targeting mTOR (Cat. # J-003008-11 and J-003008-12), Rictor (Cat. # J-016984-05 and J-016984-06), Raptor (Cat. # J-004107-05 and J-004107-06), Nrf2 (Cat. # L-003755-00-0005), G6PD (Cat. # L-008181-02-005) or 6PDG (Cat. # L-008371-00-005) obtained from Dharmacon Inc. The siRNAs (obtained at 5 nmol amounts) were reconstituted in nuclease-free water. Cells were transfected with siRNAs at a final concentration of 80 nM for mTOR, Rictor and Raptor or 100 nM for Nrf2, G6PD and 6PDG using Lipofectamine RNAiMax (Invitrogen, Cat. # 13778030) following manufacturer's recommendation. Briefly, 80 or 100 nM siRNA and Lipofectamine RNAiMax were incubated in OptiMEM medium to facilitate RNA liposome complex formation for 15 mins at room temperature (RT). A non-targeting (NT) siRNA (Qiagen, Cat. # 1027281) at 100 nM was used as negative control. These concentrations of siRNAs were found to be nontoxic to the cells and cell viability was estimated to be over 90% during the treatment. At 24 hours post siRNA transfection (hpt), the cells were replenished with DMEM containing 2% FBS and 1X antibiotics and were incubated for further 24-48 h

prior to virus infection. The extent of protein depletion was determined by western blotting as mentioned below using corresponding antibodies.

2.8 Preparation of cell lysates, SDS-PAGE and Western blotting

For western blotting, cell monolayers were washed once with cold PBS, detached with trypsin (Gibco Cat #25200056) and collected in microcentrifuge tubes. This was followed by centrifugation at 500xg for 5 min at 4ºC. The cell pellet was resuspended in RIPA lysis buffer (25 mM Tris-HCl, pH 7.6, 150 mM NaCl, 1 % Triton X-100, 1 % sodium deoxycholate, 0.1 % SDS) supplemented with the Halt Protease and Phosphatase inhibitor cocktail (ThermoFisher, Cat. # 1861281) and incubated on ice for 5 min and frozen at -80º C for 1 hr. This was followed by thawing the cells on ice and sonicating at 10% amplitude for 5-10 secs, 3 times. The cell lysates were clarified by centrifugation at 10,000xg for 5 min and total protein quantification was done using the bicinchoninic acid (BCA) assay kit (Pierce, Cat. # 23225). Twenty five µg of total protein was separated by electrophoresis on 6 % or 8 % polyacrylamide gel containing sodium dodecylsulphate (SDS-PAGE). The separated proteins were transferred onto polyvinylidene difluoride (PVDF) membranes (ThermoFisher, Cat # 88520) using a Bio-Rad semi-dry transfer system. Non-specific protein binding was blocked with 5% non-fat milk or with bovine serum albumin (for phosphorylated proteins) in Tris-buffered saline containing 0.2 % tween-20 (TBS-T) for 1 hr followed by incubation with the appropriate primary antibodies (dilution: 1:5000 for β-actin and 1:1000 for all others) at 4°C overnight. Membranes were washed three times with TBS-T and followed by incubation with goat anti-rabbit or goat anti-mouse HRP-conjugated secondary antibodies (dilution: 1:5000) at

room temperature (RT) for 2 h. The blots were washed three times with TBS-T and bands were detected using ECL western blotting substrate (Pierce, Cat. # 32106) in a BioRad imager. Protein bands were analyzed by ImageJ software (NIH).

2.9 Fluorescence activated cell sorting

A172 cells were seeded in 12-well plates at a density of 20,000 cells per well. They were left untreated or treated with pharmacological inhibitors, mock-infected or infected with ZIKV and incubated for 96 hrs. Culture media were collected and the cell monolayers were washed with PBS, detached with trypsin, resuspended with collected medium, and pelleted at 500xg for 10 mins. The cell pellet was re-suspended in staining solution containing propidium iodide (PI, 1 µg/ml, Sigma/Aldrich, Cat # P4170) for detecting loss of plasma membrane integrity and, monochlorobimane (mBCl, 10 µM, Molecular Probes, Cat # M1381MP) in PBS to determine intracellular glutathione (GSH) content and incubated at room temperature (RT) until analysis. Cell viability was determined by flow cytometry (Fluorescence Activated Cell Sorting, FACS) using Cytek-DxP-10 (BD Biosciences). PI was detected using BluYel FL-3 (488 nm excitation, 695/40 nm emission) and mBCl was detected using VioFL1 (389 nm excitation and 483 nm emission) channels. At least 10,000 events were recorded per sample. Viable cells were gated as mBCl positive (+) and PI negative (–). The data analysis was done in FlowJo 7.6.5 software.

2.10 Confocal microscopy

SK-N-SH cells stably expressing EGFP-LC3 (Garcia-Garcia *et al.*, 2013) were seeded in 35mm glass bottom cell culture dishes at a density of 200,000 cells per dish. After 24 hrs of seeding, the cells were mock-infected or infected with ZIKV at an MOI of 1 and incubated for 48 hrs. Four hours prior to the termination of the experiment, the cells were exposed to CQ (50 μM). To visualize lysosomes, cells were incubated with 1 μM LysoTracker Red DND-99 (Invitrogen, Cat. # L7528) for 10 min, the monolayer was washed once with PBS and immediately imaged as described (Garcia-Garcia *et al.*, 2013). Fluorescent imaging was done at the microscopy core facility of University of Nebraska-Lincoln using a Nikon A1R-Ti2 confocal system. Images were acquired using NIS-Elements software (Nikon). EGFP-LC3 puncta in cells were counted from three representative fields of images and were analyzed statistically.

2.11 Statistical analysis

Experimental replicas were independent and performed on separate days. The data were analyzed by using one-way or two-way ANOVA, and the appropriate post-hoc test using Graphpad Prism package. When ANOVA assumptions were not met (normality [Shapiro–Wilk test] or equal variance [Kruskal-Wallis]), one-way ANOVA on Ranks or data transformation (two-way ANOVA) were performed on the data collected. Data were plotted as mean ± standard error of mean (SEM) using the same package for statistical analysis.

CHAPTER 3: mTOR SIGNALING ACTIVATION ANTAGONIZES AUTOPHAGY TO FACILITATE ZIKA VIRUS REPLICATION

Part of the studies described in this chapter was published in the Journal of Virology, 2020. **Bikash R. Sahoo,** Aryamav Pattnaik, Arun S. Annamalai, Rodrigo Franco, Asit K. Pattnaik 2020. Mechanistic Target of Rapamycin Signaling Activation Antagonizes Autophagy to Facilitate Zika Virus Replication. **Journal of Virology, 94: e01575-20. doi:10.1128/JVI.01575-20.**

3.1. Abstract

ZIKV is a flavivirus and is transmitted by mosquitoes of the *Aedes* species. While most infections do not produce any clinical symptoms, the recent outbreak in Brazil has been linked to microcephaly and other neurological defects in neonates and Guillain-Barré syndrome in adults. The molecular mechanisms regulating ZIKV infection, and the pathogenic outcomes associated with it are not completely understood. Signaling by the mechanistic (mammalian) target of rapamycin (mTOR) kinase is important for cell survival and proliferation. Several previous studies across multiple virus families have demonstrated that virus infections hijack this critical cellular signaling cascade for their replication. In this study, we show that in human neuronal precursor cells and glial cells in culture, ZIKV infection activates both mTOR complex 1 (mTORC1) and mTORC2. When mTOR kinase was inhibited either by Torin1 or rapamycin, significant reduction in ZIKV protein expression and progeny production was observed. Depletion of the defining subunit of mTORC1, Raptor, in glial cells by small interfering RNA (siRNA) resulted in inhibition of ZIKV protein expression and viral replication. The depletion of Rictor, the unique subunit of mTORC2, or the mTOR kinase in the cells also inhibited the viral processes, albeit to a lesser extent. ZIKV infection in glial cells was seen to transiently induce autophagy at early time point post-infection. It was seen that when autophagosome elongation is impaired by the class III phosphatidylinositol 3-kinase (PI3K) inhibitor 3-methyladenine (3-MA), viral protein accumulation and progeny production was enhanced. Furthermore, the phosphorylation at S757 and the resulting inactivation of ULK1 by mTOR at later stages of ZIKV infection suggests a link between autophagy inhibition and mTOR activation by ZIKV. Accordingly, inhibition of ULK1

(by MRT68921) or autophagy (by 3-MA) reversed the effects of mTOR inhibition, leading to increased levels of ZIKV protein expression and viral progeny production. These results demonstrate that ZIKV replication requires the activation of both mTORC1 and mTORC2, which negatively regulates autophagy and facilitates the viral replication. Additionally, these findings provide a potential mechanism of the neurological diseases induced by ZIKV infection.

3.2. Introduction

Recent studies suggest that ZIKV infection leads to defective neuronal cell development and death of neuronal precursor cells and that such events might lead to the development of neurological complications (Faizan et al., 2016). The mTOR signaling cascade is a key pathway that regulates cellular growth, proliferation, and survival (Saxton and Sabatini, 2017b). mTOR is a serine/threonine kinase that belongs to the phosphatidylinositol 3-kinase (PI3K)-related protein kinase family and constitutes the catalytic subunit of two functionally distinct complexes, mTOR complex 1 (mTORC1) and mTORC2 (Saxton and Sabatini, 2017b). The regulatory associated protein of mTOR (Raptor) and the rapamycin-insensitive companion of mTOR (Rictor) are essential and distinguishing subunits of mTORC1 and mTORC2, respectively (Saxton and Sabatini, 2017b) and act as scaffold proteins to help assemble and stabilize the respective complexes (Yang et al., 2013). Phosphorylation and subsequent activation of downstream effectors of mTORC1, such as the p70 ribosomal S6 kinase 1 (p70S6K), the eukaryotic initiation factor 4E (eIF4E)-binding protein 1 (4EBP1), and Unc-51-like autophagy activating kinase 1 (ULK1), regulate cap-dependent mRNA translation, metabolism, and

protein/ organelle quality control mechanisms (Saxton and Sabatini, 2017b). mTORC2 is reported to phosphorylate several proteins of the AGC family of kinases, such as protein kinase C (PKC), protein kinase B (PKB/Akt), and the serum and glucocorticoid induced kinases (SGK) and this regulates various aspects of cytoskeletal structure modeling and cellular survival (Saxton and Sabatini, 2017b).

mTOR signaling is one of the critical pathways that is essential for proper brain development and is also known to regulate autophagy (Ganley et al., 2009). Virus infection is known to alter the mTOR complex activity (Buchkovich et al., 2008; Jan et al., 2016; Le Sage et al., 2016). While poxviruses disrupt mTORCs' regulatory cascade (Meade et al., 2018), adenoviruses are known to activate mTORC1 (de Groot et al., 1995; O'Shea et al., 2005). The NS1 protein of influenza A virus activates mTOR signaling network by phosphorylating and activating Akt, a key protein in the mTOR signaling pathway, and by inhibiting REDD1 (regulated in development and DNA damage responses 1), a key inhibitor of mTORC1 (Kuss-Duerkop et al., 2017). Flaviviruses such as west Nile virus (WNV) and dengue virus (DENV) have been reported to activate PI3K/Akt and mTORC signaling (Lee et al., 2005; Shives et al., 2014) that results in increased viral protein expression and replication (Shives et al., 2014). The NS4A and NS4B proteins of ZIKV have been shown to inhibit Akt-mTOR signaling in human fetal neuronal stem cells (Liang et al., 2016).

Autophagy is a cellular homeostatic process involving the formation of autophagosomes, which engulf protein aggregates, damaged cell organelles, and intracellular pathogens marked for degradation (Deretic et al., 2013) and is known to play a major role in eliciting a host response against virus infections (Lee and Iwasaki, 2008).

Pathogens like herpes simplex virus 1 (HSV-1) (Poppers et al., 2000)(29), human immunodeficiency virus (HIV) (Brand et al., 1997), and influenza virus (Lu et al., 1995) are known to inhibit the activation of autophagy to enhance virus replication. While induction of autophagy facilitates DENV replication (Chu et al., 2014), it restricts WNV replication and protein synthesis and acts as an antiviral response of the host cell (Kobayashi et al., 2014). In contrast, ZIKV infection has been shown to induce autophagy human fetal neural stem cells and this inhibits neurogenesis (Liang et al., 2016). Since mTOR and autophagy are key signaling cascades that regulate many cellular processes, exploring how ZIKV perturbs these pathways is important to gain better insights into the processes of ZIKV infection, and pathogenesis.

In this chapter, we demonstrate that ZIKV infection results in the activation of both mTORC1 and mTORC2 in neuronal and glial cells. Inhibition of mTOR kinase reduces ZIKV protein expression and progeny virus production. Additionally, these studies reveal that ZIKV infection induces autophagy at early stages of infection but that later in infection, autophagy is subdued by the concerted activation of both mTORC1 and mTORC2 that leads to viral protein accumulation in the infected cells and virus growth. These results demonstrate that activation of mTOR signaling, and the subsequent suppression of autophagy are events that are required for ZIKV growth *in vitro* and provide a framework for further research on the role of these two cellular pathways for understanding of the mechanism(s) underlying ZIKV induced pathogenesis.

3.3. Results

3.3.1. ZIKV infection activates mTORC1 and mTORC2 in neuronal and glial cells

in culture.

Virus infections are known to modulate mTOR signaling (Buchkovich et al., 2008; Jan et al., 2016; Le Sage et al., 2016). In order to investigate the effect of ZIKV infection on mTOR signaling in neuronal cells, we used neuronal progenitor LUHMES cells (Scholz et al., 2011) and examined the status of mTORC1 activation in these cells infected with ZIKV by determining the levels of phosphorylation (p) of eukaryotic translation initiation factor 4E binding protein (4E-BP1), a downstream substrate of mTORC1 (Saxton and Sabatini, 2017b). 4E-BP1 is phosphorylated at multiple sites resulting in its inhibition and dissociation from eIF4E which leads to cap-dependent protein translation in cells (Gingras et al., 1999; Gingras et al., 1998). Using an antibody that detects the phosphorylation of 4E-BP1 at residues Thr37 and Thr46 (residues phosphorylated by mTORC1), we observed that upon ZIKV infection, there was an increase in the levels of phosphorylated protein with time, clearly indicating the activation of mTORC1 (Fig. 3.1A). Additionally, we also sought to determine the levels of p-p70S6K, another downstream substrate of mTORC1 (Saxton and Sabatini, 2017b; Yang et al., 2013). Western blot analysis showed that the levels of p-p70S6K at threonine 389 (T389) increased following ZIKV infection (Fig. 3.1B). In the LUHMES cells, the phospho-specific antibody used also detected a second phosphorylated isoform of the protein, p-p85S6K (T412), which is derived from the same gene and contains 23 extra amino acids at the amino terminus (Pullen and Thomas, 1997). The increase in phosphorylation of both the downstream substrates of mTORC1 was evident at 12 to 24 h post-infection (hpi) and continued to increase until 48 hpi compared to the mock-infected

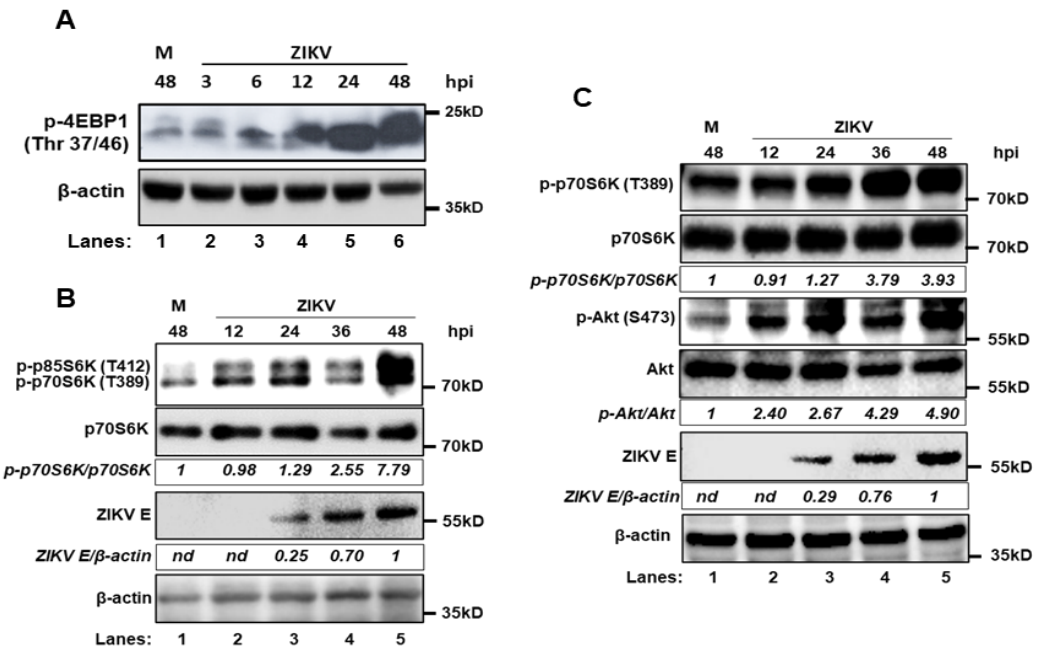

Figure 3.1: ZIKV infection activates both mTORC1 and mTORC2 in neuronal and glial cells in culture. LUHMES cells were either mock-infected (M) or infected with ZIKV at an MOI of 1 and cells lysates were prepared at the indicated hours post-infection (hpi). The lysates were subjected to Western blot analysis to detect **A** p-4E-BP1 and β-actin, **B** p-p70S6K (T389), total p70S6K, ZIKV E protein, and β-actin using the corresponding antibodies. The phospho-specific antibody against p70S6K also detected a slower migrating p-p85S6K (T412) band (1B; top panel). **C** A172 cells were mock-infected (M) or infected with ZIKV at an MOI of 1 and cells lysates were prepared at the indicated hpi. The lysates were subjected to Western blot analysis to detect p-p70S6K (T389), total p70S6K, pAkt (S473), total Akt, ZIKV E protein, and β-actin using the corresponding antibodies. The ratios p-p70S6K/p70S6K, p-Akt/Akt, and ZIKV E/β-actin from these images are shown in italics. The p-p70S6K/p70S6K and p-Akt/Akt ratios in mock-infected cells and ZIKV E/β-actin ratio in ZIKV-infected culture at 48 hpi were set at 1. Relative electrophoretic mobility of molecular mass markers in kD is shown on the right. nd, not determined.

cells (Fig. 3.1A-B). Detectable levels of ZIKV envelope (E) protein were observed at 24 hpi, suggesting that viral protein expression occurred in parallel to the activation of the mTOR signaling cascade (Fig. 3.1B). To determine if mTORC1 activation by ZIKV infection occurs in a cell type-independent manner or is restricted to the neuronal precursor cells, we examined the levels of p-p70S6K (T389) in A172 (human glioblastoma) cells infected with ZIKV. Results show that the levels of p-p70S6K (T389) were higher in ZIKV-infected A172 cells (Fig. 3.1C) than in mock-infected cells, suggesting that mTORC1 activation by ZIKV infection is independent of the type of cells used.

Since mTORC1 was found to be activated by ZIKV infection, we next examined if mTORC2 was also activated by the virus infection. mTORC2 has distinct substrates and physiological effects (Saxton and Sabatini, 2017b). Activated mTORC2 phosphorylates the downstream kinase Akt/PKB at serine 473 (S473); therefore, we examined the levels of p-Akt (S473) in A172 cells infected with ZIKV. The results showed a progressive increase in the levels of p-Akt (S473) with time compared to the mock-infected cells (Fig. 3.1C), suggesting that activation of mTORC2 also occurs in ZIKV-infected cells. Thus, the results clearly show for the first time that ZIKV infection activates both mTORC1 and mTORC2 in different cell types, including neuronal and glial cells in culture, and that this effect is paralleled with ZIKV protein expression.

3.3.2. ZIKV replication is dependent on mTORC1 and mTORC2 activity.

Enhanced mTOR cascade activity has been shown to be associated with both increased and decreased viral replication (Le Sage et al., 2016). Since the previous results

suggested that ZIKV infection activates mTOR, we next investigated whether activation of mTORCs is required for ZIKV replication. To this end, we used Torin1 that is known to inhibit mTOR kinase activity, potently and selectively, by an ATP-competitive mechanism (Thoreen et al., 2009; Zask et al., 2009). To examine the effect of mTOR kinase inhibition on ZIKV replication, cells were pretreated with or without Torin1 for 1 h followed by infection with ZIKV. The cells were then incubated in the presence of Torin1 for 48 h. Western blot analysis of infected cell lysates showed that while the levels of p-p70S6K (T389) were considerably higher in ZIKV-infected cells than in mock-infected cells, the presence of Torin1 led to nearly undetectable levels of p-p70S6K (T389) in the virus-infected cells (Fig. 3.2A). Likewise, the levels of p-Akt (S473), which were higher in ZIKV-infected cells, were undetectable in the presence of Torin1 (Fig. 3.2A). Importantly, ZIKV E protein expression was greatly reduced in the presence of Torin1 (Fig. 3.2A).

Examination of infectious virus yield from the infected cell culture supernatants revealed significantly lower virus titers in cells treated with Torin1 at 48 hpi and 72 hpi than in untreated cells (Fig. 3.2B). These results clearly demonstrated that mTOR kinase activity is essential for viral protein expression and progeny production. Although the virus growth at 24 hpi and 96 hpi was less in the presence of Torin1 than in its absence, the inhibitory effect was not significant. The observed lack of significant inhibitory effect of Torin1 at these time points could be due to the fact that ZIKV growth is not substantial at 24 hpi, as has been seen previously (Annamalai et al., 2017), or to a decrease in the viability of cells at 96 hpi because of virus-induced cell death. Indeed, viability of ZIKV-infected cells was significantly reduced at 96 hpi, and the presence of Torin1 reversed

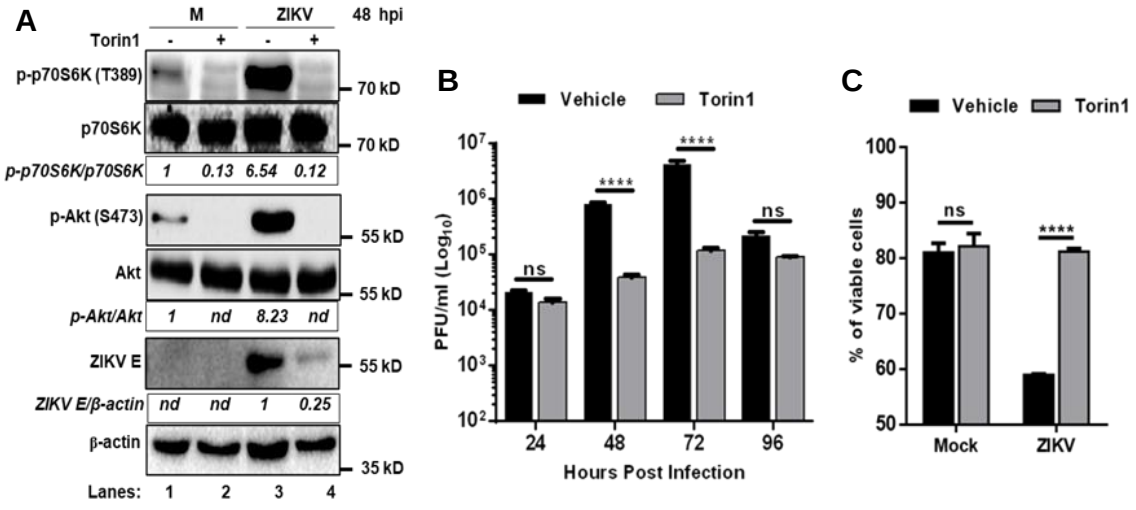

Figure 3.2: ZIKV replication requires both mTORC1 and mTORC2 activity. A A172 cells were either left untreated (-) or pre-treated (+) with torin1 for 1 h prior to being mock-infected or infected with ZIKV at an MOI of 1 in the continued presence of torin1. Cell lysates were prepared at 48 hpi and subjected to Western blot analyses to detect p-p70S6K (T389), total p70S6K, pAkt (S473), total Akt, ZIKV E protein, and β-actin using the corresponding antibodies. The ratios p-p70S6K/p70S6K, p-Akt/Akt, and ZIKV E/β-actin from these images are shown in italics. The p-p70S6K/p70S6K and p-Akt/Akt ratios in mock-infected, torin1-untreated cells and ZIKV E/β-actin ratio in ZIKV-infected, torin1-untreated culture were arbitrarily set at 1. Relative electrophoretic mobility of molecular mass markers in kD is shown on the right. nd, not determined. **B** Cell culture supernatants from untreated (vehicle) or torin1-treated and ZIKV-infected cells were collected every 24 hpi for quantitation of virus yield by plaque assay. **C** Cell viability was evaluated by flow cytometry in mock-infected (mock) and ZIKV-infected (ZIKV) cells at 96 hpi in the presence or absence (vehicle) of torin1. Error bars represent ± SEM. ns, non-significant; ****, $p \leq 0.0001$.

ZIKV-induced cell death (Fig. 3.2C). These results clearly revealed an essential role for mTOR activity in viral protein expression, infectious-progeny production, and ZIKV-induced cell death.

To determine if ZIKV replication is dependent on either mTORC1, mTORC2, or both, we used rapamycin. Rapamycin has been reported to complex with FK506-binding protein (FKBP), a nonobligate component of mTORC1. The FKBP-rapamycin complex interacts with mTOR kinase and is known to inhibit its activity (Dumont and Su, 1996; Feldman et al., 2009). A172 cells were pretreated with rapamycin for 1 h, infected with ZIKV, and subsequently incubated in the presence of rapamycin for 48 h. We observed that ZIKV-induced p-p70S6K (T389) was considerably reduced in the presence of rapamycin (Fig. 3.3A, lane 4) along with reduction in the levels of the viral E protein. While rapamycin is known to primarily inhibit mTORC1, resulting in inhibition of p70S6K (T389) phosphorylation, it can also suppress the assembly and function of mTORC2 upon extended exposure, leading to the inhibition of Akt phosphorylation at S473 as well (Sarbassov et al., 2006). Accordingly, the levels of p-Akt (S473) were also reduced in the presence rapamycin (Fig. 3.3A, lane 4), indicating that mTORC2 activity induced by ZIKV infection is also inhibited by rapamycin. Similar to what was observed in the presence of Torin1, culture supernatants showed significantly reduced virus titers from infected cell culture supernatants treated with rapamycin at 48 hpi and 72 hpi (Fig. 3.3B). Again, the reduced virus yield and observed lack of significant difference in infectious virus titers at 96 hpi was due to increased virus-induced cell death at 96 hpi, which was prevented by rapamycin (Fig. 3.3C). Overall, these results demonstrated that activation of mTOR signaling is required for ZIKV protein expression and virus growth.

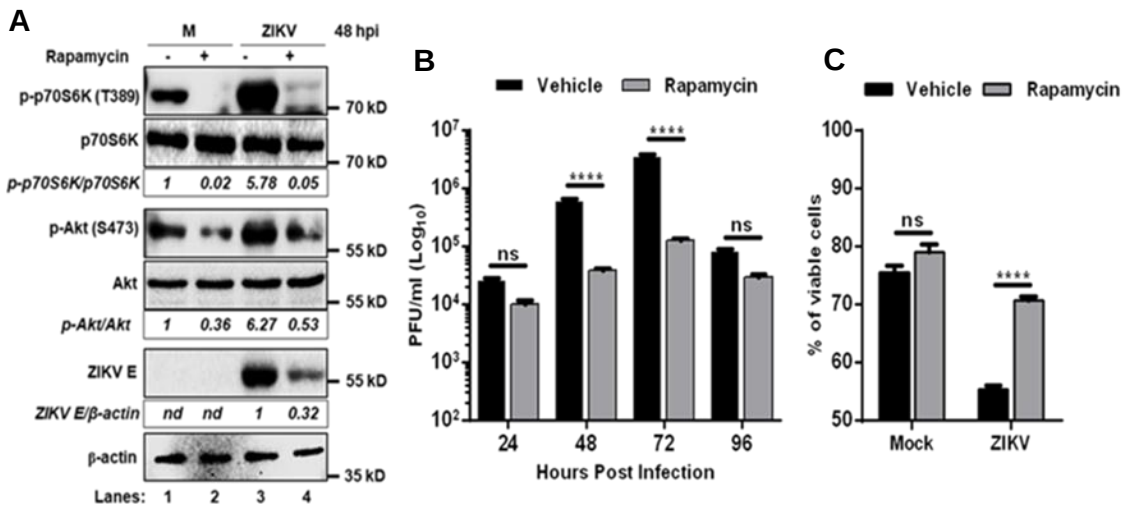

Figure 3.3: ZIKV replication requires both mTORC1 and mTORC2 activity. **A** A172 cells were either left untreated (-) or pre-treated (+) with rapamycin for 1 h prior to being mock-infected or infected with ZIKV at an MOI of 1 in the continued presence of rapamycin. Cell lysates were prepared at 48 hpi and subjected to Western blot analyses to detect p-p70S6K (T389), total p70S6K, pAkt (S473), total Akt, ZIKV E protein, and β-actin using the corresponding antibodies. The ratios p-p70S6K/p70S6K, p-Akt/Akt, and ZIKV E/β-actin from these images are shown in italics. The p-p70S6K/p70S6K and p-Akt/Akt ratios in mock-infected, rapamycin-untreated cells and ZIKV E/β-actin ratio in ZIKV-infected, rapamycin-untreated culture were arbitrarily set at 1. Relative electrophoretic mobility of molecular mass markers in kD is shown on the right. nd, not determined. **B** Cell culture supernatants from untreated (vehicle) or rapamycin-treated and ZIKV-infected cells were collected every 24 hpi for quantitation of virus yield by plaque assay. **C** Cell viability was evaluated by flow cytometry in mock-infected (mock) and ZIKV-infected (ZIKV) cells at 96 hpi in the presence or absence (vehicle) of rapamycin. Error bars represent ± SEM. ns, non-significant; ****, $p \leq 0.0001$.

However, the pharmacological inhibition of mTOR signaling was inconclusive with regard to whether activation of either mTORC1 or mTORC2 is required for virus replication.

3.3.3. Both mTORC1 and mTORC2 are required for ZIKV replication.

To unequivocally examine the role of mTOR in ZIKV replication, we conducted experiments in which critical protein components of the mTORC1, mTORC2, or both were depleted. Since the mTOR kinase is the central component of both complexes, whereas Raptor and Rictor are the unique scaffolding subunits of mTORC1 and mTORC2, respectively, we used specific small interfering RNAs (siRNAs) against the proteins to deplete the cells of these proteins and examine the effects on ZIKV E protein expression and progeny production. In cells transfected with siRNA targeting mTOR kinase, the levels of mTOR protein were greatly reduced compared to that seen with non-targeting (NT) siRNA (Fig. 3.4A, lanes 3 and 4). Similarly, when siRNAs targeting Raptor (Fig. 3.4A, lanes 7 and 8) or Rictor (lanes 5 and 6) were used, depletion of the corresponding proteins was also observed. Importantly, the reduction in these protein levels was associated with downregulation of phosphorylation of the corresponding substrates: p70S6K for mTORC1 (Raptor) (Fig. 3.4B, lanes 7 and 8) and Akt for mTORC2 (Rictor) (Fig. 3.4B, lanes 5 and 6). These results corroborate that siRNA-mediated depletion of Raptor or Rictor leads to significant downregulation of the activities of mTORC1 or mTORC2.

In cells infected with ZIKV, a dramatic reduction in the levels of E protein was observed when mTOR kinase was depleted (Fig. 3.5A, compare lane 4 with lane 2),

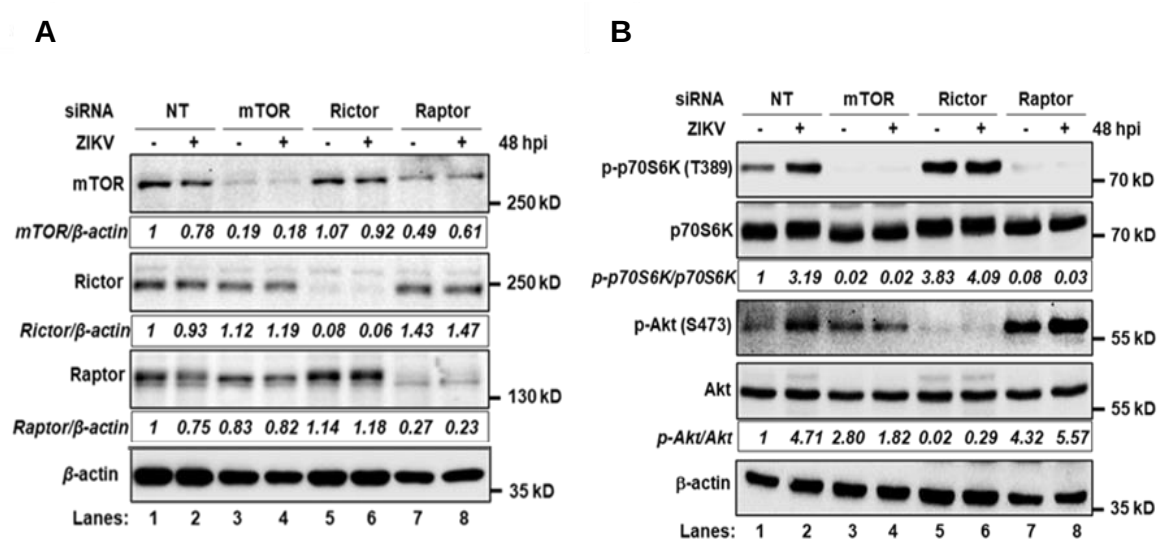

Figure 3.4: siRNA mediated depletion of mTOR complex 1 (mTORC1) and 2 (mTORC2) components. A A172 cells were transfected with either non-targeting (NT) siRNA or siRNAs targeting mTOR kinase (mTOR), Rictor or Raptor for 72 h and mock-infected (M) or infected with ZIKV for 48 h. Cell lysates were prepared and subjected to Western blot analyses to detect mTOR, Raptor, Rictor, and β-actin using the corresponding antibodies. The ratios mTOR/β-actin, Rictor/β-actin, and Raptor/β-actin, from these images are shown in italics. The ratios for mTOR/β-actin, Rictor/β-actin, and Raptor/β-actin from uninfected and NT siRNA-treated cells were set at 1. Relative electrophoretic mobility of molecular mass markers in kD is shown on the right. **B** Cell lysates from the same experiment were subjected for Western blot analysis to detect p-p70S6K (T389), total p70S6K, pAkt (S473), total Akt, and β-actin using the corresponding antibodies. The ratios p-p70S6K/p70S6K and p-Akt/Akt, from these images are shown italics.

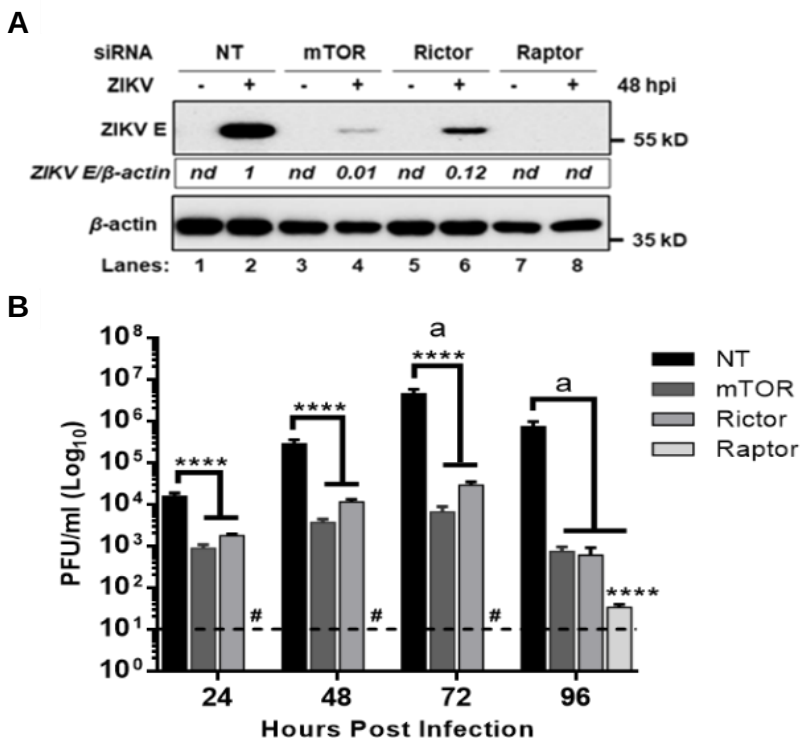

Figure 3.5: mTOR complex 1 (mTORC1) and 2 (mTORC2) regulate ZIKV replication. A A172 cells were transfected with either non-targeting (NT) siRNA or siRNAs targeting mTOR kinase (mTOR), Rictor or Raptor for 72 h and mock-infected (M) or infected with ZIKV for 48 h. Cell lysates were prepared and subjected to Western blot analyses to detect ZIKV E and β-actin using the corresponding antibodies. The ratios ZIKV E/β-actin from these images are shown in italics. The ratio for ZIKV/β-actin, from infected and NT siRNA-treated cells were set at 1. Relative electrophoretic mobility of molecular mass markers in kD is shown on the right. **B** Infectious virus production in cells depleted of mTOR, Rictor, or Raptor. The experiments were conducted as described in panel A, culture supernatants from infected cells were collected at various hpi and assayed for infectious virus yield by plaque assay. Horizontal discontinuous line represents limit of detection. #, virus titer is below the limit of detection. Error bars represent ± SEM. a, two-way ANOVA, $p \leq 0.0001$; ****, $p \leq 0.0001$.

consistent with the results in Fig. 3.2 and 3.3 obtained with the use of Torin1 and rapamycin, respectively. When Raptor (Fig. 3.5A, lane 8) or Rictor (lane 6) was depleted from the cells through the use of the corresponding siRNAs, the levels of the viral E protein in these infected cells were also dramatically reduced. These results suggest that both mTORC1 and mTORC2 are necessary for optimal levels of viral protein expression. It is interesting to note that while the depletion of Raptor led to nearly undetectable levels of E protein expression (Fig. 3.5A, lane 8), the depletion of Rictor led to detectable but significantly reduced (lane 6) levels of the viral E protein expression. These results show that the requirement for mTORC1 in viral E protein expression is more important than the requirement for mTORC2. However, the role of mTORC2 as a critical regulator of ZIKV replication cannot be ignored.

Consistent with drastic reduction in viral E protein expression, we also observed significant reduction in infectious progeny production in cells with depleted mTOR kinase, Raptor, or Rictor (Fig. 3.5B). Although depletion of mTOR kinase or Rictor led to levels of production of infectious progeny that were significantly lower than those in cells treated with NT siRNA, the effect of Raptor depletion was most dramatic in that infectious virus production was below the level of detection at 24, 48, or 72 hpi, whereas at 96 hpi, the virus titers were significantly lower than those from NT siRNA-treated cells (Fig. 3.5B). Thus, these results show that both mTORC1 and mTORC2 are required for ZIKV protein expression and infectious virus production; however, mTORC1 appears to play a more important role in these processes than mTORC2.

3.3.4. ZIKV infection induces autophagy, which suppresses the virus replication.

As mTOR signaling is known to regulate autophagy (Ganley et al., 2009), a cellular homeostatic pathway that can also function as an antiviral response to virus infection (Lee and Iwasaki, 2008), we investigated the role of autophagy in ZIKV infection. Flaviviruses, including ZIKV, infection is known to activate autophagy (Ke, 2018; Liang et al., 2016). Microtubule-associated protein 1A/1B-light chain 3 (LC3) is a soluble protein that is recruited to autophagosomal membranes and is commonly used as a marker for changes in autophagosome dynamics. Therefore, we examined the distribution of LC3 in cells infected with ZIKV at various times points post infection. Human neuroblastoma SK-N-SH cells stably expressing LC3 labeled with enhanced green fluorescent protein (EGFP-LC3) (Garcia-Garcia et al., 2013) were mock infected or infected with ZIKV (Fig. 3.6A). Following incubation for indicated lengths of time, the cells were either untreated or treated with chloroquine (CQ) 4 h prior to the termination of the experiment to avoid any unintended negative effects of CQ on ZIKV infection and block autophagosome cargo degradation (Delvecchio et al., 2016). The cells were subsequently stained with LysoTracker Red (a marker for lysosomes) and examined by fluorescence microscopy. Results showed that ZIKV infection significantly increased the accumulation of EGFP-LC3 punctum clusters at 12 and 24 hpi compared to mock infected cells in the presence or absence of CQ, an inhibitor of lysosomal cargo degradation (Fig. 3.6A-B). These results suggest that ZIKV infection increases autophagy flux at early time points of infection.

To corroborate these observations, we evaluated changes in the levels of lipidated LC3-II and the levels p62, an autophagy receptor with the ability to co-aggregate in the

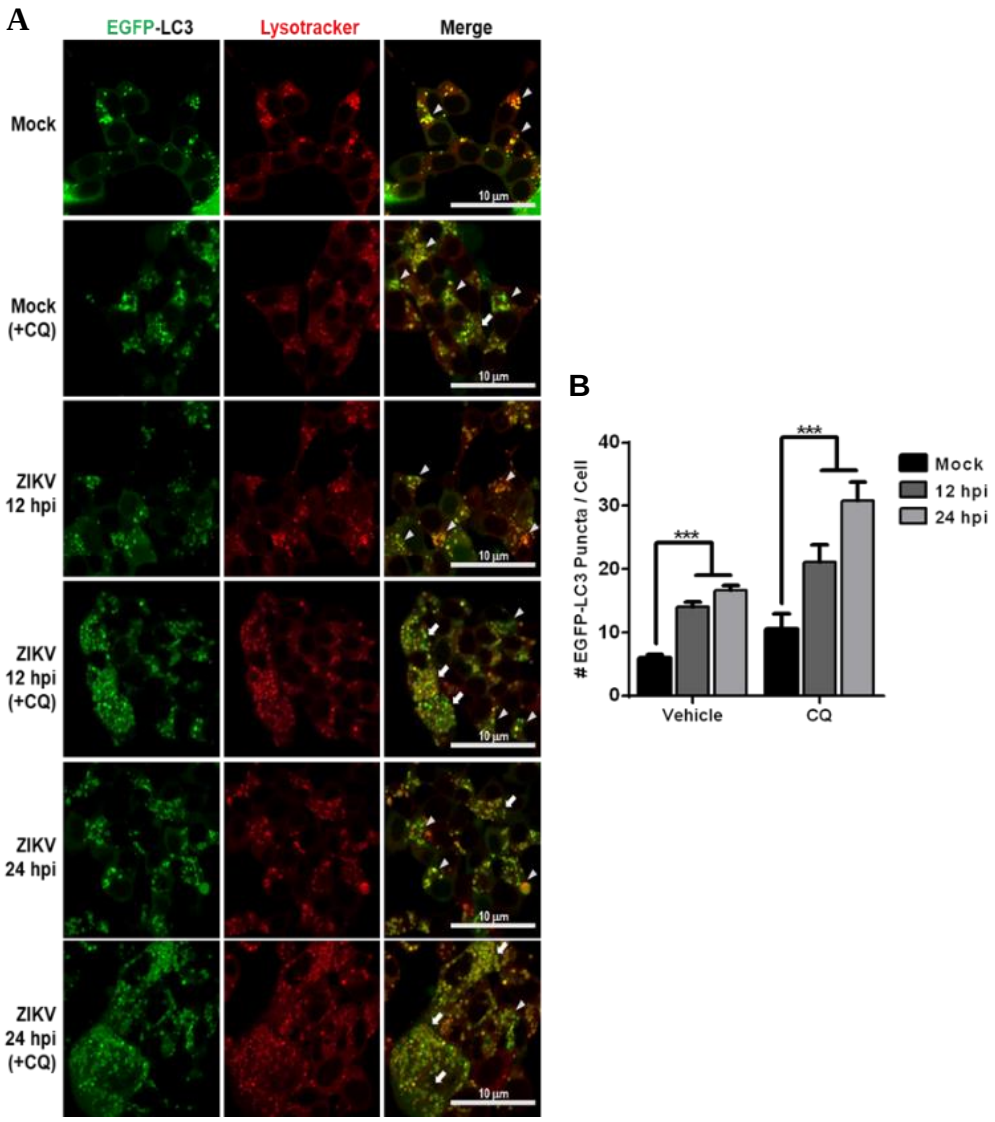

Figure 3.6: Autophagy is induced in cells infected with ZIKV. A SK-N-SH cells stably expressing EGFP-LC3 were mock-infected or infected with ZIKV at an MOI of 1. The cells were left untreated or treated with CQ for 4 h prior to the termination of the experiment followed by staining with LysoTracker Red before being examined by fluorescence microscopy. Arrowheads in merged images indicate EGFP-LC3 puncta clusters. Arrows indicate enlarged cells with higher abundance of EGFP-LC3 clusters. Scale bar: 10 µm. **B** Quantification of EGFP-LC3 puncta per cell ($n \geq 37$) from three representative fields is shown. Error bars represent ± SEM. One-Way ANOVA on Ranks; ***, $p \leq 0.001$.

presence of ubiquitinated substrates (Lamark et al., 2017). A172 cells infected with ZIKV showed an early increase in the levels of p62 monomers as well as aggregates at 12 and 24 hpi in comparison to mock infected cells (Fig. 3.7A). Interestingly, the p62 levels decreased over time, and by 48 hpi, they were comparable to those in mock-infected cells (Fig. 3.7A). The levels of p62 aggregates were also similar to that of monomeric p62 at the indicated times post ZIKV infection. Similarly, an increase in LC3-II level was observed between 12 and 24 hpi, which decreased at later time points (Fig. 3.7A). These results clearly show that ZIKV infection results in activation of autophagy at early times after infection and is suppressed as infection proceeds. In the presence of CQ, the levels of p62 and LC3-II increased slightly further in the infected cells at 12 hpi (Fig. 3.7B, lane 6) in comparison to mock-infected cells (lane 2) and tapered off at later times post infection. These results corroborate that ZIKV infection induces an increase in autophagy flux at early times (12 to 24 h) following infection. To assess the effect of autophagy induction on viral protein expression, we examined the levels of viral E protein expression in cells infected with ZIKV in the presence or absence of 3-methyladenine (3-MA), a purine analog known to block autophagosome elongation by inhibiting the class III PI3K signaling cascade (Petiot et al., 2000; Seglen and Gordon, 1982). Inhibiting autophagy by 3-MA resulted in the accumulation of p62 that was paralleled by a decrease in the levels of lipidated LC3-II in infected and mock-infected cells (Fig. 3.8A). Importantly, we observed that there was an increase in the accumulation of viral E protein in infected cells treated with 3-MA compared to cells not treated with 3-MA (Fig. 3.8A), which suggests that autophagy prompts the degradation of viral treated with 3-MA compared to untreated cells (Fig. 3.8B). Taken together, these results show that early

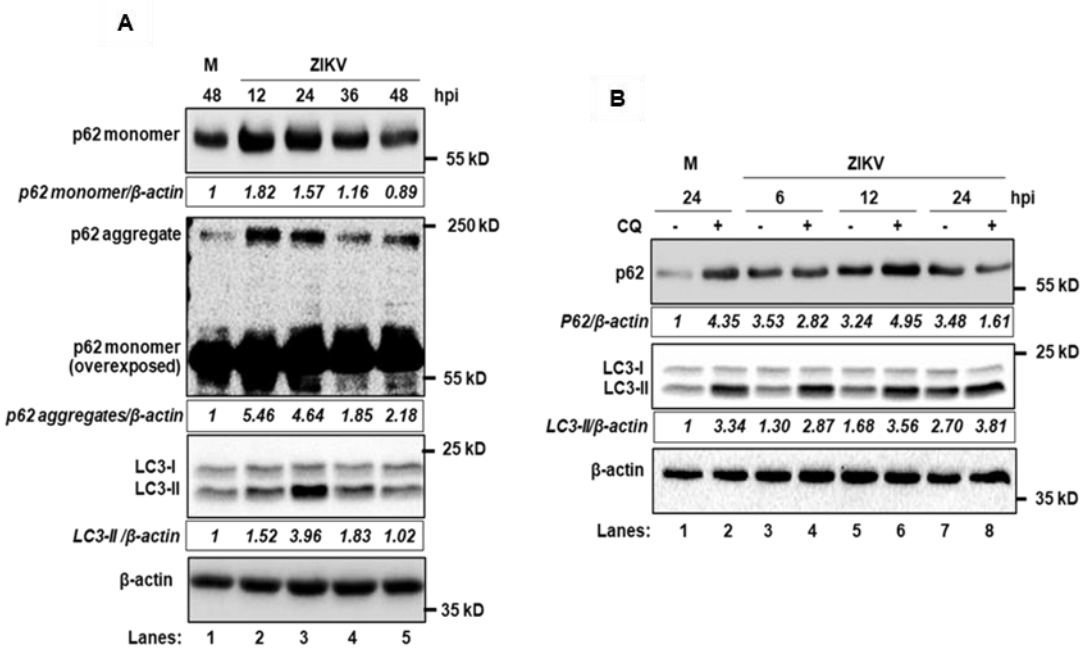

Figure 3.7: ZIKV induced autophagy. A A172 cells were either mock-infected (M) or infected with ZIKV at an MOI of 1. Cell lysates were prepared at various hpi, subjected to Western blot analysis to detect levels of p62 and LC3-II using corresponding antibodies. Monomeric p62 levels are presented on top panel. A longer exposure of the same blot showing the p62 monomer as well as the p62 aggregates towards the top of the blot is shown in the panel below that. Ratios of p62 monomer/β-actin, p62 aggregates/β-actin, and LC3-II/β-actin are shown in italics with the ratios in mock-infected culture set arbitrarily at 1. Relative electrophoretic mobility of molecular mass markers in kD is shown on the right. **B** A172 cells were either mock-infected (M) or infected with ZIKV at an MOI of 1. CQ was added 4 h prior to harvesting cell lysates at the indicated time points. Levels of p62, LC3-II, and β-actin were analyzed by Western blotting. Representative image from three independent experiments is shown. Ratios of p62/β-actin, and LC3-II/β-actin are shown in italics with the ratios in mock-infected culture set arbitrarily at 1.

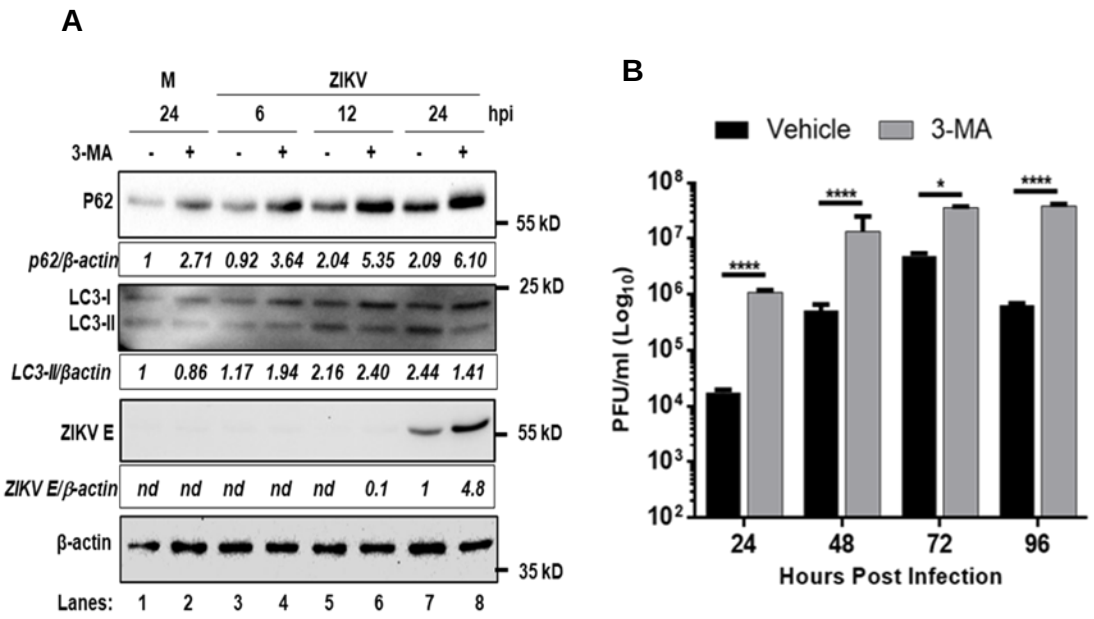

Figure 3.8: ZIKV-induced autophagy suppresses virus replication. A A172 cells were mock-infected (M) or infected with ZIKV at an MOI 1 in the presence (+) or absence (-) of 3-MA, cell lysates were prepared at the indicated time points and the levels of p62, LC3-II, viral E protein, and β-actin were examined by Western blot analysis. Ratios of p62/β-actin, LC3-II/β-actin and ZIKV E/β-actin are shown in italics with the ratios set arbitrarily at 1 as shown. **B** Infectious progeny virus titers as determined by plaque assay from ZIKV-infected cells untreated (Vehicle) or treated with 3-MA. Error bars represent ± SEM. *, $p \leq 0.05$; ****, $p \leq 0.0001$.

induction of autophagy upon ZIKV infection (12 to 24 hpi) is indeed a cellular defense mechanism that suppresses viral protein accumulation and progeny production, but at later stages in ZIKV infection (24 hpi), autophagy is suppressed to allow ZIKV protein accumulation and progeny production.

3.3.5. mTOR activation suppresses autophagy and allows ZIKV replication.

I next wanted to investigate if the role of mTOR in the regulation of viral protein expression and progeny production is linked to autophagy. mTORC1 has been shown to phosphorylate ULK1 at serine 757 (S757) to negatively regulate autophagy (Kim et al., 2011). To this end, we examined cell lysates of ZIKV-infected cells harvested at different times following infection for the expression of p-ULK1 (S757). The results showed an increase in the levels of p-ULK1 (S757) with time after the virus infection (Fig. 3.9A) that parallels the gradual decline in the levels of p62 and LC3-II (Fig. 3.7A), suggesting that ZIKV-induced phosphorylation of ULK1 suppresses autophagy. Accordingly, inhibition of mTORC1 by Torin1 ablated ULK1 phosphorylation (Fig. 3.9B) with a concomitant increase in autophagy, as evidenced by the enhanced degradation of p62 and LC3-II (Fig. 3.9B). As shown before, the level of ZIKV E protein was reduced substantially in the presence of Torin1 (Fig. 3.9B). These results suggest that during ZIKV infection, phosphorylation, and the subsequent inhibition of ULK1 by mTOR inhibit autophagy and facilitate ZIKV E protein accumulation.

Since inhibiting mTOR kinase resulted in increased autophagy with a concomitant decrease in viral E protein levels, we wanted to investigate if inhibiting autophagy with 3-MA (class III PI3K inhibitor) or MRT6891 (ULK1 inhibitor) under conditions in which

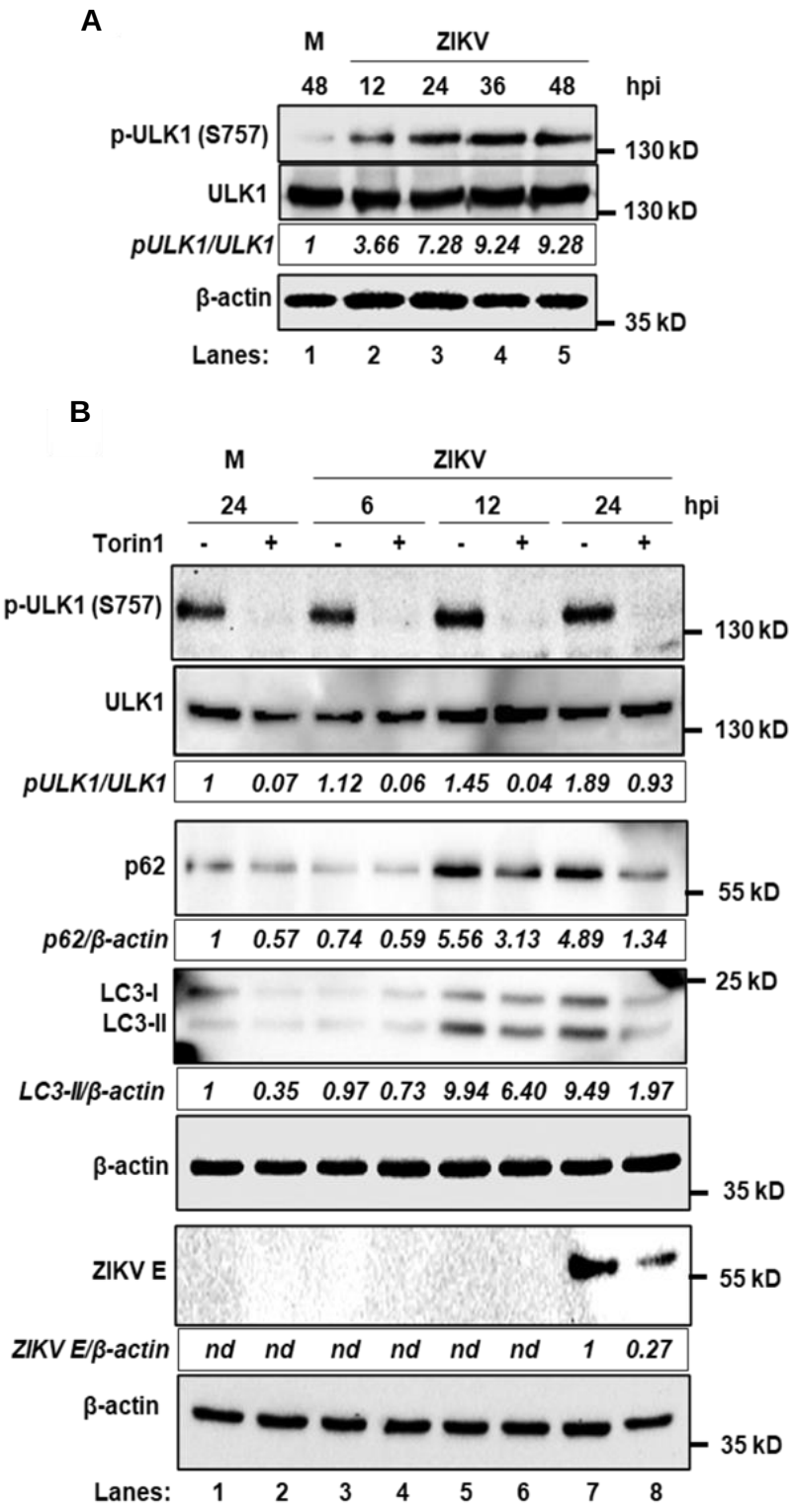
A
M
ZIKV
48
12
24
36
48
hpi
p-ULK1 (S757)
130 kD
ULK1
130 kD
pULK1/ULK1
1
3.66
7.28
9.24
9.28
β-actin
35 kD
Lanes:
1
2
3
4
5
B
M
ZIKV
24
6
12
24
hpi
Torin1
-
+
-
+
-
+
-
+
p-ULK1 (S757)
130 kD
ULK1
130 kD
pULK1/ULK1
1
0.07
1.12
0.06
1.45
0.04
1.89
0.93
p62
55 kD
p62/β-actin
1
0.57
0.74
0.59
5.56
3.13
4.89
1.34
LC3-I
LC3-II
25 kD
LC3-II/β-actin
1
0.35
0.97
0.73
9.94
6.40
9.49
1.97
β-actin
35 kD
ZIKV E
55 kD
ZIKV E/β-actin
nd
nd
nd
nd
nd
nd
1
0.27
β-actin
35 kD
Lanes:
1
2
3
4
5
6
7
8

Figure 3.9: ZIKV infection induces ULK1 phosphorylation and suppresses autophagy. A Phosphorylation of ULK1 is enhanced in ZIKV-infected cells. A172 cells were either mock-infected (M) or infected with ZIKV at an MOI of 1. Cell lysates were prepared at various hpi and subjected to Western blot analysis for p-ULK (S757), total ULK1 and β-actin. Ratio of p-ULK1/ULK1 is shown in italics with the ratio in mock-infected culture set arbitrarily at 1 **B** Inhibition of mTORC1 by torin1 leads to reduced ULK1 phosphorylation and reduced detection of the viral E protein. A172 cells treated with (+) or without (-) torin1 were mock-infected (M) or infected with ZIKV. Cell extracts were prepared at 49 hpi and the levels of p-ULK1 (S757), total ULK, p62, LC3-II, ZIKV E protein, and β-actin were examined by Western blotting. Ratios of p-ULK1/ULK1, p62/β-actin, LC3-II/β-actin and ZIKV E/β-actin are shown in italics with the ratios set arbitrarily at 1 as shown.

mTOR kinase activity has already been impaired would result in rescue of viral E protein levels and infectious-progeny production. Data from such an experiment would provide unequivocal evidence for a direct link between mTOR activation, suppression of autophagy, and viral replication. The enhanced autophagy induced by Torin1, as evidenced by the increased degradation of p62 and LC3-II, was reversed by 3-MA (Fig. 3.10A, compare lanes 3 and 4 with lanes 9 and 10) or MRT68921 (Fig. 3.10A, compare lanes 3 and 4 with lanes 11 and 12) in cells infected with ZIKV or left uninfected. However, only in cells infected with ZIKV did 3-MA and MRT68921 prevent the decrease in E protein levels induced by Torin1 (Fig. 3.10A, compare lane 4 with 10 and lane 4 with 12). Furthermore, infectious virus production, which is also inhibited significantly in the presence of Torin1, was seen to be rescued to the untreated-control levels in the presence of 3-MA or MRT68921 (Fig. 3.10B). Overall, these observations clearly show that activation of mTOR in ZIKV infected cells suppresses autophagy to allow virus protein expression and progeny production.

3.4. Discussion

Studies have demonstrated that ZIKV infection hinders growth and development of neurospheres and organoid cultures *in vitro* (Garcez et al., 2016; Garcez et al., 2017; Qian et al., 2017). It has also been demonstrated that ZIKV infection causes abnormal neurological development and fetal demise in mice (Lazear and Diamond, 2016; Li et al., 2016a; Miner et al., 2016). Yet, the molecular mechanisms of ZIKV induced pathogenesis are not entirely understood. mTOR signaling is critically involved in and

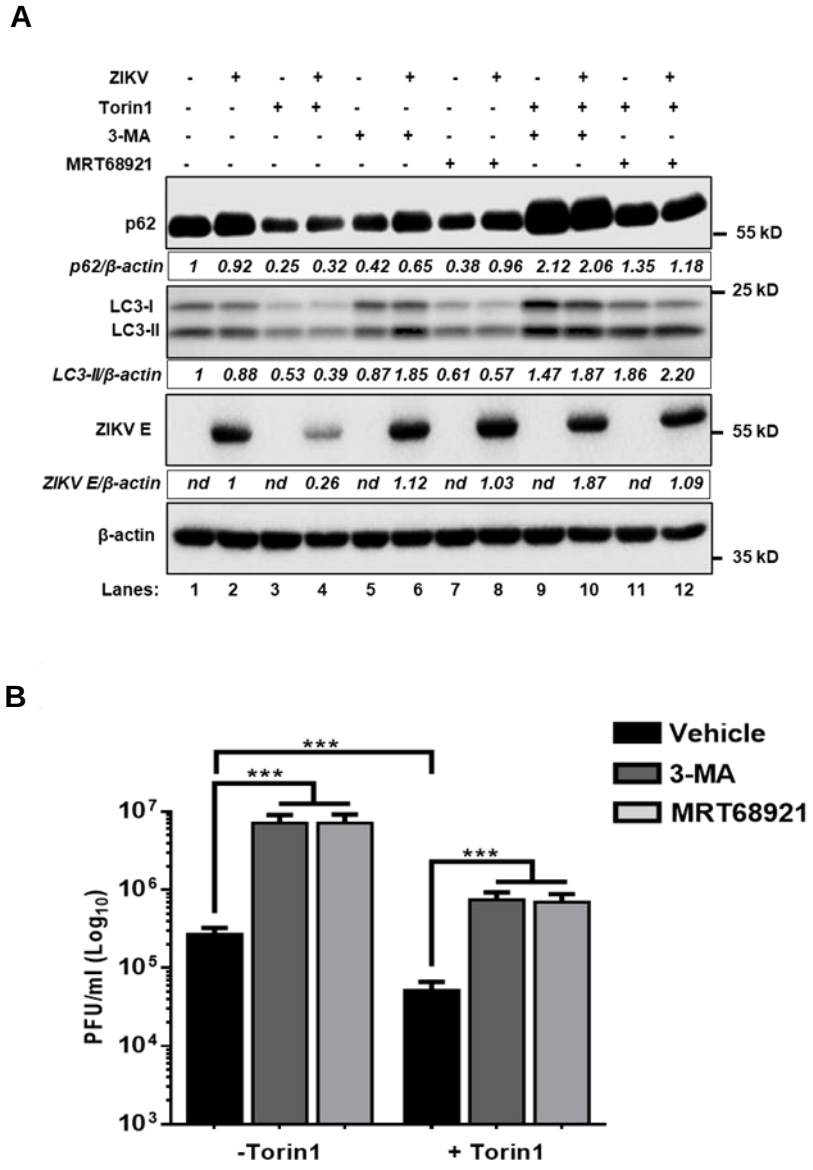

Figure 3.10: Inhibition of autophagy under condition of mTORC inhibition rescues ZIKV replication. A and B Inhibiting autophagy under condition of mTORC inhibition rescues viral E protein accumulation **A** and progeny production **B**. A172 cells were either mock-infected (-) or infected with ZIKV (+) and treated without (-) or with (+) various inhibitors as shown on top of each lane in panel A. Cell extracts were prepared at 48 hpi and analyzed by Western blotting for p62, LC3-II, ZIKV E protein, and β-actin. Ratios of

p62/β-actin, LC3-II/β-actin, and ZIKV E/β-actin are shown in italics with the ratios set arbitrarily at 1 as shown. Under similar experimental conditions, culture supernatants from the infected cells at 72 hpi were assayed for infectious progeny production **B** by plaque assay. Error bars represent ± SEM. ***, $p \leq 0.001$.

regulates many cellular processes such as growth, survival, and proliferation (Saxton and Sabatini, 2017a).

Many viruses are known to either activate or suppress mTORC signaling to facilitate viral replication (Le Sage et al., 2016). Additionally, prototypic flaviviruses such as the WNV, DENV, Japanese encephalitis virus (JEV) and hepatitis C virus (HCV) are known to activate the Akt/mTOR pathway and this activation may be proviral or an antiviral role in nature (Le Sage et al., 2016). While inhibition of mTOR activates autophagy and enhances DENV replication (Jan et al., 2016), mTORC1 supports WNV replication (Shives et al., 2014). With regard to HCV, the role of mTOR appears to be controversial in that some studies suggest a proviral role of mTOR activation (Peng et al., 2010; Stohr et al., 2016) while others advocate for an antiviral role (Johri et al., 2019; Shao et al., 2010; Shrivastava et al., 2012). Additionally, activation of mTOR and mTOR-dependent mechanisms have been implicated in the enzootic transmission cycle of some flaviviruses involving the mosquito vector (Hansen et al., 2004). Therefore, modulation of mTOR signaling appears to be integral to flavivirus transmission, replication, and pathogenesis.

Using human neuronal progenitor (LUHMES) and glioblastoma (A172) cells, we observed activation of mTORC1 following infection with ZIKV. Further studies revealed that ZIKV infection activated not only mTORC1 but also mTORC2 to facilitate viral protein expression, accumulation, and progeny virus production. These studies also revealed that early during ZIKV infection, autophagy is activated that results in the restriction of viral protein accumulation to undetectable levels but at later times, autophagy is suppressed by the inhibitory phosphorylation of ULK1 via activation of

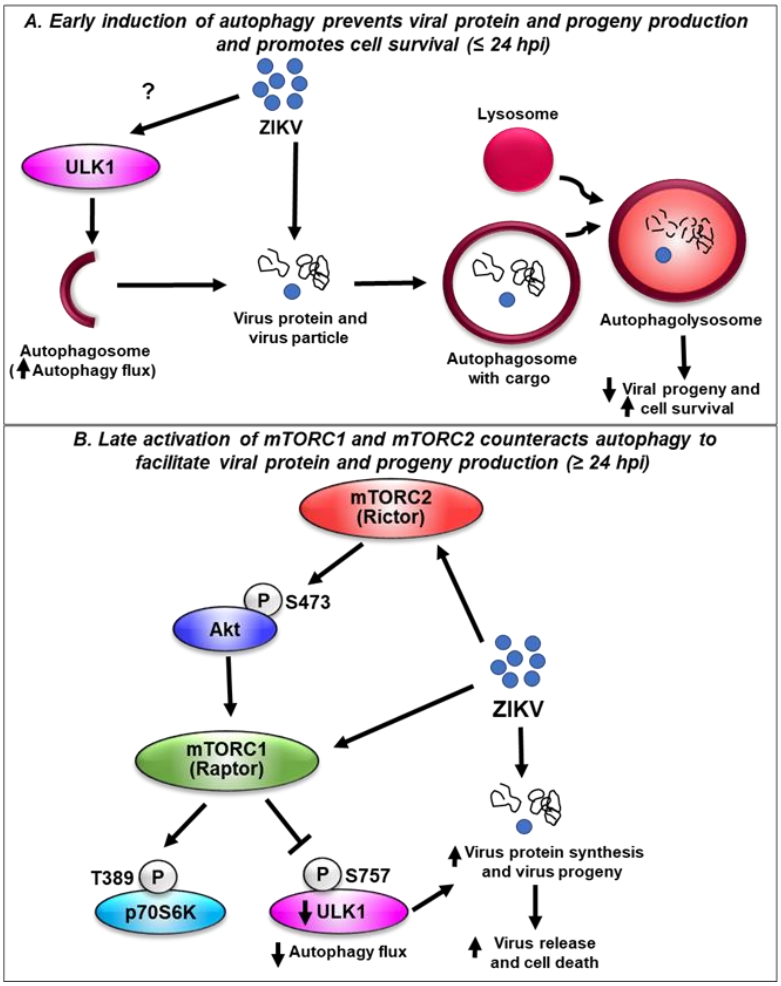

Figure 3.11: Scheme of ZIKV-induced regulation of autophagy, mTOR signaling, and effects on viral protein accumulation, progeny virus production and cell death in infected cells. (A) ZIKV infection induces an early activation of autophagy (≤ 24 hpi) that mediates the degradation of viral proteins preventing viral assembly. (B) Later stages of infection (≥ 24 hpi) activate mTORC1 and mTORC2 to mediate the phosphorylation and inhibition of ULK1, whose activity is necessary for autophagy initiation. Inhibition of autophagy facilitates accumulation of viral proteins, infectious progeny release, and cell death. The timeframe of the events delineated here is likely dependent on the cell type for infection, the exposure time and dosage of the virus.

mTORC1. This leads to increased levels of viral protein accumulation in the infected cells and enhanced viral progeny production.

ZIKV infection induces autophagy (Cao et al., 2017; Cugola et al., 2016; Hamel et al., 2015) but there are conflicting results as to the effect of autophagy on ZIKV infection. Some studies report that inhibition of autophagy reduces viral replication and limits viral transmission (Abernathy et al., 2019; Cao et al., 2017; Hamel et al., 2015). ZIKV-induced autophagy was also shown to be mediated by inhibition of the Akt-mTOR pathway by the viral NS4A and NS4B proteins, leading to defective neurogenesis (Liang et al., 2016). In contrast, other studies have reported that autophagy facilitates virus clearance in phagocytes (Huang et al., 2020) and protects cells against ZIKV infection (Karuppan et al., 2020; Liu et al., 2018). On the other hand, pharmacological and genetic inhibition of autophagy was shown to have no adverse effect on ZIKV replication in glial cells (Ojha et al., 2019).

While the conflicting findings in regard to the role of autophagy and mTOR in ZIKV infection could be attributed to the different cell types and experimental model systems that these cellular events were tested in, it could also be linked to the temporality of the events being analyzed. In addition, the experimental tools used to study mTOR signaling might be a point of discrepancy. While phosphorylation of mTOR at S2448 has been used in many studies as a marker for mTOR activation, there is clear evidence that pS2448 does not correlate with mTOR activity (Figueiredo et al., 2017). Using different cell types, we demonstrated that mTORC1 and mTORC2 are consistently activated by evaluating the phosphorylation status of their direct substrates, p70S6K, ULK1 (mTORC1) and Akt (mTORC2), which are considered as more reliable readouts of

mTOR activation (Saxton and Sabatini, 2017a). We have clearly defined that while autophagy is initiated early during the infection process, it is later on suppressed by ZIKV-induced mTOR activation. Very few studies have addressed the time-course of changes in such events and thus point to the importance of these results.

The role of the individual complexes in ZIKV protein expression and progeny production could not be ascertained using torin1 or rapamycin due to the lack of specificity of these compounds. By using siRNAs to deplete the critical components of the two complexes, we was able to firmly conclude that both mTORC1 and mTORC2 are required for efficient ZIKV replication, although a differential effect was noted in their requirements. mTORC1 appears to play a more dominant role in ZIKV replication compared to mTORC2. This is borne out from the observations that Raptor depletion led to extremely low to undetectable levels of viral protein expression and infectious progeny production (Fig. 3.5), while Rictor depletion led to significantly reduced but still detectable levels of E protein expression and progeny production.

Several studies have provided evidence for a major role for mTORC1 in virus replicative processes, but the role for mTORC2 has been less clear. Replication of WNV, HCV, influenza virus, Andes virus and herpesviruses require mTORC1 but not mTORC2 (Clippinger et al., 2011; Kuss-Duerkop et al., 2017; McNulty et al., 2013; Moorman and Shenk, 2010; Shives et al., 2014; Stohr et al., 2016). Only one previous study showed that Rictor (mTORC2) is primarily involved in HCMV replication (Kudchodkar et al., 2006). Although the NS5A protein of HCV activates mTORC2 (George et al., 2012), no experimental evidence links this activation to viral replication. Therefore, one important finding from my studies reported here is the significant involvement of mTORC2 in

replication of ZIKV. The mTORC2 may play an indirect role, likely upstream of mTORC1 activation through phosphorylation of Akt, an activator of mTORC1 (Sarbassov et al., 2005). Since a negative feedback loop between mTORC1 activation and mTORC2 has been described where p70S6K phosphorylates Rictor and decreases mTORC2 function (Efeyan and Sabatini, 2010; Julien et al., 2010), it is possible that ZIKV also overcomes this negative feedback loop to facilitate the potentiation of mTORC1 activation by mTORC2.

It is interesting to note that depletion of mTOR kinase itself resulted in still detectable levels of E protein expression and progeny production, while knockdown of Raptor exerted a more robust negative effect. Knockdown of Rictor induced a more pronounced decrease in Akt phosphorylation than mTOR downregulation (Fig. 3.4). Since mTOR kinase is central to both mTORC1 and mTORC2, our expectation was that depletion of mTOR would have the most significant negative impact on viral E protein expression and progeny production as well as on the corresponding downstream substrates compared to the Raptor or Rictor depletion. A direct comparison between the knockdown of mTOR, Rictor, and Raptor cannot be made by just comparing the changes in protein levels or the phosphorylation of the corresponding substrates as this would require that the antibodies used for detection had similar signal-to-noise ratio efficiencies. However, a possibility exists that Raptor might partially regulate ZIKV replication independent from mTOR. Indeed, a recent study reports mTOR-independent functions for Raptor (Kim et al., 2016). Similarly, Rictor has been shown to form mTOR-less complexes that mediate different processes including Akt phosphorylation (Gkountakos et al., 2018; McDonald et al., 2008). To address an mTOR-independent role of Raptor

and Rictor in ZIKV infection is an interesting area of research that requires further experimentation.

The inability to detect viral proteins in ZIKV-infected cells prior to 24 hpi was surprising given that the viral genome is a competent template for translation immediately after entry into cells. We considered the possibility that autophagy was being activated early in ZIKV infected cells resulting in inhibition of viral protein accumulation to undetectable levels. Flaviviruses are known to activate autophagy, which plays an important role in replication and/or pathogenesis (Ke, 2018). For example, the viral NS4A-induced autophagy protects DENV- and Modoc virus (a murine flavivirus)-infected cells and enhances virus replication (McLean et al., 2011) whereas ZIKV NS4A- and NS4B-induced autophagy inhibits neurogenesis (Liang et al., 2016). Autophagy is also induced in DENV- and HCV-infected cells to support viral replication (Chu et al., 2014; Dreux et al., 2009) while in a separate study, autophagy was found to play no role in WNV infection (Beatman et al., 2012).

Our results (Fig. 3.7) show that autophagy was indeed induced early (within 24 hpi) in ZIKV-infected cells and thereafter there was a gradual decline in the autophagy flux. The decline in autophagy flux was concomitant with increase in mTOR activation as seen by increased phosphorylation of ULK1. In addition to p-ULK1, mTORC1 activation has been shown to inhibit autophagy at other signaling steps, so we cannot rule out other targets that mediate the negative regulation of autophagy by ZIKV-induced mTORC1 activation (Kim and Guan, 2015). Based on the findings reported here, we propose that activation of autophagy is an early antiviral response against ZIKV infection (Fig. 3.11A) that is then suppressed by the virus-induced activation of mTORC signaling, leading to

enhanced viral protein accumulation and progeny production (Fig. 3.11B). However, it is important to recognize that the temporality of these events might change depending on the cell types or experimental model systems used and the conditions of infection including virus dose and length of infection. While inhibition of autophagy increased viral protein accumulation, it only occurred at 24 hpi, which also suggests the existence of other unexplored mechanisms by which the cell limits viral replication at early time points of infection.

The mechanisms involved in autophagy activation by ZIKV are incompletely understood. Although NS4A and NS4B proteins have been shown to induce autophagy through inhibition of mTOR signaling (Liang et al., 2016), we have observed that the induction of autophagy precedes viral protein accumulation with no evidence of inhibition of mTOR signaling. A recent report demonstrated that ZIKV induces an NF-κB-dependent autophagy pathway mediated by STING (Liu et al., 2018). Another report demonstrates that in astrocytes activation of NF-κB and autophagy by ZIKV infection seems to depend on TL3 receptors (Ojha et al., 2019). Thus, autophagy could be triggered by the induction of antiviral innate immune responses prior to viral replication. It is also possible that adenosine-monophosphate (AMP)-activated kinase (AMPK), which is activated by ZIKV (Thaker et al., 2019a) could induce autophagy. It is unknown at this time what viral factors drive activation of autophagy early in infection and mTORC signaling. However, we have observed that autophagy is not activated when UV-inactivated ZIKV is used in the experiments, suggesting that live virus infection is necessary. Which antiviral immune responses and viral structural and/or non-structural proteins are involved in the activation of autophagy and the later induction of mTOR

signaling are not known at this time and remains to be investigated. Bystander effects from infected cells could also contribute to the modulation of autophagy. Indeed, previous reports have demonstrated that the release of soluble factors including cytokines can regulate autophagy in non-infected cells (Kong et al., 2018; Van Grol et al., 2010; Wu et al., 2016).

Since hyperactive mTOR signaling is linked to exhaustion of stem cell niches and loss of mTOR activity leads to depletion of progenitor cells responsible for the normal development of the brain (Takei and Nawa, 2014), these results might also point to potential mechanism(s) of ZIKV-induced neurological deficits in developing fetal brains. Further exploration in this aspect can provide a better understanding into the molecular mechanism(s) of ZIKV induced microcephaly and other neurological deficits.

CHAPTER 4: REDOX REGULATION OF ZIKA VIRUS REPLICATION

4.1. Abstract

ZIKV is a mosquito-transmitted flavivirus and its association with microcephaly, other congenital abnormalities in the developing fetus and Guillain-Barré syndrome, neuropathy, and myelitis in adults and older children is a major concern to public health. The molecular machinery regulating ZIKV infection are still unclear. While it is well known that viral infections alter host cell redox homeostasis that can either be pro-viral or anti-viral in nature, exact mechanisms and consequences for different viruses are not clearly understood. The results show that ZIKV infection induces oxidative stress in neuronal and glial cells in culture which transiently activates the nuclear factor erythroid 2 p45-related transcription factor 2 (Nrf2) signaling cascade. We demonstrate that downregulation of Nrf2 or inhibition of *de novo* GSH synthesis was shown to increase viral protein synthesis and infectious particle production. Additionally, depletion of the enzymes, glucose 6-phosphate dehydrogenase (G6PD) and 6-phosphogluconate dehydrogenase (6PGD), critical contributors to the generation of NADPH increased viral replication. Although pharmacologic inhibition of G6PD and 6PGD by 6-amino nicotinamide (6-AN) resulted in significant inhibition of viral protein synthesis and infectious progeny production, the inhibition could not be rescued by D-ribose, indicating that pentose phosphate pathway (PPP) does not appear to play a major role in viral replication. These results highlight the importance of cellular redox homeostasis in the regulation of ZIKV replication.

4.2. Introduction

Several studies have shown that prototypic flaviviruses including HCV, DENV as well as JEV induce oxidative stress upon infection and which correlates with disease pathogenesis (Gil et al., 2004; Korenaga et al., 2005; Liao et al., 2002; Zhang et al., 2019). Upon infection, the virus hijacks host cell metabolism which triggers stress on the cell. Generally, cellular metabolism leads to the generation of reactive oxygen species (ROS) such as superoxide anion ($O2^{\bullet-}$), singlet oxygen ($^1O_2$) and hydrogen peroxide (H_2O_2) in mitochondria, ER, and peroxisomes. These ROSs at moderate levels can serve as critical cofactors in cellular signaling and are promptly neutralized by antioxidant defense system (Birben et al., 2012). But in an infected cell, the redox homeostasis is altered by virus induced metabolic changes and resulting in the induction of oxidative stress (Zhang et al., 2019).

Increased oxidative stress can have a multitude of consequences including lipid peroxidation, protein carbonyl formation, DNA damage and activates multiple stress induced transcription factors that further downregulate antioxidant response and amplify oxidant induced cellular damage (Birben et al., 2012; Cooke et al., 2003; Dalton et al., 1999). It has been shown that the induction of oxidative stress can be beneficial to viral replication in host cells. Flaviviruses are known to control 5’ RNA genome capping by inducing oxidative stress in infected cells (Gullberg et al., 2015). Dengue virus (DENV) is known to induce oxidant-triggered autophagy in infected cells leading to inhibition of apoptotic cell death and increased viral replication (Datan et al., 2016). Additionally, DENV infection has been reported to reduce cellular GSH pool, which generally downregulates ROS and maintains redox homeostasis and pharmacological inhibition of

GSH synthesis enhanced viral replication (Tian et al., 2010). HCV causes chronic hepatitis in infected patients by triggering oxidative stress and downregulating antioxidant response (Ivanov et al., 2013; Rebbani and Tsukiyama-Kohara, 2016; Vasallo and Gastaminza, 2015).

The nuclear factor erythroid 2–related transcription factor 2 (Nrf2) signaling cascade is a key player in the cellular antioxidant system (Hayes and Dinkova-Kostova, 2014). When the redox homeostasis is maintained, Nrf2 stably associates with kelch-like ECH- associated protein 1 (Keap1) and is constitutively ubiquitinated and degraded via the ubiquitin- proteasome pathway (Cullinan et al., 2004; Hayes and Dinkova-Kostova, 2014). Upon oxidative stress induction, stable association of Nrf2 and Keap1 is altered by conformational changes in Keap1 leading to its dissociation and resultant activation of Nrf2 (Cullinan et al., 2004; Hayes and Dinkova-Kostova, 2014). Subsequently, the heterodimerization of Nrf2 with small Maf (sMaf) proteins leads to nuclear translocation of Nrf2 where it induces the activation of antioxidant response elements (AREs), a cluster of genes involved in antioxidant response, cellular protection, and regulation of autophagy (Hayes and Dinkova-Kostova, 2014; Pajares et al., 2016; Pajares et al., 2018). Additionally, Nrf2 is involved in the *de novo* synthesis of GSH, an important intracellular antioxidant, by directly modulating the activity of Glutamate-Cysteine Ligase Catalytic subunit (GCLC), and reduced Nicotinamide adenine dinucleotide phosphate (NADPH), by inducing the activity of the enzymes G6PD and 6PGD (Hayes and Dinkova-Kostova, 2014).

Although few studies have implicated the induction of oxidative stress in ZIKV infected cells, a detailed understanding of the molecular mechanisms involved therein is

poorly understood. In this study, we demonstrate that ZIKV infection of neuronal and glial cells in culture results in the induction of oxidative stress that triggers transient activation of Nrf2 signaling cascade. The activation of Nrf2 is found to be antagonistic to ZIKV replication since its depletion promotes ZIKV protein synthesis and infectious virion production. Furthermore, transient activation of Nrf2 in ZIKV infected cells leads to the activation of its downstream effectors, GCLC and G6PD which are known to be involved in the synthesis of glutathione (GSH) and generation of NADPH, critical contributors to the cell's antioxidant system. Both, inhibition of *de novo* GSH synthesis by BSO or depletion of NADPH generating enzymes, G6PD or 6PGD, resulted in enhanced ZIKV replication. These results highlight the antiviral role played cellular antioxidant response in ZIKV infection.

4.3. Results

4.3.1. ZIKV infection induces oxidative stress in neuronal and glial cells in culture

ZIKV has been reported to have a wide cellular tropism (Lazear and Diamomd, JVI review in 2016?) and is known to infect cells of neuronal origin. Using the neuronal progenitor LUHMES cells, we first sought to determine the susceptibility of these cells to ZIKV infection as it had not been reported previously. Immunofluorescence imaging for ZIKV E protein shows that LUHMES are permissive to infection by ZIKV, and this is dependent on the multiplicity of infection (MOI) (Fig. 4.1A). Western blot analysis revealed that the expression of ZIKV E protein in LUHMES cells was also MOI-dependent (Fig. 4.1B).

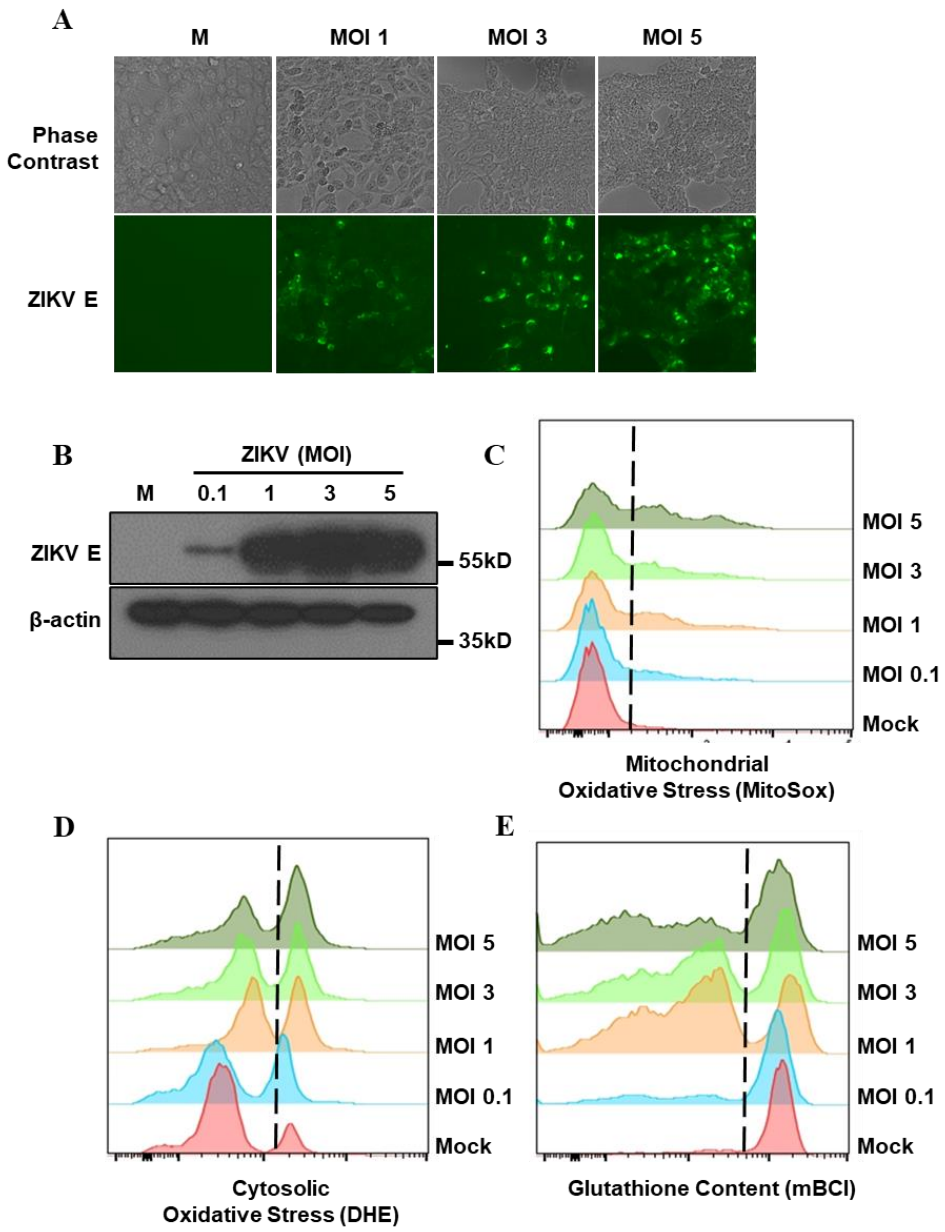

Figure 4.1: ZIKV infection induces oxidative stress in LUHMES cells. A Cells were either mock-infected (M) or infected with ZIKV at the indicated MOI and at 24 hpi, the cells were fixed and stained with anti-flavivirus E antibody followed by Alexa 488 conjugated secondary antibody. Fluorescence images show cells infected with ZIKV (green) at indicated MOIs. **B** Cells were either mock-infected (M) or infected with ZIKV at the indicated MOI and at 24 hpi, lysates were prepared and subjected to Western blot

analysis to detect ZIKV E protein and β-actin using the corresponding antibodies. Relative electrophoretic mobility of molecular mass markers in kilo Daltons (kD) is shown on the right. Flowcytometry analysis show the MOI dependent induction of mitochondrial **C** and cytosolic **D** oxidative stress measured using MitoSox and Dihydroethidium (DHE) respectively in mock-infected vs ZIKV-infected cells . **(E)** Flowcytometry analysis show the MOI dependent reduction on Glutathione content in ZIKV-infected vs mock-infected cells.

Additionally, ZIKV infection triggered an MOI dependent increase in ROS, both mitochondrial (Fig. 4.1C) and cytosolic (Fig. 4.1D), which was paralleled with the reduction of cellular GSH content (Fig. 4.1E). Similarly, infection of A172 human glioblastoma cells led to expression of viral E protein which was detectable at 24 hpi with a maximal expression between 48 and 72 hpi (Fig. 4.2A). The virus infection also led to an increase in the accumulation of mitochondrial ROS that is evident at 48 hpi (Fig. 4.2B and C) and increased significantly by 72 hpi. A parallel significant reduction in cellular GSH content was also evident at 72 hpi in infected cells (Fig. 4.2D and E). These results unequivocally demonstrate that ZIKV infection induces oxidative stress in neuronal precursor and glial cells.

4.3.2. Nrf2 activation precedes oxidative stress and antagonizes viral replication

Previous studies have demonstrated that ZIKV induces oxidative stress (Almeida et al., 2020; Ledur et al., 2020; Li et al., 2017a; Simanjuntak et al., 2018), but conflicting results exist in regards to the activation of the antioxidant response by Nrf2 (Almeida et al., 2020). Nrf2 is a functionally active transcription factor constitutively expressed in the cell. However, under normal conditions of cell growth, it is negatively regulated by its ubiquitination and degradation via the proteasome. Nrf2 degradation is interrupted upon oxidative stress to become stabilized and transcriptionally active (Nguyen et al., 2009). In contrast to ROS formation, ZIKV induced an early stabilization of Nrf2 at 12 hpi that peaked between 24-48 hpi (Fig. 4.3). In mock-infected cells, Nrf2 was undetectable (Fig. 4.3, lane 1). This is likely attributed to the observation that under normal conditions Nrf2 has a short lifespan and is degraded rapidly in cells

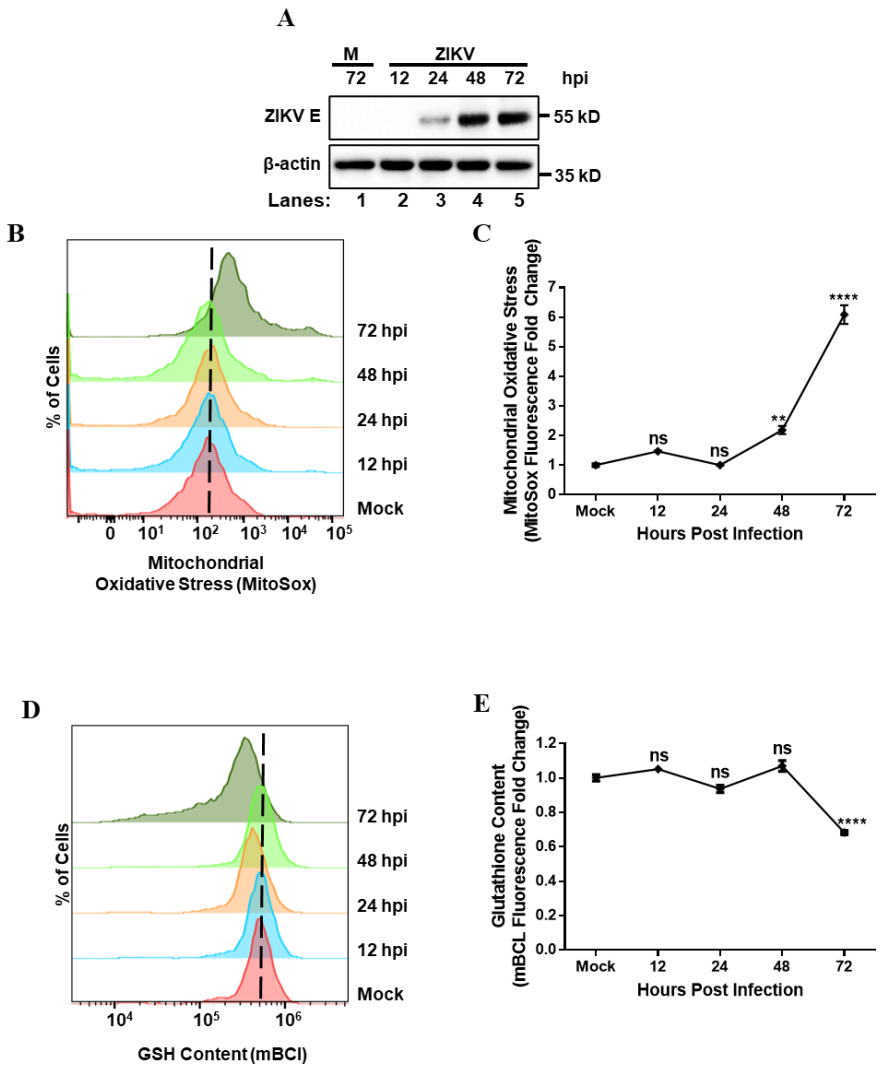

Figure 4.2: ZIKV infection induces oxidative stress in A172 cells. A Cells were either mock-infected (M) or infected with ZIKV at MOI 1 and at the indicated hpi, lysates were prepared and subjected to Western blot analysis to detect ZIKV E protein and β-actin using corresponding antibodies. Relative electrophoretic mobility of molecular mass markers in kD is shown on the right. **B** Flowcytometry analysis show time-dependent induction of mitochondrial oxidative stress **C and D** measured using MitoSox and GSH content **E and F** in mock-infected vs ZIKV-infected cells.

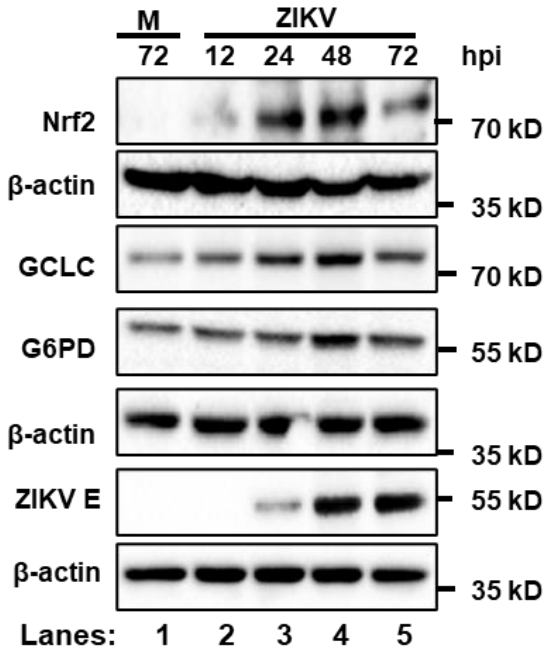

Figure 4.3: Nrf2 activation precedes oxidative stress and antagonizes ZIKV replication. Cells were either mock-infected (M) or infected with ZIKV at MOI 1 and at the indicated hpi, lysates were prepared and subjected to Western blot analysis to detect Nrf2, GCLC, G6PD, ZIKV E and β-actin using corresponding antibodies. Relative electrophoretic mobility of molecular mass markers in kD is shown on the right.

(Stewart et al., 2003; Tonelli et al., 2018). Subsequent downregulation of Nrf2 at 72 hpi coincided with the increase in ROS accumulation in A172 cells (Fig. 4.2B and C). Activation of Nrf2 resulted in concomitant increase in the protein levels of the glutamate cysteine ligase (GCLC, catalytic subunit) and glucose 6-phosphate (P) dehydrogenase (G6PD) (Fig. 4.3), whose gene transcription is driven by AREs recognized by Nrf2. The temporality of increased expression of both GCLC and G6PD was coincident with the stabilization of Nrf2. Describe data on viral E protein!

While pharmacological activation of Nrf2 has been previously shown to inhibit ZIKV genome replication (Huang et al., 2017), the effect of Nrf2 depletion in ZIKV replication has not been determined. siRNA mediated depletion significantly reduced the levels of Nrf2 in ZIKV infected cells (Fig. 4.4A, lanes 3 and 4). The inability of detecting Nrf2 in mock-infected cells transfected with siNT or siNrf2 (Fig. 4.4A, lanes 1 and 2) is consistent with our previous observation (Fig. 4.3). The depletion of Nrf2 also resulted in reduced expression of both GCLC and G6PD in ZIKV infected cells that were transfected with siNrf2 in comparison to cells transfected with siNT (Fig. 4.4A, lanes 3 and 4). Nrf2 knockdown increased ZIKV protein expression (Fig. 4.4A). At least a two- to three-fold increase in E protein expression at 48 hpi was observed in multiple repeat experiments. Interestingly, infectious virus particle release was significantly increased from cells depleted of Nrf2 as compared to cells treated with siNT (Fig. 4.4B). The increase in virus yield ranged from nearly 200-fold at 72 hpi to about 20-fold at 96 hpi with nearly 40-fold and 70-fold increase at 24 hpi and 48 hpi, respectively (Fig. 4.4B). It should be noted that the reduced fold-increase in virus titer at 96 hpi is likely due to ZIKV-induced cell death that we have observed in previous experiments. Furthermore, downregulation of Nrf2

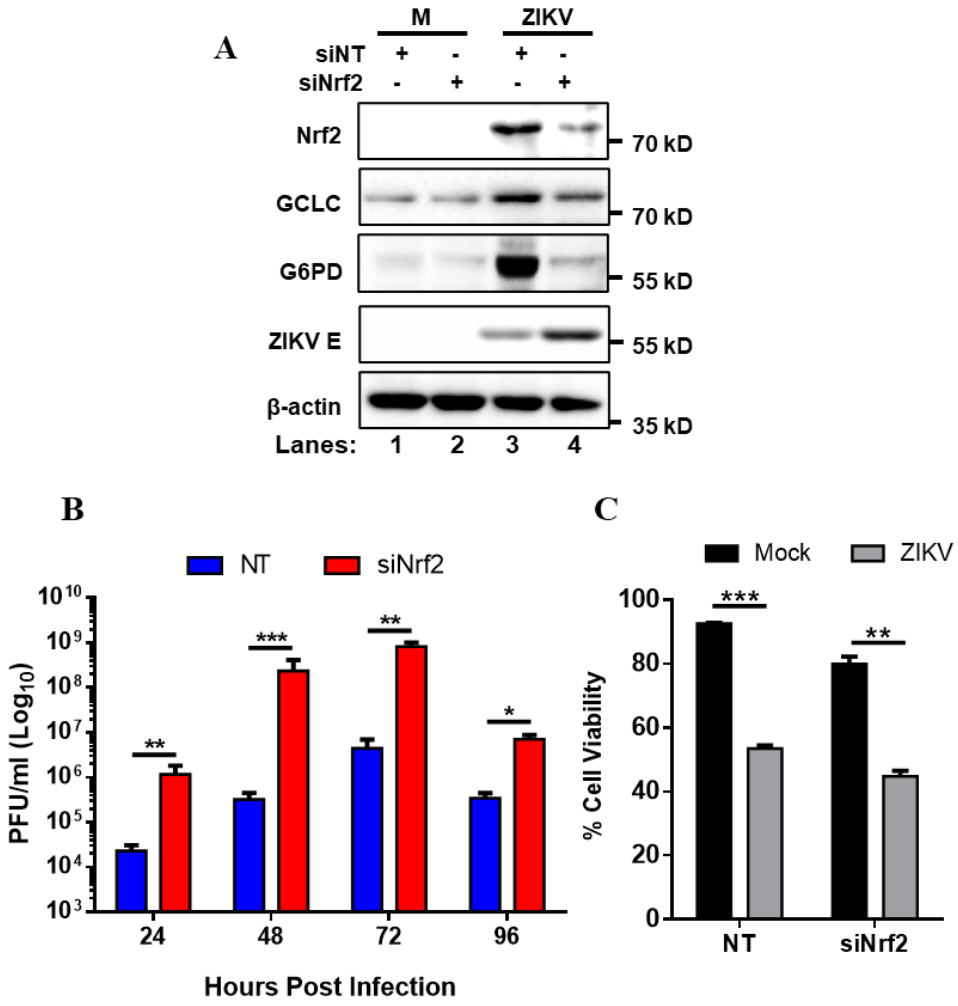

Figure 4.4: siRNA mediated depletion of Nrf2 enhances ZIKV replication. A Cells were transfected with either non-targeting (NT) siRNA (siNT) or siRNAs targeting Nrf2 (siNrf2) and mock-infected (M) or infected with ZIKV at MOI 1 and at 48 hpi, lysates were prepared and subjected to Western blot analysis to detect Nrf2, GCLC, G6PD, ZIKV E and β-actin using corresponding antibodies. Relative electrophoretic mobility of molecular mass markers in kD is shown on the right. **B** Cell culture supernatants from NT or siNrf2 transfected and ZIKV-infected cells were collected at the indicated times for quantitation of virus yield by plaque assay. **C** Cell viability was evaluated by flow cytometry in siNT or siNrf2 transfected, mock-infected (mock) or ZIKV-infected (ZIKV) cells at 96 hpi. Error bars represent ± SEM. *, $p \leq 0.1$; **, $p \leq 0.01$; ***, $p \leq 0.001$.

increased cell death induced by ZIKV (Fig. 4.4C). These results demonstrate that Nrf2 activation counters ZIKV replication and its depletion leads to enhanced replication of the virus.

4.3.3. Glutathione reduces ZIKV replication and cell death

I next decided to evaluate the role of the antioxidant response triggered by Nrf2 on ZIKV replication. The Nrf-2-dependent increase in GCLC observed upon ZIKV infection (Fig. 4.4A) suggested a role of glutathione (GSH) synthesis in viral infection, as GCLC mediates the rate-limiting step in *de novo* GSH formation by the synthesis of its precursor, γ-glutamylcysteine (Franco and Cidlowski, 2012). Since I had observed that ZIKV infection induced GSH depletion (Fig. 4.1E, 4.2D and E) that paralleled the downregulation of Nrf2/GCLC at 72 hpiobserved after its initial peak between 24-48 hpi (Fig. 4.3), we examined the effect of buthionine sulfoximine (BSO), an irreversible inhibitor of GCLC (Franco and Cidlowski, 2012) on ZIKV replication. In the presence of BSO, ZIKV protein expression was increased approximately 2- to 3-fold (Fig. 4.5A) while infectious virus yield in the supernatants was significantly enhanced (Fig. 4.5B). Again, the increase in virus yield ranged from nearly 120-fold at 72 hpi to about 20-fold at 96 hpi with nearly 80-fold and 85-fold increase at 24 hpi and 48 hpi, respectively, as compared to BSO-untreated cells. These results correlate well with the results obtained when Nrf2 is downregulated (Figs. 4.4A and B). Similarly, ZIKV-induced cell death was also enhanced (Fig. 4.5C). These results demonstrate an antiviral role of Nrf2 via GSH synthesis in ZIKV infection.

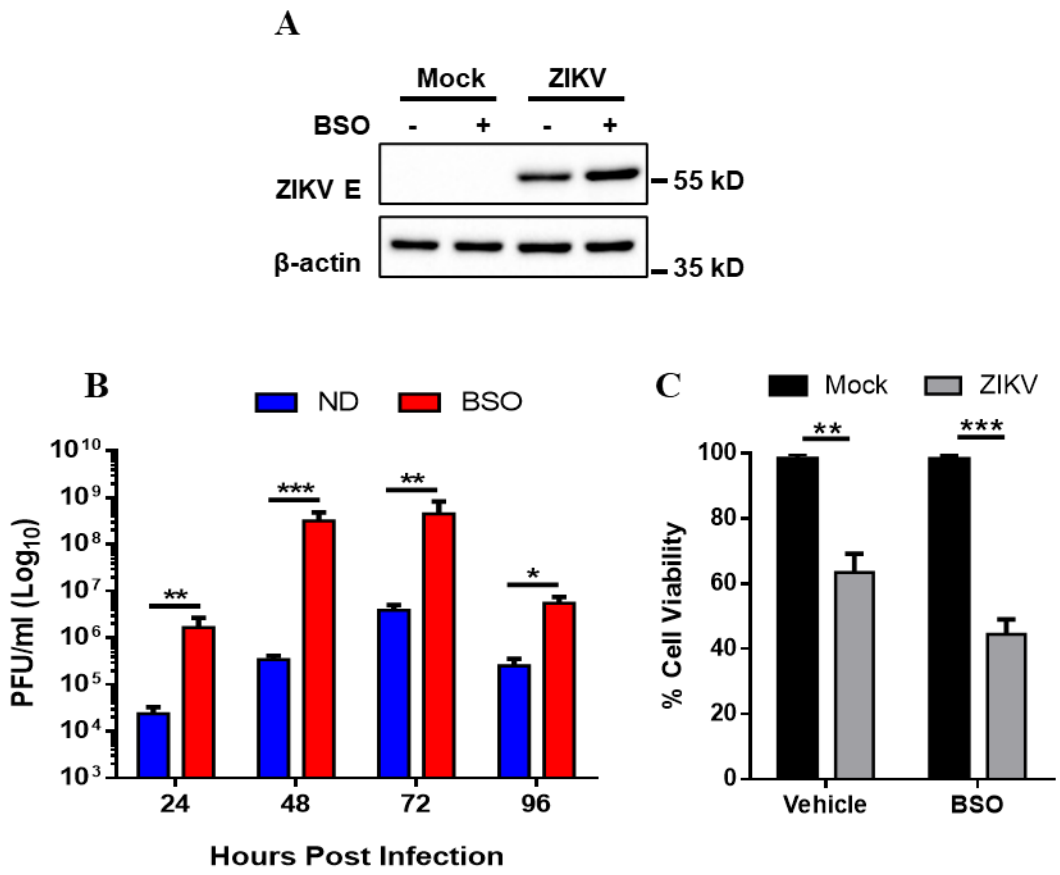

Figure 4.5: Glutathione reduces ZIKV replication and cell death . A Cells were mock-infected (M) or infected with ZIKV at MOI 1 followed by treatment with vehicle (-) or BSO (+) and at 48 hpi, lysates were prepared and subjected to Western blot analysis to detect ZIKV E and β-actin using corresponding antibodies. Relative electrophoretic mobility of molecular mass markers in kD is shown on the right. **B** Cell culture supernatants from vehicle (ND) or BSO treated, and ZIKV-infected cells were collected at the indicated times for quantitation of virus yield by plaque assay. **C** Cell viability was evaluated by flow cytometry in Vehicle or BSO treated mock-infected (Mock) or ZIKV-infected (ZIKV) cells at 96 hpi. Error bars represent ± SEM. *, $p \leq 0.1$; **, $p \leq 0.01$; ***, $p \leq 0.001$.

4.3.4. ZIKV replication is augmented by NADPH depletion

Similar to GCLC, G6PD was transiently upregulated in an Nrf2-dependent manner during ZIKV replication (Fig. 4.3). G6PD and 6-phosphogluconate dehydrogenase (6PGD) are NADP-dependent oxidoreductases within the pentose phosphate pathway (PPP) that regenerate nicotinamide adenine dinucleotide phosphate (NADPH) whose reductive power fuels numerous antioxidant/reductive systems (Stanton, 2012). The antioxidant function of GSH is primarily mediated by the activity of GSH peroxidases (GPx), which catalyze the reduction of peroxides (hydrogen peroxide [H_2O_2], peroxynitrite [$ONOO^-$] or lipid peroxides [LOOH]). The resultant GSH disulfide or oxidized GSH (GSSG) is reduced by GSH reductase (GR) using NADPH as cofactor (Fig. 4.9) (Franco and Cidlowski, 2012). Because GSH synthesis exerted an inhibitory effect on ZIKV replication, it was expected that G6PD and 6PGD would also be inhibitory. In line with this assumption, we found that the depletion of G6PD and 6PGD enhanced viral protein and infectious virion production (Fig. 4.6A and B). In contrast, pharmacological inhibition of G6PD and 6PGD by 6-AN significantly inhibited viral replication (Fig. 4.7A and C). The inhibitory effect 6-AN was not cell specific as it was also observed in VeroE6 (African green monkey kidney epithelial cells) cells (Fig. 4.7B). 6-AN also inhibited ZIKV-induced cell death (Fig. 4.7D). In addition to its role in replenishing NADPH pool, the PPP generates ribose 5P, a precursor for the synthesis of nucleotides. We next explored the possibility that supplementing cells with D-Ribose under the condition of pharmacologic inhibition of G6PD and 6PGD by 6-AN would result in rescue of ZIKV replication. Interestingly, even in the presence of D-Ribose, 6-

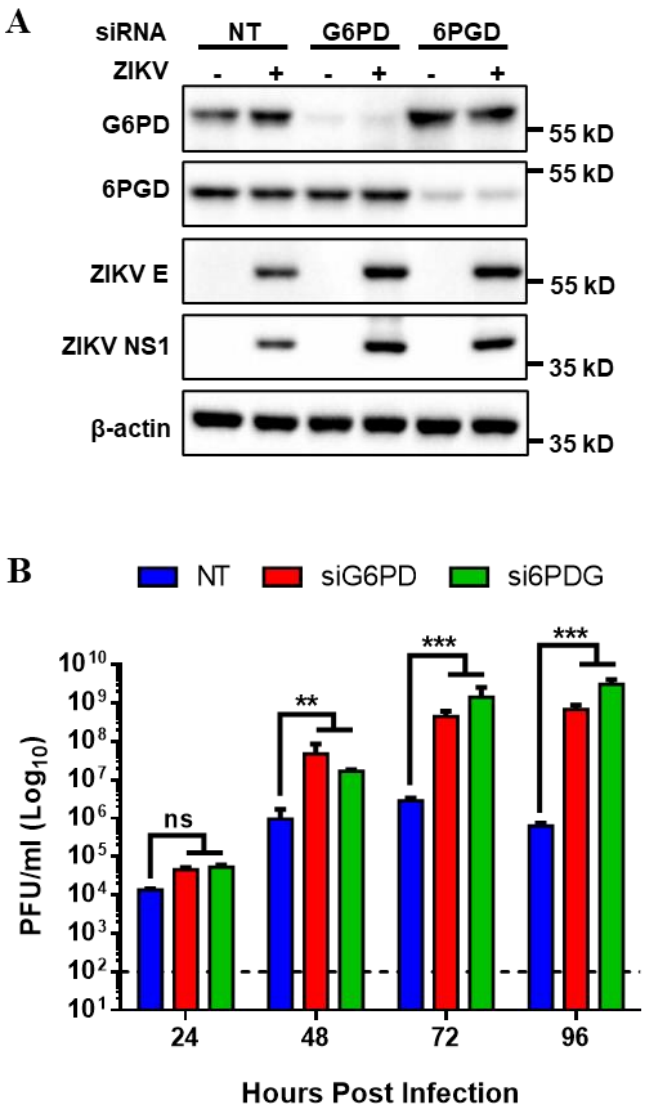

Figure 4.6: siRNA mediated depletion of G6PD and 6PGD. A A172 cells were transfected with either non-targeting (siNT) siRNA or siRNAs targeting G6PD or 6PGD for 48 h and subsequently mock-infected (M) or infected with ZIKV for 48 h. Cell lysates were prepared and subjected to Western blot analyses to detect G6PD, 6PGD, ZIKV E and β-actin using the corresponding antibodies. Relative electrophoretic mobility of molecular mass markers in kD is shown on the right. **B** Infectious virus production in cells depleted of G6PD or 6PGD in comparison to siNT transfected cells. The experiments were conducted as described in panel **A,** culture supernatants from infected cells were collected at the indicated hpi and assayed for infectious virus yield by plaque assay. Horizontal discontinuous line represents limit of detection. Error bars represent ± SEM. ns, non significant; **, $p \leq 0.01$; ***, $p \leq 0.001$

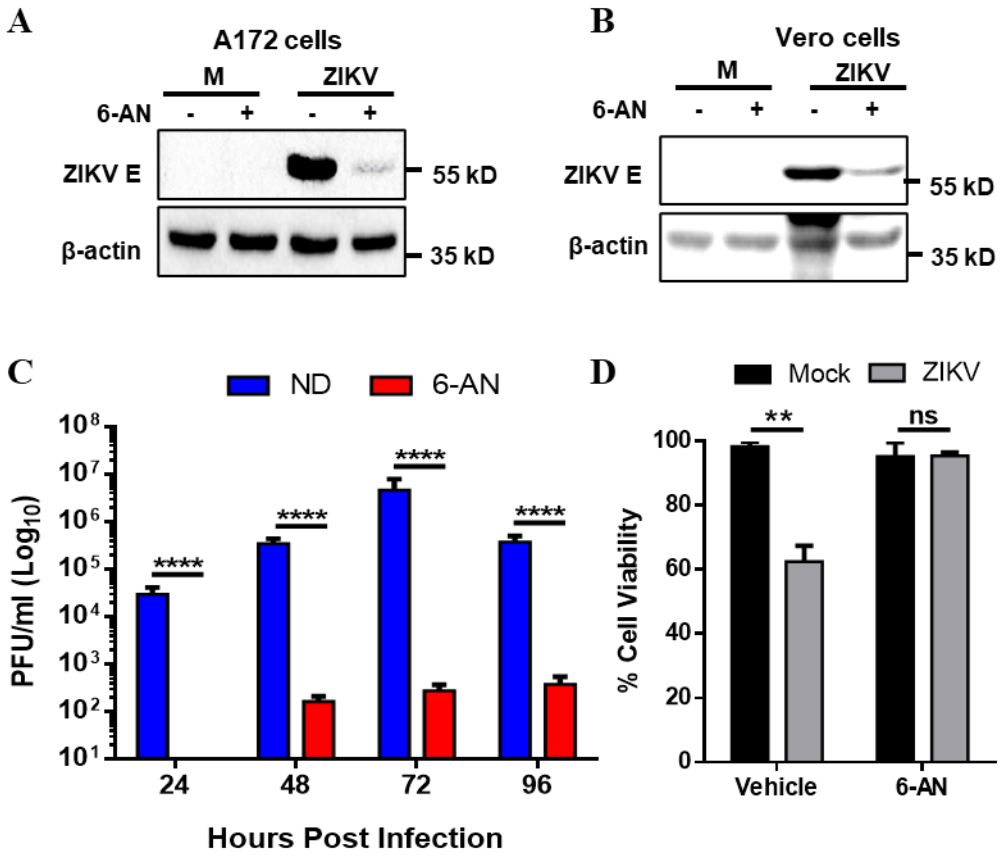

Figure 4.7: 6-AN inhibits ZIKV replication. A A172 **B** VeroE6 cells were mock-infected (M) or infected with ZIKV at MOI 1 followed by treatment with vehicle (-) or 6-AN (+) and at 48 hpi, lysates were prepared and subjected to Western blot analysis to detect ZIKV E and β-actin using corresponding antibodies. Relative electrophoretic mobility of molecular mass markers in kD is shown on the right. **C** Cell culture supernatants from vehicle (-) or 6-AN (+) treated, and ZIKV-infected cells were collected at indicated times for quantitation of virus yield by plaque assay. **D** Cell viability was evaluated by flow cytometry in vehicle or 6-AN treated and (+) mock-infected (Mock) or ZIKV-infected (ZIKV) cells at 96 hpi. Error bars represent ± SEM. Ns, non significant; **, $p \leq 0.01$; ****, $p \leq 0.0001$.

AN still inhibited ZIKV replication and no rescue of ZIKV protein levels was observed (Fig. 4.8). Considering the contrasting results obtained by siRNA mediated depletion and pharmacological inhibition of PPP enzymes, G6PD and 6PGD, it is possible that the inhibitory effect of 6-AN on ZIKV replication is independent of the PPP and is likely by hitherto unknown mechanism.

4.4 Discussion

The recent outbreak of ZIKV in the Americas revealed serious neurological and developmental pathologies in fetuses and adults. The interplay between ZIKV infection and the resultant induction of oxidative stress in infected cells can contribute to serious outcomes such congenital defects and developmental abnormalities. Yet a clear understanding of the molecular mechanisms involved is still absent. This study focused on the effect of ZIKV infection on the redox homeostasis in neuronal and glial cells.

ZIKV infection of human neuronal progenitor LUHMES cells revealed that these cells are permissive to virus infection and that ZIKV infection resulted in a significant increase in the accumulation of ROS. Additionally, a marked reduction of the GSH content was observed. The presence of higher amounts of reduced GSH in a cell is indicative of good overall cellular health and a balanced redox state. ZIKV infection resulted in a significant decrease in the cellular GSH pool indicating oxidative stress induction and resulting damage. Similarly, infection of human glioblastoma A172 cells showed accumulation of ROS and a marked decrease in GSH levels signifying oxidative damage.

Nrf2 is central to the cellular antioxidant system and is known to act as a

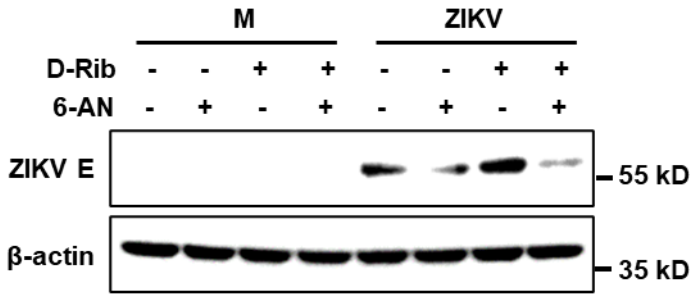

Figure 4.8: Inhibition of ZIKV E expression by 6-ASN is not rescued by D-Ribose. A172 cells were mock-infected (M) or infected with ZIKV at MOI 1 followed by treatment with vehicle (-) or 6-AN (+) in the absence (-) or presence (+) of D-Ribose and at 48 hpi, lysates were prepared and subjected to Western blot analysis to detect ZIKV E and β-actin using corresponding antibodies. Relative electrophoretic mobility of molecular mass markers in kD is shown on the right.

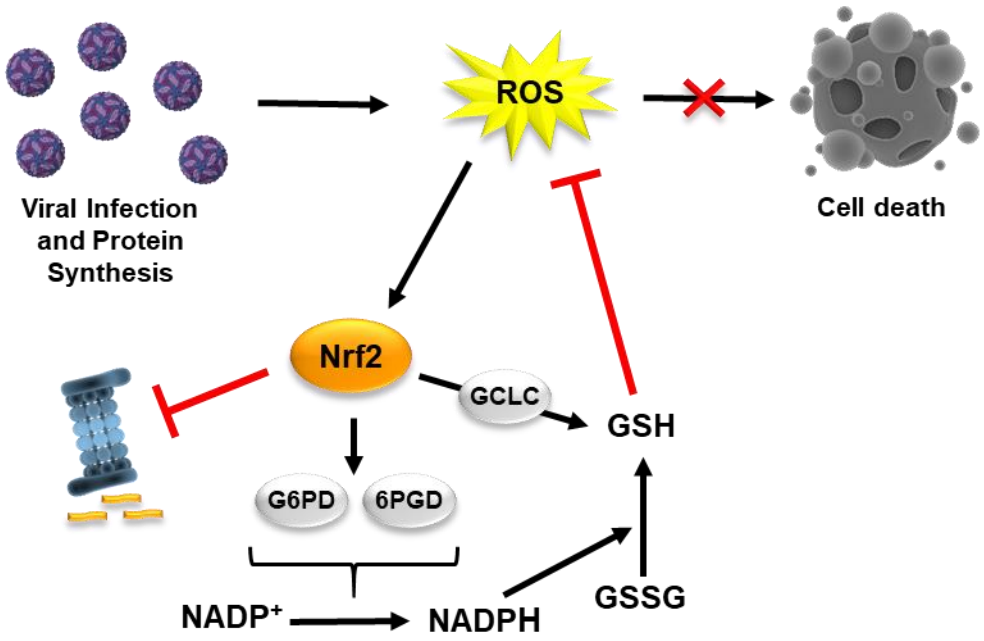

Figure 4.9: ZIKV induces oxidative stress and activates Nrf2/antioxidant pathway. ZIKV infection and protein synthesis in infected cells generate oxidative stress that inhibits the proteasomal degradation of Nrf2 and activates it. Activated Nrf2 directly modulates the activity of NADPH generating enzymes, G6PD and 6PGD resulting in higher generation of the reducing power and increasing *de novo* synthesis of GSH by modulating the enzyme, GCLC. This leads to the conversion of oxidized GSH (GSSG) to reduced GSH and increased accumulation of intracellular GSH which maintains redox homeostasis and prevents ZIKV induced cell death.

transcription factor inducing the expression of several genes involved in the antioxidant response carbohydrate metabolism, lipid metabolism as well as *de novo* glutathione synthesis and NADPH generation (Hayes and Dinkova-Kostova, 2014). With observation of oxidative stress induction, we looked for the expression of Nrf2 in ZIKV infected cells. A transient upregulation of Nrf2 and its downstream effectors, GCLC and G6PD, was seen upon ZIKV infection with time. The temporality of these events preceded the marked decrease in cellular GSH pool and the accumulation of ROS. Additionally, with the depletion of Nrf2, ZIKV replication was enhanced, as was evident with increased viral protein synthesis and infectious virion production, indicating that the cellular antioxidant network plays a key role in regulating virus replication. Indeed, inhibition of *de novo* GSH synthesis, an important modulator of redox homeostasis in a cell, by BSO enhanced both ZIKV protein expression and infectious viral progeny titers, corroborating the observation that cellular antioxidant defense plays an antiviral role in ZIKV replication. Cellular viability in Nrf2 depleted or BSO treated, ZIKV-infected cells was also significantly reduced due to increased cell death as a result of virus replication.

Nrf2 directly modulates the cellular reduced GSH pool by regulating key enzymes that generate the reducing fuel, NADPH. ZIKV infected cells transiently upregulate Nrf2 and its downstream effector, G6PD, which along with 6PGD serves to generate NADPH. This temporary upregulation leads to increased generation of NADPH that works to maintain redox homeostasis in the infected cells. Depletion of either G6PD or 6PDG resulted in the enhancement of viral protein expression and progeny virion production again corroborating the finding that antioxidant defense system inhibits ZIKV replication.

It has been reported previously that replication of several different of viruses such as DENV (Chao et al., 2008), entroviruses (Ho et al., 2008), and coronaviruses (Wu et al., 2008) is enhanced under conditions of G6PD deficiency. Additionally, individuals with genetic deficiency in G6PD have been shown to exhibit more severe complications of hepatitis E virus infection (Au et al., 2011; Thapa et al., 2009). Since G6PD enhances cellular antiviral response pathways by upregulating certain antiviral genes such as tumor necrosis factor a (TNF-a) and myxomavirus resistance 1 (MX1) (Wu et al., 2015), G6PD depletion may downregulate antiviral gene expression and support virus replication more robustly. Additionally, in G6PD-knowdown cells, expression of HSCARG protein, an NADPH sensor, has been demonstrated to be upregulated, which in turn has been shown to enhanced antiviral response. Therefore, it is possible that a combination of redox imbalance and the inability to generate NADPH and glutathione as well as reduced antiviral response due to G6PD depletion may contribute to the increased susceptibility to ZIKV infections.

Interestingly, 6-AN, a known inhibitor of both G6PD or 6PDG did not enhance ZIKV replication but in stark contrast to siRNA mediated depletion, significantly reduced ZIKV replication as was evident from viral E protein expression and infectious virus production. We explored the possibility that supplementing 6-AN treated ZIKV infected cells with D-Ribose may antagonize the effect of 6-AN and recover ZIKV protein expression. But it was observed that supplementing 6-AN treated ZIKV infected cells with D-Ribose did not rescue ZIKV replication, suggesting that the role of PPP is dispensable for ZIKV replication in these cells. Additionally, the inhibitory effect of 6-AN was found to be cell type independent. This suggests that the inhibitory effect of 6-

AN on ZIKV replication may be by a different mechanism and is not associated with the downregulation of enzymes involved in PPP such as G6PD and 6GPD. A detailed exploration into the inhibitory mechanism of 6-AN is essential for it to be developed as an anti-ZIKV drug. In conclusion, we demonstrate a pivotal role of the Nrf2 signaling cascade in ZIKV replication and highlights the antiviral nature of the cascade. This observation may lead to the development of antioxidant supplementation as a strategy to alleviate ZIKV pathogenesis.

CHAPTER 5: METABOLIC REGULATION OF ZIKV INFECTION

5.1. Abstract

Virus infection is known to modulate cellular metabolism which drives cellular energetics to a state conducive to viral replication. Increased rate of glycolysis, enhanced synthesis of lipids and modifications to lipid membranes, increased production of nucleotides and enzymatic cofactors, etc. are hallmark metabolic changes in virus-infected cells. Therefore, a better understanding of the specific metabolic changes induced by virus infection can be useful in the development of antiviral therapies. Previous studies have revealed that the pentose phosphate pathway does not appear to play a major role in ZIKV replication. To examine if other cellular pathways namely glycolysis, gluconeogenesis, or mitochondrial pathways such as fatty acid oxidation, glutaminolysis, etc are required for the viral replication, we used pharmacologic inhibitors to determine their effect on ZIKV. Results show that inhibition of the rate limiting enzyme, hexokinase in the glycolysis pathway, by 2-Deoxy-D-glucose (2-DG), a glucose analog, reduced viral protein expression and infectious progeny production. The inhibition by 2-DG recovered transiently at 48 h post-infection. This transient recovery was prevented when oxidative metabolism was inhibited by blockage of the mitochondrial pyruvate carrier, inhibition of fatty acid oxidation, or gluaminolysis. These results suggest that gluconeogenesis plays a role in virus replication. Further studies examining various metabolites may reveal pathways that are critical for ZIKV replication.

5.2. Introduction

The recent re-emergence of ZIKV and the associated serious disease outcomes such as microcephaly and other neurological deficits in infants and adults poses a major threat to public health (Faizan et al., 2016). While several reports have studied the molecular mechanisms involved in the infection, replication, and pathogenesis of ZIKV, detailed elucidation of ZIKV-induced metabolic changes is not yet available (Jordan and Randall, 2016; Rothan et al., 2019; Thaker et al., 2019b). Generally, virus infection leads to enhanced cellular metabolism to meet the biosynthetic needs of viral replication. Flavivirus replication is known to increase the production of nucleotides and associated enzymatic cofactors (Jordan and Randall, 2016). DENV infection has been reported to significantly increase the biosynthesis of carbohydrates, amino acids, and lipids (Fontaine et al., 2015; Jordan and Randall, 2016). Furthermore, DENV infection also increases early glycolytic intermediates while decreasing late glycolytic intermediates indicating an active glycolytic flux (Allonso et al., 2015; Fontaine et al., 2015). Proteomic analysis of HCV-infected Huh-7.5 cells showed perturbations in cellular metabolic pathways namely glycolysis, citric acid cycle and the pentose phosphate pathway that favor virus replication (Diamond et al., 2010). While this happens early in infection, a shift in cellular metabolism towards cell viability and maintaining energy homeostasis is observed later in the infection cycle (Diamond et al., 2010).

Glycolysis is also essential for addition of glycan moieties to proteins for glycosylation, the most common form of post translational modifications (Schjoldager et al., 2020). Glycosylation of viral proteins is critical to virion assembly, infection as well as evasion of immune responses (Annamalai et al., 2019; Annamalai et al., 2017;

Watanabe et al., 2019). It has been reported that removal of glycosylation sites from the viral envelope (E) and non-structural protein 1 (NS1) of ZIKV leads to attenuation of progeny virions and defective in neuroinvasion (Annamalai et al., 2019; Annamalai et al., 2017; Carbaugh et al., 2019). Furthermore, lipid biosynthesis and intracellular accumulation of sphingolipids, phospholipids and cholesterol have been shown to facilitate replication of several prototypic flaviviruses such as WNV and DENV (Heaton et al., 2010; Mackenzie et al., 2007; Merino-Ramos et al., 2016). DENV activates autophagy-mediated lipid catabolism and upregulates β-oxidation and energy metabolism that are essential for efficient virus replication (Heaton and Randall, 2010; Khakpoor et al., 2009; Lee et al., 2013). Studies with ZIKV have shown that human cells infected with ZIKV utilize more glucose and feed into the TCA cycle whereas mosquito cells feed into the pentose phosphate pathway suggesting differential metabolic pathways between species (Thaker et al., 2019b).

In this study, we demonstrate that the dependency of ZIKV on glycolysis may be indispensable for optimal viral replication. With pharmacological inhibition of glycolysis by 2-Deoxy-D-glucose (2-DG), viral protein production and infectious virus yield were significantly reduced, although a transient increase at 48 hpi was observed. Glycosylated E protein levels were also reduced suggesting an important role for glycolysis in ZIKV replication. This observation suggested a virus-induced shift in cellular metabolism towards gluconeogenesis. We found that with pharmacological inhibition of the mitochondrial pyruvate carrier, fatty acid oxidation or gluaminolysis, a marked reduction in viral protein production was noted even at 48 hpi. Taken together, these results suggest that glycolysis and gluconeogenesis are needed for optimal replication of ZIKV and

demonstrate the complex dependency of ZIKV on cellular metabolism.

5.3. Results

5.3.1. Glycolysis is necessary for ZIKV protein expression and progeny virion production

Since virus replication is critically dependent on glycolysis for viral protein synthesis, post translational modifications of viral proteins, and progeny virion production (Watanabe et al., 2019),, we sought to first determine the effect of inhibition of glycolysis on ZIKV replication. By using 2-DG to inhibit the activity of hexokinase, the enzyme that catalyzes the first irreversible step of the glycolytic pathway where glucose is phosphorylated to glucose-6-phosphate (G6P), we found a marked decrease in viral E protein expression across all the time points in comparison to cells infected with ZIKV and treated with the vehicle (Fig. 5.1A). Interestingly, we observed a transient increase in the levels of E proteins at 48 hpi (lane 6) but at later times, the E protein levels were reduced (lanes 8 and 10). Several studies have reported the N-glycosylation of ZIKV E protein and its importance for viral assembly and infectivity (Annamalai et al., 2017; Carbaugh et al., 2019; Fontes-Garfias et al., 2017). A follow up study demonstrated that the major proportion of N-glycan on ZIKV E include N-acetylglucosamine (GlcNAc) and glucose among others (Routhu et al., 2019). Glucose 6P and Fructose 6P, two intermediates in glycolytic pathway, are precursors of the nucleotide activated sugars donors UDP-glucose and UDP-GlcNac, respectively, that mediate protein N-glycosylation. Interestingly, we observed that the inhibition of glycolysis by 2-DG resulted in the detection of two bands for ZIKV E protein, one representing the fully

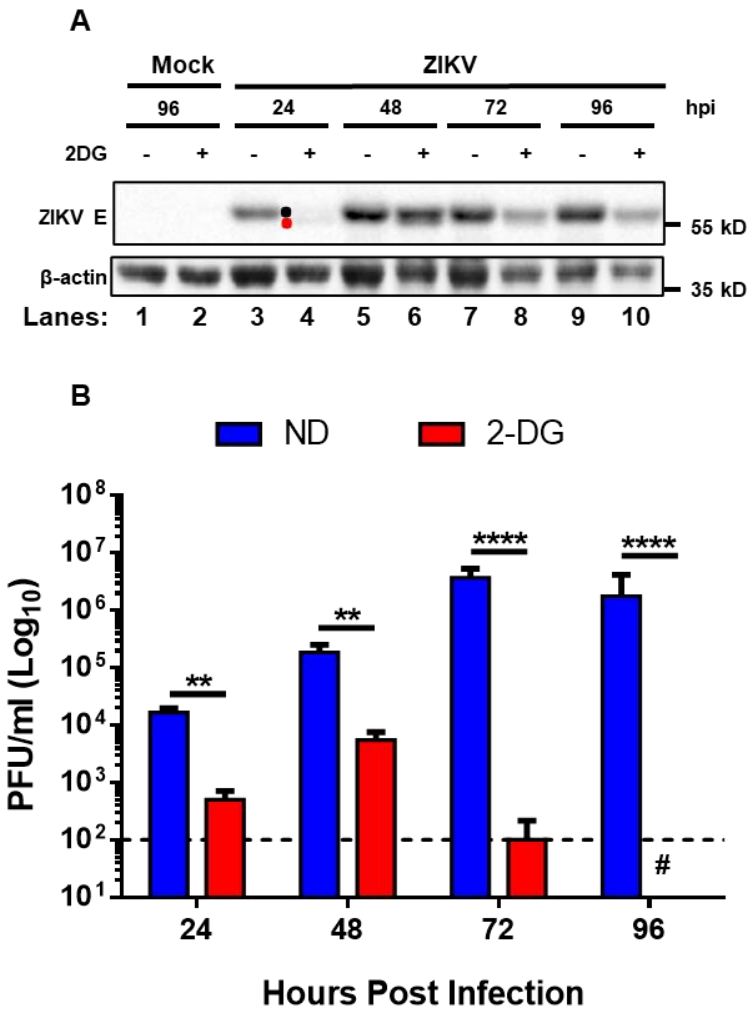

Figure 5.1: Glycolysis is necessary for ZIKV protein expression and progeny virion production. A A172 cells were either mock-infected (M) or infected with ZIKV at an MOI of 1 and treated with vehicle or the glycolytic inhibitor, 2-DG. Cell lysates were prepared at the indicated hours post-infection (hpi) and subjected to Western blot analysis to detect ZIKV E and β-actin using the corresponding antibodies. Relative electrophoretic mobility of molecular mass markers in kD is shown on the right. **B** Culture supernatants from vehicle or 2-DG treated and ZIKV-infected cells were collected every 24 hpi for quantitation of virus yield by plaque assay. #, number of plaques were below the limit of detection (LOD). **, $p \leq 0.01$; ****, $p \leq 0.0001$.

glycosylated E protein (top band, identified with a black dot on the left of lane 4) and a faster migrating unglycosylated E protein (bottom band, identified with a red dot on the left of lane 4) (Fig. 5.1A). The results indicate that exposure of ZIKV infected cells to 2-DG leads to significant reduction in viral protein levels but also glycosylation of the viral E protein.

Since, viral protein levels as well as glycosylation are critical to the production of infectious progeny virions, we examined the yield of infectious virus in the culture supernatants of infected cells treated with 2-DG. Results show a dramatic inhibition of infectious progeny production at all times examined (Fig. 5.1B). Interestingly, at 96 hpi, when E protein was readily detectable (Fig. 5A, lane 10), infectious progeny was undetectable (Fig. 5.1B), indicating that factors other than the protein levels or glycosylation are important for progeny virus production.

5.3.2. Gluconeogenesis partially contributes to ZIKV replication

The transient recovery of ZIKV protein synthesis at 48 hpi under condition of glycolysis inhibition suggests additional carbon sources are likely fueling viral replication. Glucose 6P can also be generated by the recycling of phosphoenolpyruvate via gluconeogenesis, which involves carbon metabolism via the mitochondrial TCA cycle. Three primary carbon sources can fuel the TCA cycle independent from glycolysis are (i) pyruvate, originated by either its reverted synthesis from lactate via lactate dehydrogenase or pyruvate uptake from culture media; (ii) fatty acid oxidation (FAO) to acetyl-CoA; and (iii3) glutamine lysis (glutaminolysis) to glutamate that is subsequently incorporated to the TCA cycle upon its metabolism to α-ketoglutarate. Progressive

oxidation of these carbon sources is coupled to the electron transport chain (ETC). In addition, reductive carboxylation of pyruvate and glutamine can bypass the ETC to produce oxaloacetate/malate that can fuel gluconeogenesis as well (Yip et al., 2016).

Therefore, we next evaluated the potential role of mitochondrial metabolism by inhibiting the ETC complex I by rotenone (ROT) and the mitochondrial pyruvate carrier by UK5099 (UK). A marginal decrease in the levels of viral E proteins was observed (Fig. 5.2A). In the presence of ROT or UK, the viral E protein was fully glycosylated (lanes 7, 8, 11, and 12). Examining NS1, another viral glycoprotein that is critically involved in genome replication, we observed two species of NS1 (glycosylated and unglycosylated) in the presence of 2-DG, consistent with our observation with the E protein. Significant inhibitory effect production of infectious progeny virions was seen with ROT and UK (Fig. 5.2B). On the other hand, inhibition of FAO by etomoxir (ETO) and glutaminolysis by BPTES did not produce any significant effect on viral protein synthesis (Fig. 5.3A) or infectious virus yield (Fig. 5.3B). Interestingly, blocking any of the pathways that supply carbons to gluconeogenesis under condition of glycolysis inhibition resulted in reversal of the transient increase in ZIKV protein expression seen at 48 hpi when glycolysis was inhibited (Fig. 5.4A and B). These results indicate that when glycolysis is inhibited, ZIKV replication is facilitated, albeit in part, by gluconeogenesis.

5.4. Discussion

Viruses have evolved to alter cellular metabolism for creating an environment optimal for their replication in host cells (Jordan and Randall, 2016). The development of

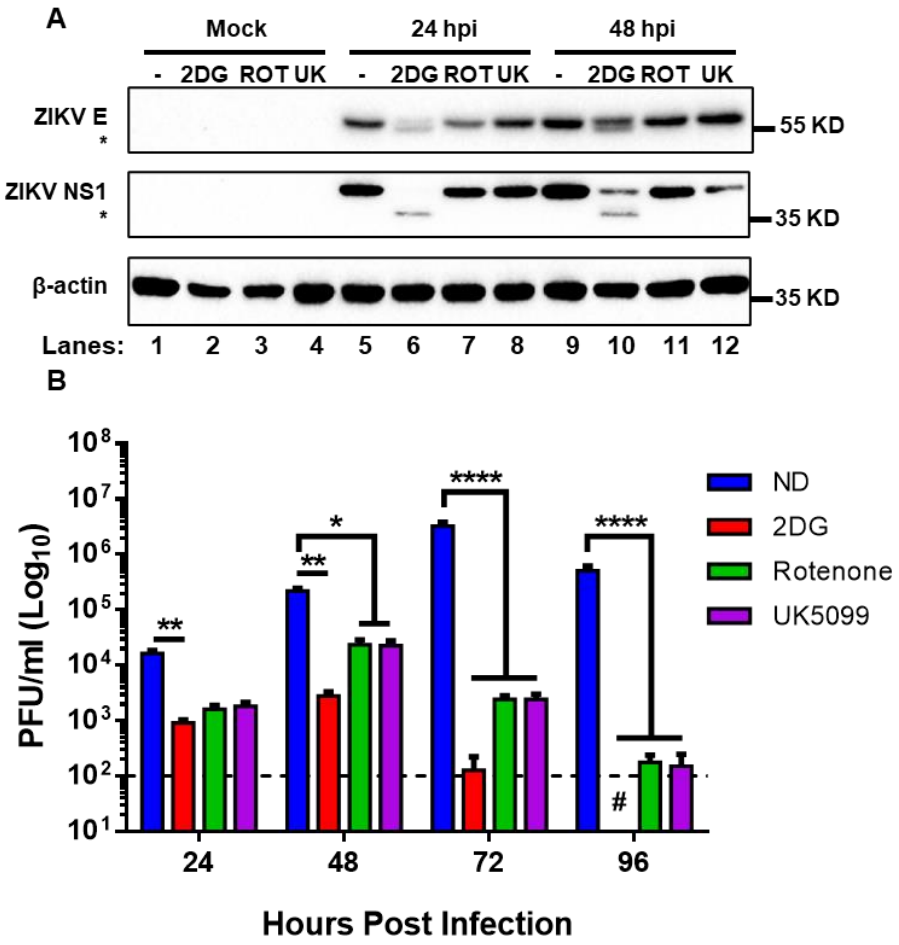

Figure 5.2: Inhibition of mitochondrial metabolism affects ZIKV replication. A A172 cells were either mock-infected (M) or infected with ZIKV at an MOI of 1 and treated with vehicle or 2-DG or mitochondrial ETC complex I inhibitor, Rotenone (ROT) or the mitochondrial pyruvate carrier inhibitor, UK5099 (UK). Cell lysates were prepared at the indicated hours post-infection (hpi) and subjected to Western blot analysis to detect ZIKV E, NS1, and β-actin using the corresponding antibodies. Relative electrophoretic mobility of molecular mass markers in kD is shown on the right. **B** Culture supernatants from a similar experiment were collected every 24 hpi for quantitation of virus yield by plaque assay. #, number of plaques were below the limit of detection (LOD). *, $p \leq 0.05$; **, $p \leq 0.01$; ****, $p \leq 0.0001$.

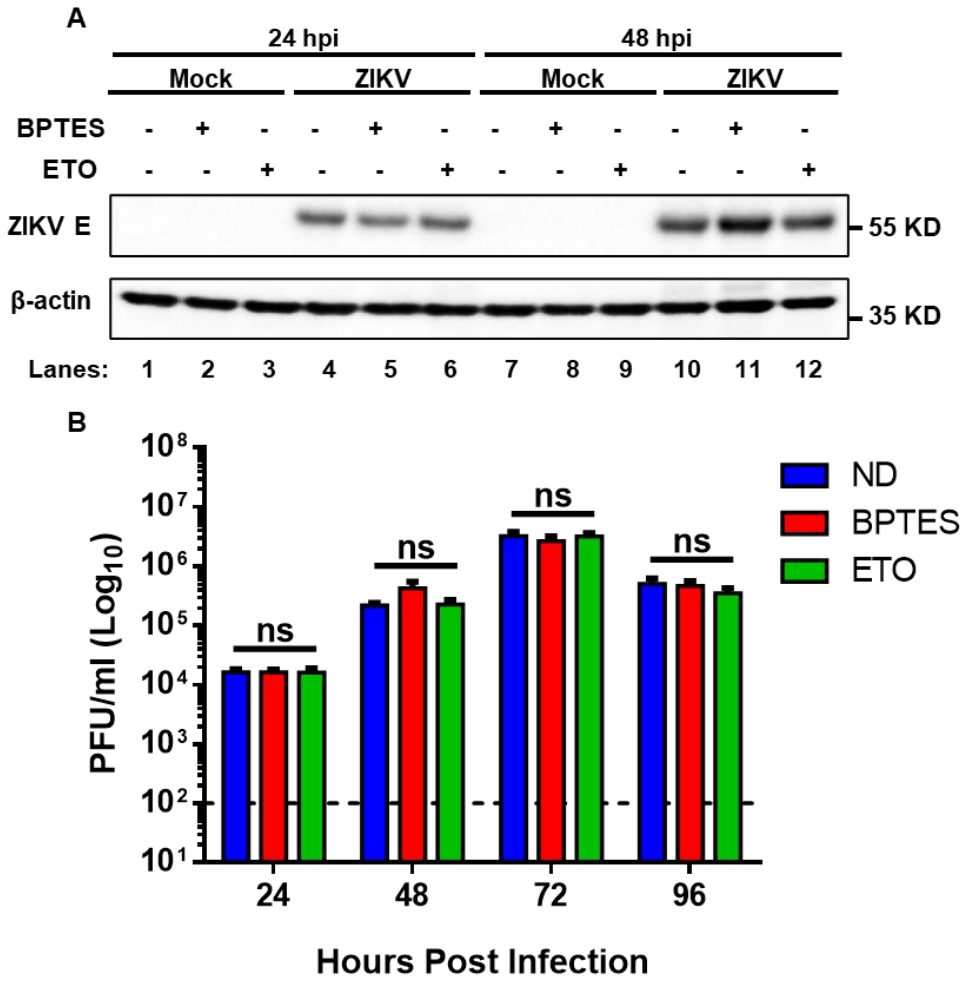

Figure 5.3: Inhibition of fatty acid oxidation or glutaminolysis does not affect ZIKV replication. A A172 cells were either mock-infected (M) or infected with ZIKV at an MOI of 1 and treated with vehicle or fatty acid oxidation inhibitor, Etomoxir (ETO) or glutaminolysis inhibitor, BPTES. Cell lysates were prepared at the indicated hours post-infection (hpi) and subjected to Western blot analysis to detect ZIKV E and β-actin using the corresponding antibodies. Relative electrophoretic mobility of molecular mass markers in kD is shown on the right. **B** Culture supernatants from a similar experiment were collected every 24 hpi for quantitation of virus yield by plaque assay. ns, non-significant. Horizontal dashed lines indicated the limit of detection in plaque assay. **, $p \leq 0.01$; ****, $p \leq 0.0001$.

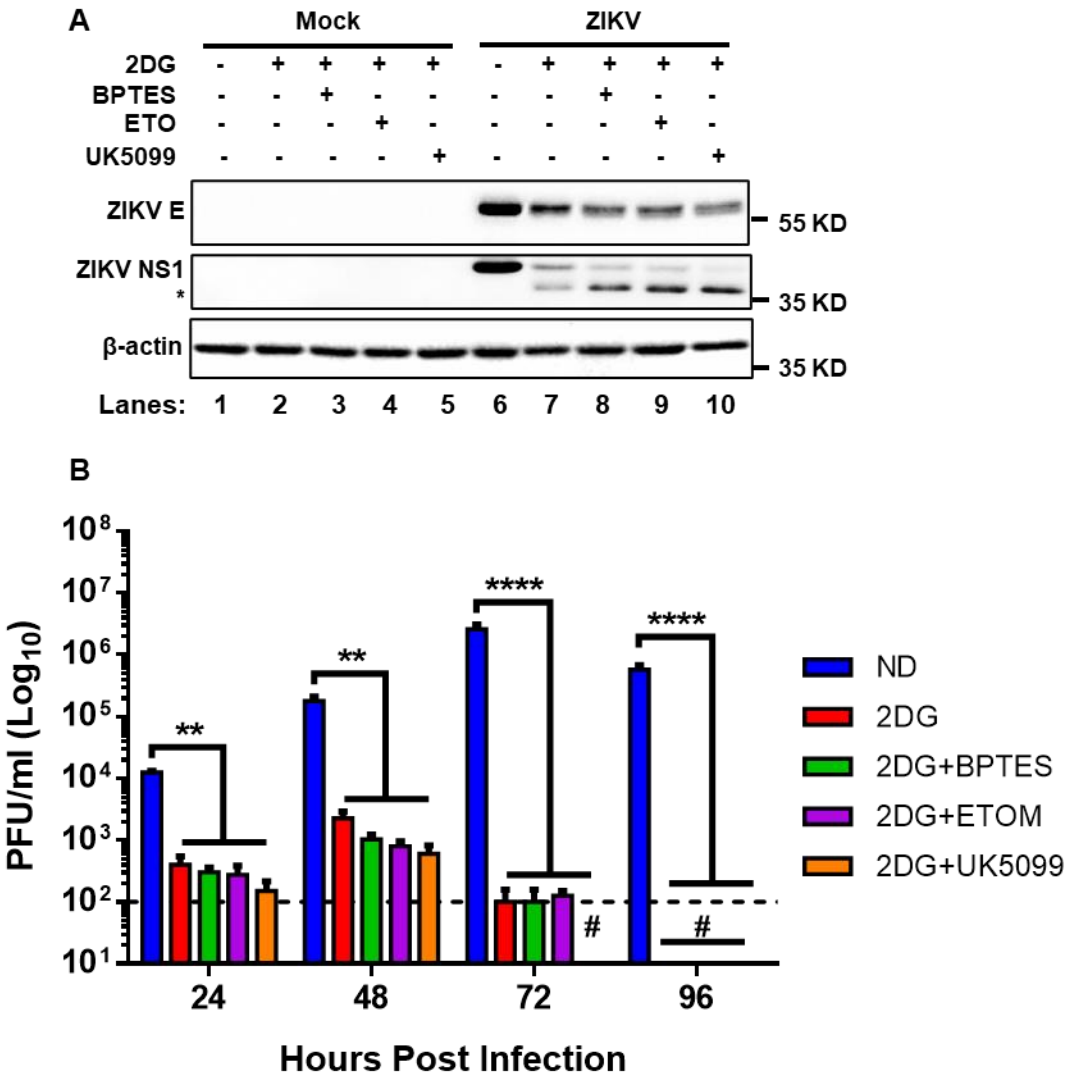

Figure 5.4: Gluconeogenesis partially regulates ZIKV replication A A172 cells were either mock-infected (M) or infected with ZIKV at an MOI of 1 and treated with vehicle or 2-DG along with BPTES or ETO or UK. Cell lysates were prepared at 48 hpi and subjected to Western blot analysis to detect ZIKV E, NS1, and β-actin using the corresponding antibodies. Relative electrophoretic mobility of molecular mass markers in kD is shown on the right. **B** Culture supernatants from a similar experiment were collected every 24 hpi for quantitation of virus yield by plaque assay. #, no plaques were detected.

metabolomic approaches to study the alterations in cellular metabolism induced by virus infection have significantly contributed to a better understanding of the role of metabolism in virus infection, replication as well as pathogenesis (Jordan and Randall, 2016; Sanchez and Lagunoff, 2015). Furthermore, elucidation of specific metabolic changes induced by specific viruses has led to the development of antiviral strategies targeting host cell processes (Sanchez and Lagunoff, 2015). In this study, we explored the role of cellular metabolic pathways and associated signaling cascade in ZIKV protein expression and replication.

The increase in glycolysis reported in a variety of virus infections demonstrates the required surge in cellular bioenergetics in infected cells. Increased glycolysis leads to the generation of nucleotides and other cofactors that are involved in the replication of the infecting virus. Indeed, in ZIKV infected cells, inhibition of hexokinase, the first enzyme of glycolysis, by 2-DG, led to a significant loss in viral protein expression and infectious virus titers indicating a strong dependence of ZIKV on cellular glucose metabolism. Glycosylation of viral proteins is essential to the production of mature infectious virus particles and pathogenesis (Annamalai et al., 2019; Annamalai et al., 2017; Bagdonaite and Wandall, 2018; Watanabe et al., 2019). The downregulation of viral E and NS1 protein glycosylation status demonstrates a two-fold effect of 2-DG on inhibition of ZIKV. While blocking the activity of hexokinase by 2-DG reduced ZIKV replication, a transient increase in the expression of viral E protein as well as infectious virus yield was observed at 48 hpi. This pointed towards the involvement of other carbon sources being fed into glucose metabolism via gluconeogenesis (Fig. 5.5).

Standalone inhibition of the ETC complex I by ROT or the mitochondrial

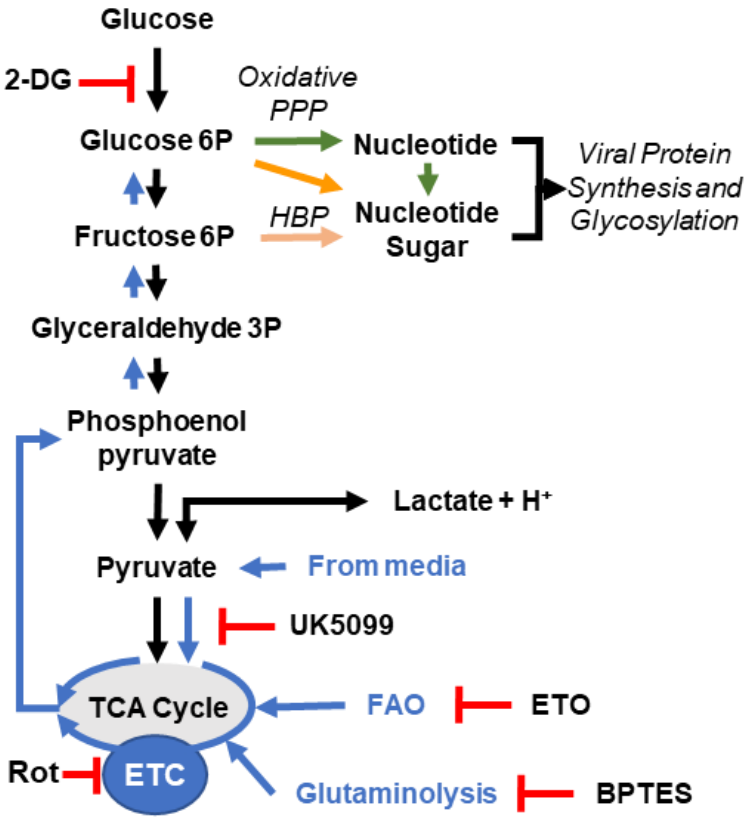

Figure 5.5: Cellular metabolism and ZIKV replication. Schematic of cellular metabolism showing glycolysis, PPP, TCA cycle and gluconeogenesis (indicated by blue arrows). Also shown are the targets for metabolic inhibitors 2-DG, Rotenone (ROT), Etomoxir (ETO), BPTES, andUK5099 (UK). When glycolysis is blocked by 2-DG, carbons are cycled into the metabolism from pyruvate, fatty acids and glutamine which leads to generation of glucose 6P by gluconeogenesis to support ZIKV replication.

pyruvate carrier by UK led to marginal inhibition of ZIKV protein expression but a more pronounced effect on infectious progeny production suggesting a contributing role of mitochondrial metabolism in ZIKV replication. In contrast, standalone inhibition of FAO by ETO and glutaminolysis by BPTES did not inhibit the accumulation of ZIKV proteins suggesting the non-involvement of these metabolic processes in ZIKV replication. Furthermore, when any of above mentioned pathways were blocked under condition of glycolysis inhibition by 2-DG, the transient increase in ZIKV protein accumulation in cells was not observed corroborating the finding that gluconeogenesis plays a contributing role in ZIKV replication.

CHAPTER 6: SUMMARY, CONCLUSIONS, AND FUTURE DIRECTIONS

6.1 Summary

Viruses are obligate parasites that co-opt the host cell machinery to synthesize their proteins, replicate their genomes, produce progeny virions, and cause disease. On the other hand, the host cell also employs several strategies in response to virus infection that can be pro- or anti-viral in nature. Therefore, studying the alterations in host cell processes induced by virus infection is key to understanding viral pathogenesis as well as to the development of antiviral strategies. The studies presented in this dissertation demonstrate activation of both mTORC1 and mTORC2 upon ZIKV infection and this facilitates viral protein expression and progeny virion production (Fig 6.1). We also observed that early in infection, autophagy is activated in ZIKV-infected cells. But later in the infection process, a gradual decline in autophagy flux was observed which coincided with the activation of mTORC1. The inhibitory effect of mTORC1 on autophagy induction was found to be mediated by the phosphorylation of ULK1 (Fig 6.1). These findings point to an antiviral nature of autophagy induction in ZIKV infected cells that is countered by virus-induced activation of mTORC1. Virus infection is also known to trigger oxidative stress in infected cells, and this is a critical contributor to virus-induced pathogenesis. ZIKV infection was found to induce oxidative stress in infected cells which led to a transient activation of Nrf2 mediated antioxidant response. Both genetic depletion of Nrf2 and pharmacological inhibition of glutathione (GSH) synthesis, led to increased expression of viral proteins and infectious virus production (Fig 6.1). Additionally, downregulation of NADPH generation also increased ZIKV

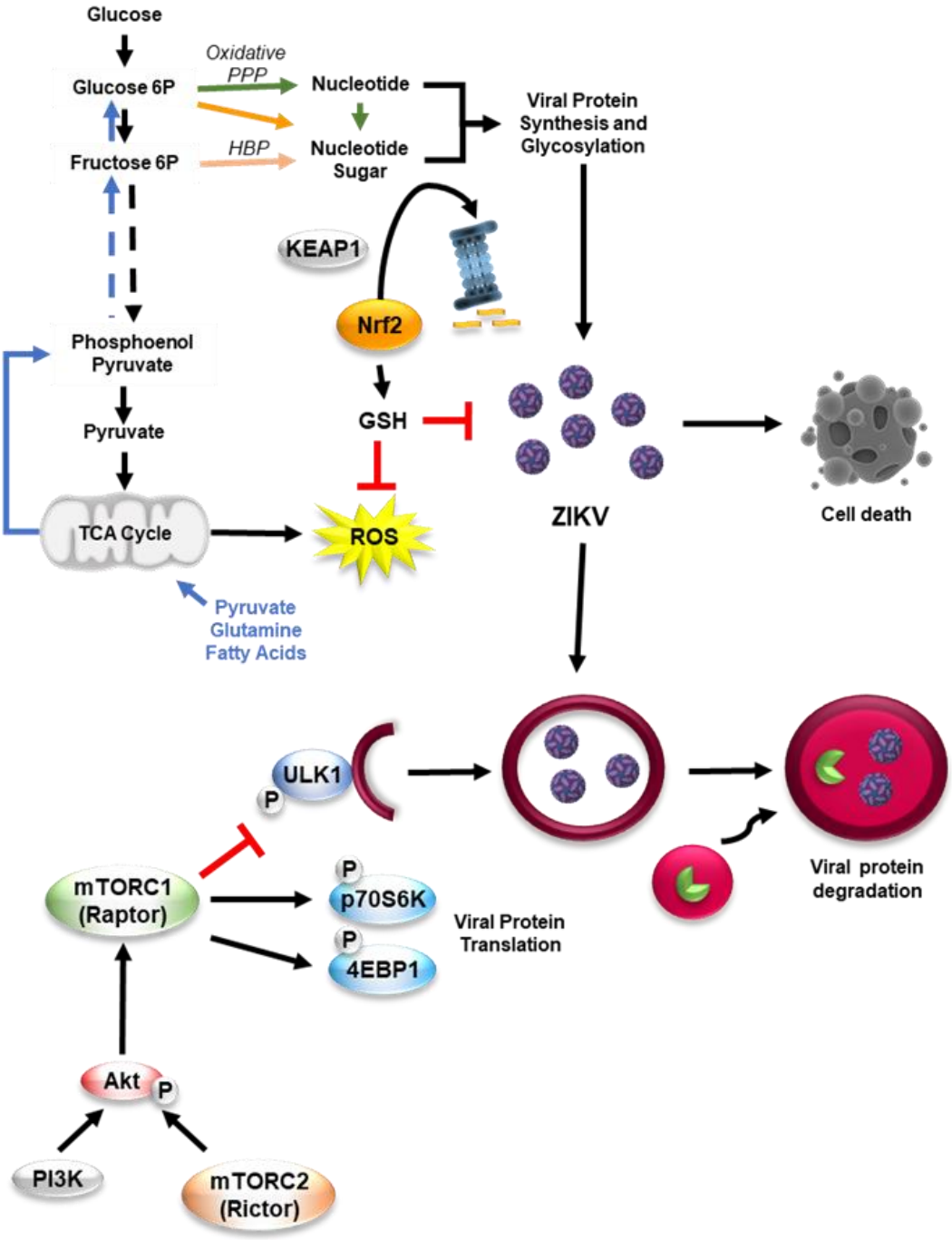

Figure 6.1: Host cell responses to ZIKV infection. Nrf2 mediated cellular antioxidant system negatively regulates ZIKV replication in infected cells as well as counters virus

infection induced oxidative stress at early time points post infection. But at later time points, the increased accumulation of viral proteins and replication of ZIKV exerts an imbalance in the generation and scavenging of oxidants that leads to cellular damage and cell death (upper part of the illustration). ZIKV replication is dependent on cellular metabolic processes like glycolysis and gluconeogenesis. Inhibition of glycolysis results in significant suppression of ZIKV protein expression and infectious virus yield. But a transient increase is observed at 48 hpi because of the activation of gluconeogenesis which cycles carbons from sources other than glucose (upper part of the illustration). ZIKV infection induces the activation of autophagy that degrades viral proteins at early time points thereby resulting in our ability to not detect them. But at later time points, activation of the mTORCs phosphorylates ULK1 and suppresses autophagy and this leads to increased ZIKV protein expression and progeny production (lower part of the illustration).

replication, suggesting an anti-viral role of cellular antioxidant system in ZIKV infection.

Viruses are dependent on cellular metabolism and are known to significantly alter them. We found that ZIKV replication in infected cells is heavily dependent on glycolysis because the inhibition of glycolysis by 2-DG significantly reduced viral protein expression and glycosylation as well as infectious virion production (Fig 6.1). We have also demonstrated that upon inhibition of glycolysis, gluconeogenesis contributes to ZIKV replication, albeit to a lesser extent. Overall, these findings provide insights into the molecular mechanisms regarding mTORCs activation, redox homeostasis and metabolic alterations that are involved in ZIKV infection and replication. The major conclusions from the above studies are outlined below.

6.2 Conclusions

1. ZIKV infection induced activation of both mTORCs is necessary for viral protein expression and replication.
2. Autophagy is activated in ZIKV infected cells at early time points post infection and blockage of autophagy induction favors ZIKV replication.
3. ZIKV induced activation of mTORC1 downregulates autophagy which promotes ZIKV replication in infected cells.
4. Increased generation of ROS leads to oxidative stress induction in ZIKV infected cells.
5. Nrf2 mediated cellular antioxidant response plays an antiviral role and inhibits ZIKV replication.

6. Cellular GSH and NADPH are critical players in the antioxidant response to ZIKV infection.
7. Glycolysis is essential to ZIKV protein synthesis and glycosylation and infectious progeny production.
8. ZIKV replication is partially regulated by gluconeogenesis.

6.3 Future directions

6.3.1 Elucidate the mTOR-independent role of Raptor in ZIKV replication.

Studies reported in chapter 3 of this dissertation show that while depletion of mTOR kinase resulted in still-detectable levels of ZIKV E protein expression and progeny production, the siRNA mediated knockdown of Raptor exerted a more robust negative effect. Therefore, it would be very interesting to explore the molecular mechanisms involved in the mTOR-independent roles of Raptor in ZIKV replication. We intend to conduct proteomic analysis of mock- and ZIKV-infected cells and compare the interactome of Raptor under both conditions. This approach may help me identify unique proteins other than those involved in the mTOR pathway that Raptor interacts with which could potentially regulate ZIKV replication.

6.3.2 Which ZIKV proteins are involved in the early activation of autophagy and late activation of mTORCs?

The molecular mechanisms involved in the activation of autophagy in ZIKV infected cells are not yet clearly elucidated. While it is shown that NS4A and NS4B proteins of ZIKV can induce autophagy (Liang et al., 2016), such observations can be

dependent on several factors including the cell type, virus strain as well as the duration of infection. While the studies reported in chapter 3 of this dissertation demonstrate induction of autophagy early in infection, they do not dissect which viral proteins are involved in this process. Upon infection, the structural proteins of ZIKV are responsible for the interaction of the infecting virion with the cell surface receptors and subsequent internalization. Therefore, it is possible that one or a combination of the structural proteins or the viral genome itself, upon uncoating, may trigger autophagy in the infected cell. Furthermore, the role of the other NS proteins in the induction of autophagy cannot be ruled out. To identify the viral protein(s) that trigger autophagy in ZIKV infected cells, we intend to study the effect of ectopic expression of each of the viral proteins. Such a study will help identify the viral protein(s) responsible for the early induction of autophagy. Additionally, using a similar approach, we plan to identify the viral protein(s) that interact with the components of the mTOR signaling pathway leading to its activation. The findings from these studies will significantly contribute to the understanding of ZIKV induced modulations of cellular signaling pathways.

6.3.3. Explore the effect of ZIKV infection in neuron differentiation using LUHMES cells.

The human neuronal progenitor LUHMES cells are an interesting and physiologically relevant model system to study neuron differentiation. These cells can be differentiated into mature neurons given the right conditions (Scholz et al., 2011). Studies done in chapter 3 and 4 of this dissertation have shown that ZIKV infection activates mTOR signaling pathway as well as induces oxidative stress in these cells. While these

studies were conducted in undifferentiated LUHMES cells, we intend to determine the effect of ZIKV infection induced activation of mTOR cascade and oxidative stress on neuronal differentiation and maturation using these cells. By examining specific markers of mature neuron development from immature progenitor cells, we hope to dissect the mechanisms involved in ZIKV infection induced pathogenesis.

6.3.4. Study the genes involved in causing microcephaly.

Multiple studies have implicated the involvement of the mTOR signaling pathway in the regulation of brain development and induction of microcephaly (Cloetta et al., 2013; Lipton and Sahin, 2014; Thomanetz et al., 2013). It has also been shown that during brain development, the activation of the mTOR pathway is tightly regulated and any aberration results in developmental disorders. The MCPH class of proteins (MCPH 1-27) are known to regulate proper neurological development in fetuses (Siskos et al., 2021). While the direct involvement of mTOR signaling in modulation of these proteins has not yet been studied, it is possible that ZIKV induced activation of mTORCs differentially regulates their expression leading to improper brain development and neurological disease in infants. Additionally, ZIKV infection could alter the relative levels of these proteins leading to imbalances in the ratios of these proteins that may also result in microcephaly. Therefore, evaluation of the MCPH group of proteins in ZIKV infected cells by RNA-seq analysis as well as by Western blotting can be investigated and a possible link between ZIKV induced activation of the mTOR pathway with the expression status of the proteins can be established. This will provide important information on the molecular mechanisms of ZIKV induced microcephaly.

6.3.5. Mechanism of 6-AN induced inhibition of ZIKV.

The contrasting results obtained by the siRNA mediated depletion and pharmacological inhibition, by 6-AN, of PPP enzymes G6PD and 6PGD suggests a PPP-independent role of 6-AN in the inhibition of ZIKV replication. 6-AN is known to be metabolized in cells to 6-amino NAD and 6-amino NADP that act as antimetabolites and lead to a depletion of cellular pools of NAD and NADP, both of which are essential for the generation of NADPH. Therefore, it would be interesting to study the cellular processes, apart from PPP, that are affected by the exposure of cells to 6-AN and how such processes contribute to the inhibition of ZIKV replication. This will help elucidate the mechanisms involved inhibition of ZIKV by 6-AN.

6.3.6. Metabolomic analysis to determine the changes in cellular metabolism upon ZIKV infection.

The experimental findings described in chapter 5 highlight the dependency of ZIKV on cellular metabolic processes, such glycolysis and gluconeogenesis, for its replication. While these studies focus on the central carbon metabolism, a holistic understanding of overall cellular metabolic alterations induced by ZIKV infection is necessary to better understand the dynamics of host-virus interactions, identify unique features of virus infection as well as develop novel antiviral strategies. To this end, it would be interesting to conduct metabolomic analysis of cells infected with ZIKV and compare the metabolomic profile with that of uninfected cells. Such studies will significantly contribute to the understanding of host-virus interactions and may provide novel targets for drugs against ZIKV infections.

6.3.7. How does cellular GSH antagonize ZIKV?

Studies conducted in chapter 4 show that ZIKV infection causes a Nrf-2-dependent increase in GCLC which mediates the rate-limiting step in *de novo* GSH formation by the synthesis of its precursor, γ-glutamylcysteine. Cellular GSH is known to negatively affect the replication of prototypic flaviviruses such as DENV and ZIKV by inhibiting the activity of viral NS5 protein (Saisawang et al., 2018; Tian et al., 2010). While such studies have focused on the viral NS5 protein, the effect of glutathionylation of other viral proteins on virus replication cannot be overlooked. Therefore, we intend to examine the effect of the redox regulated post translational modification, glutathionylation, of other ZIKV proteins on viral protein expression and infectious virion production.

REFERENCES

2017. Chapter 29 - Flaviviridae. Academic Press, Boston.

Abernathy, E., Mateo, R., Majzoub, K., van Buuren, N., Bird, S.W., Carette, J.E., Kirkegaard, K., 2019. Differential and convergent utilization of autophagy components by positive-strand RNA viruses. PLoS Biol 17, e2006926.

Akiyama, B.M., Laurence, H.M., Massey, A.R., Costantino, D.A., Xie, X., Yang, Y., Shi, P.Y., Nix, J.C., Beckham, J.D., Kieft, J.S., 2016. Zika virus produces noncoding RNAs using a multi-pseudoknot structure that confounds a cellular exonuclease. Science 354, 1148-1152.

Aktepe, T.E., Mackenzie, J.M., 2018. Shaping the flavivirus replication complex: It is curvaceous! Cell Microbiol 20, e12884.

Allonso, D., Andrade, I.S., Conde, J.N., Coelho, D.R., Rocha, D.C., da Silva, M.L., Ventura, G.T., Silva, E.M., Mohana-Borges, R., 2015. Dengue Virus NS1 Protein Modulates Cellular Energy Metabolism by Increasing Glyceraldehyde-3-Phosphate Dehydrogenase Activity. J Virol 89, 11871-11883.

Almeida, L.T., Ferraz, A.C., da Silva Caetano, C.C., da Silva Menegatto, M.B., Dos Santos Pereira Andrade, A.C., Lima, R.L.S., Camini, F.C., Pereira, S.H., da Silva Pereira, K.Y., de Mello Silva, B., Perucci, L.O., Talvani, A., de Magalhaes, J.C., de Brito Magalhaes, C.L., 2020. Zika virus induces oxidative stress and decreases antioxidant enzyme activities in vitro and in vivo. Virus Res 286, 198084.

Annamalai, A.S., Pattnaik, A., Sahoo, B.R., Guinn, Z.P., Bullard, B.L., Weaver, E.A., Steffen, D., Natarajan, S.K., Petro, T.M., Pattnaik, A.K., 2019. An Attenuated Zika Virus Encoding Non-Glycosylated Envelope (E) and Non-Structural Protein 1 (NS1) Confers Complete Protection against Lethal Challenge in a Mouse Model. Vaccines (Basel) 7.

Annamalai, A.S., Pattnaik, A., Sahoo, B.R., Muthukrishnan, E., Natarajan, S.K., Steffen, D., Vu, H.L.X., Delhon, G., Osorio, F.A., Petro, T.M., Xiang, S.H., Pattnaik, A.K., 2017. Zika Virus Encoding Nonglycosylated Envelope Protein Is Attenuated and Defective in Neuroinvasion. J Virol 91.

Antoniou, E., Orovou, E., Sarella, A., Iliadou, M., Rigas, N., Palaska, E., Iatrakis, G., Dagla, M., 2020. Zika Virus and the Risk of Developing Microcephaly in Infants: A Systematic Review. Int J Environ Res Public Health 17.

Arfin, S., Jha, N.K., Jha, S.K., Kesari, K.K., Ruokolainen, J., Roychoudhury, S., Rathi, B., Kumar, D., 2021. Oxidative Stress in Cancer Cell Metabolism. Antioxidants (Basel) 10.

Arias, C.F., Preugschat, F., Strauss, J.H., 1993. Dengue 2 virus NS2B and NS3 form a stable complex that can cleave NS3 within the helicase domain. Virology 193, 888-899.

Au, W.Y., Ngai, C.W., Chan, W.M., Leung, R.Y., Chan, S.C., 2011. Hemolysis and methemoglobinemia due to hepatitis E virus infection in patient with G6PD deficiency. Ann Hematol 90, 1237-1238.

Avirutnan, P., Punyadee, N., Noisakran, S., Komoltri, C., Thiemmeca, S., Auethavornanan, K., Jairungsri, A., Kanlaya, R., Tangthawornchaikul, N., Puttikhunt, C., Pattanakitsakul, S.N., Yenchitsomanus, P.T., Mongkolsapaya, J., Kasinrerk, W., Sittisombut, N., Husmann, M., Blettner, M., Vasanawathana, S., Bhakdi, S., Malasit, P., 2006. Vascular leakage in severe dengue virus infections: a potential role for the nonstructural viral protein NS1 and complement. J Infect Dis 193, 1078-1088.

Bagdonaite, I., Wandall, H.H., 2018. Global aspects of viral glycosylation. Glycobiology 28, 443-467.

Baird, L., Swift, S., Lleres, D., Dinkova-Kostova, A.T., 2014. Monitoring Keap1-Nrf2 interactions in single live cells. Biotechnol Adv 32, 1133-1144.

Barbelanne, M., Tsang, W.Y., 2014. Molecular and cellular basis of autosomal recessive primary microcephaly. Biomed Res Int 2014, 547986.

Barrows, N.J., Campos, R.K., Liao, K.C., Prasanth, K.R., Soto-Acosta, R., Yeh, S.C., Schott-Lerner, G., Pompon, J., Sessions, O.M., Bradrick, S.S., Garcia-Blanco, M.A., 2018. Biochemistry and Molecular Biology of Flaviviruses. Chem Rev 118, 4448-4482.

Beatman, E., Oyer, R., Shives, K.D., Hedman, K., Brault, A.C., Tyler, K.L., Beckham, J.D., 2012. West Nile virus growth is independent of autophagy activation. Virology 433, 262-272.

Beltramello, M., Williams, K.L., Simmons, C.P., Macagno, A., Simonelli, L., Quyen, N.T., Sukupolvi-Petty, S., Navarro-Sanchez, E., Young, P.R., de Silva, A.M., Rey, F.A., Varani, L., Whitehead, S.S., Diamond, M.S., Harris, E., Lanzavecchia, A., Sallusto, F., 2010. The human immune response to Dengue virus is dominated by highly cross-reactive antibodies endowed with neutralizing and enhancing activity. Cell Host Microbe 8, 271-283.

Birben, E., Sahiner, U.M., Sackesen, C., Erzurum, S., Kalayci, O., 2012. Oxidative stress and antioxidant defense. World Allergy Organ J 5, 9-19.

Boyer, S., Calvez, E., Chouin-Carneiro, T., Diallo, D., Failloux, A.B., 2018. An overview of mosquito vectors of Zika virus. Microbes Infect 20, 646-660.

Brand, S.R., Kobayashi, R., Mathews, M.B., 1997. The Tat protein of human immunodeficiency virus type 1 is a substrate and inhibitor of the interferon-induced, virally activated protein kinase, PKR. J Biol Chem 272, 8388-8395.

Brecher, M., Zhang, J., Li, H., 2013. The flavivirus protease as a target for drug discovery. Virol Sin 28, 326-336.

Brinton, M.A., Dispoto, J.H., 1988. Sequence and secondary structure analysis of the 5'-terminal region of flavivirus genome RNA. Virology 162, 290-299.

Brinton, M.A., Fernandez, A.V., Dispoto, J.H., 1986. The 3'-nucleotides of flavivirus genomic RNA form a conserved secondary structure. Virology 153, 113-121.

Buchkovich, N.J., Yu, Y., Zampieri, C.A., Alwine, J.C., 2008. The TORrid affairs of viruses: effects of mammalian DNA viruses on the PI3K-Akt-mTOR signalling pathway. Nat Rev Microbiol 6, 266-275.

Burger-Calderon, R., Gonzalez, K., Ojeda, S., Zambrana, J.V., Sanchez, N., Cerpas Cruz, C., Suazo Laguna, H., Bustos, F., Plazaola, M., Lopez Mercado, B., Elizondo, D., Arguello, S., Carey Monterrey, J., Nunez, A., Coloma, J., Waggoner, J.J., Gordon, A., Kuan, G., Balmaseda, A., Harris, E., 2018. Zika virus infection in Nicaraguan households. PLoS Negl Trop Dis 12, e0006518.

Byk, L.A., Gamarnik, A.V., 2016. Properties and Functions of the Dengue Virus Capsid Protein. Annu Rev Virol 3, 263-281.

Cao-Lormeau, V.M., Blake, A., Mons, S., Lastere, S., Roche, C., Vanhomwegen, J., Dub, T., Baudouin, L., Teissier, A., Larre, P., Vial, A.L., Decam, C., Choumet, V., Halstead, S.K., Willison, H.J., Musset, L., Manuguerra, J.C., Despres, P., Fournier, E., Mallet, H.P., Musso, D., Fontanet, A., Neil, J., Ghawche, F., 2016. Guillain-Barre Syndrome outbreak associated with Zika virus infection in French Polynesia: a case-control study. Lancet 387, 1531-1539.

Cao-Lormeau, V.M., Roche, C., Teissier, A., Robin, E., Berry, A.L., Mallet, H.P., Sall, A.A., Musso, D., 2014. Zika virus, French polynesia, South pacific, 2013. Emerg Infect Dis 20, 1085-1086.

Cao, B., Parnell, L.A., Diamond, M.S., Mysorekar, I.U., 2017. Inhibition of autophagy limits vertical transmission of Zika virus in pregnant mice. J Exp Med 214, 2303-2313.

Carbaugh, D.L., Baric, R.S., Lazear, H.M., 2019. Envelope Protein Glycosylation Mediates Zika Virus Pathogenesis. J Virol 93.

Carteaux, G., Maquart, M., Bedet, A., Contou, D., Brugieres, P., Fourati, S., Cleret de Langavant, L., de Broucker, T., Brun-Buisson, C., Leparc-Goffart, I., Mekontso Dessap, A., 2016. Zika Virus Associated with Meningoencephalitis. N Engl J Med 374, 1595-1596.

Chambers, T.J., Grakoui, A., Rice, C.M., 1991. Processing of the yellow fever virus nonstructural polyprotein: a catalytically active NS3 proteinase domain and NS2B are required for cleavages at dibasic sites. J Virol 65, 6042-6050.

Chambers, T.J., Hahn, C.S., Galler, R., Rice, C.M., 1990. Flavivirus genome organization, expression, and replication. Annu Rev Microbiol 44, 649-688.

Chambers, T.J., Nestorowicz, A., Amberg, S.M., Rice, C.M., 1993. Mutagenesis of the yellow fever virus NS2B protein: effects on proteolytic processing, NS2B-NS3 complex formation, and viral replication. J Virol 67, 6797-6807.

Chao, Y.C., Huang, C.S., Lee, C.N., Chang, S.Y., King, C.C., Kao, C.L., 2008. Higher infection of dengue virus serotype 2 in human monocytes of patients with G6PD deficiency. PLoS One 3, e1557.

Christian, K.M., Song, H., Ming, G.L., 2019. Pathophysiology and Mechanisms of Zika Virus Infection in the Nervous System. Annu Rev Neurosci 42, 249-269.

Chu, L.W., Huang, Y.L., Lee, J.H., Huang, L.Y., Chen, W.J., Lin, Y.H., Chen, J.Y., Xiang, R., Lee, C.H., Ping, Y.H., 2014. Single-virus tracking approach to reveal the interaction of Dengue virus with autophagy during the early stage of infection. J Biomed Opt 19, 011018.

Clippinger, A.J., Maguire, T.G., Alwine, J.C., 2011. The changing role of mTOR kinase in the maintenance of protein synthesis during human cytomegalovirus infection. J Virol 85, 3930-3939.

Cloetta, D., Thomanetz, V., Baranek, C., Lustenberger, R.M., Lin, S., Oliveri, F., Atanasoski, S., Ruegg, M.A., 2013. Inactivation of mTORC1 in the developing brain causes microcephaly and affects gliogenesis. J Neurosci 33, 7799-7810.

Cooke, M.S., Evans, M.D., Dizdaroglu, M., Lunec, J., 2003. Oxidative DNA damage: mechanisms, mutation, and disease. FASEB J 17, 1195-1214.

Costin, J.M., Zaitseva, E., Kahle, K.M., Nicholson, C.O., Rowe, D.K., Graham, A.S., Bazzone, L.E., Hogancamp, G., Figueroa Sierra, M., Fong, R.H., Yang, S.T., Lin, L., Robinson, J.E., Doranz, B.J., Chernomordik, L.V., Michael, S.F., Schieffelin, J.S., Isern, S., 2013. Mechanistic study of broadly neutralizing human monoclonal antibodies against dengue virus that target the fusion loop. J Virol 87, 52-66.

Coyne, C.B., Lazear, H.M., 2016. Zika virus - reigniting the TORCH. Nat Rev Microbiol 14, 707-715.

Cruz-Oliveira, C., Freire, J.M., Conceicao, T.M., Higa, L.M., Castanho, M.A., Da Poian, A.T., 2015. Receptors and routes of dengue virus entry into the host cells. FEMS Microbiol Rev 39, 155-170.

Cugola, F.R., Fernandes, I.R., Russo, F.B., Freitas, B.C., Dias, J.L., Guimaraes, K.P., Benazzato, C., Almeida, N., Pignatari, G.C., Romero, S., Polonio, C.M., Cunha, I., Freitas, C.L., Brandao, W.N., Rossato, C., Andrade, D.G., Faria Dde, P., Garcez, A.T., Buchpigel, C.A., Braconi, C.T., Mendes, E., Sall, A.A., Zanotto, P.M., Peron, J.P., Muotri, A.R., Beltrao-Braga, P.C., 2016. The Brazilian Zika virus strain causes birth defects in experimental models. Nature 534, 267-271.

Cullinan, S.B., Gordan, J.D., Jin, J., Harper, J.W., Diehl, J.A., 2004. The Keap1-BTB protein is an adaptor that bridges Nrf2 to a Cul3-based E3 ligase: oxidative stress sensing by a Cul3-Keap1 ligase. Mol Cell Biol 24, 8477-8486.

D'Ortenzio, E., Matheron, S., Yazdanpanah, Y., de Lamballerie, X., Hubert, B., Piorkowski, G., Maquart, M., Descamps, D., Damond, F., Leparc-Goffart, I., 2016. Evidence of Sexual Transmission of Zika Virus. N Engl J Med 374, 2195-2198.

Dai, L., Song, J., Lu, X., Deng, Y.Q., Musyoki, A.M., Cheng, H., Zhang, Y., Yuan, Y., Song, H., Haywood, J., Xiao, H., Yan, J., Shi, Y., Qin, C.F., Qi, J., Gao, G.F., 2016. Structures of the Zika Virus Envelope Protein and Its Complex with a Flavivirus Broadly Protective Antibody. Cell Host Microbe 19, 696-704.

Dalton, T.P., Shertzer, H.G., Puga, A., 1999. Regulation of gene expression by reactive oxygen. Annu Rev Pharmacol Toxicol 39, 67-101.

Dandekar, A., Mendez, R., Zhang, K., 2015. Cross talk between ER stress, oxidative stress, and inflammation in health and disease. Methods Mol Biol 1292, 205-214.

Dang, J., Tiwari, S.K., Lichinchi, G., Qin, Y., Patil, V.S., Eroshkin, A.M., Rana, T.M., 2016. Zika Virus Depletes Neural Progenitors in Human Cerebral Organoids through Activation of the Innate Immune Receptor TLR3. Cell Stem Cell 19, 258-265.

Datan, E., Roy, S.G., Germain, G., Zali, N., McLean, J.E., Golshan, G., Harbajan, S., Lockshin, R.A., Zakeri, Z., 2016. Dengue-induced autophagy, virus replication and protection from cell death require ER stress (PERK) pathway activation. Cell Death Dis 7, e2127.

de Groot, R.P., Schouten, G.J., de Wit, L., Ballou, L.M., van der Eb, A.J., Zantema, A., 1995. Induction of the mitogen-activated p70 S6 kinase by adenovirus E1A. Oncogene 10, 543-548.

DeBlasi, J.M., DeNicola, G.M., 2020. Dissecting the Crosstalk between NRF2 Signaling and Metabolic Processes in Cancer. Cancers (Basel) 12.

Delgado, T., Sanchez, E.L., Camarda, R., Lagunoff, M., 2012. Global metabolic profiling of infection by an oncogenic virus: KSHV induces and requires lipogenesis for survival of latent infection. PLoS Pathog 8, e1002866.

Delvecchio, R., Higa, L.M., Pezzuto, P., Valadao, A.L., Garcez, P.P., Monteiro, F.L., Loiola, E.C., Dias, A.A., Silva, F.J., Aliota, M.T., Caine, E.A., Osorio, J.E., Bellio, M., O'Connor, D.H., Rehen, S., de Aguiar, R.S., Savarino, A., Campanati, L., Tanuri, A., 2016. Chloroquine, an Endocytosis Blocking Agent, Inhibits Zika Virus Infection in Different Cell Models. Viruses 8.

Deretic, V., Saitoh, T., Akira, S., 2013. Autophagy in infection, inflammation and immunity. Nat Rev Immunol 13, 722-737.

Diamond, D.L., Syder, A.J., Jacobs, J.M., Sorensen, C.M., Walters, K.A., Proll, S.C., McDermott, J.E., Gritsenko, M.A., Zhang, Q., Zhao, R., Metz, T.O., Camp, D.G., 2nd, Waters, K.M., Smith, R.D., Rice, C.M., Katze, M.G., 2010. Temporal proteome and lipidome profiles reveal hepatitis C virus-associated reprogramming of hepatocellular metabolism and bioenergetics. PLoS Pathog 6, e1000719.

Diamond, M.S., Pierson, T.C., 2015. Molecular Insight into Dengue Virus Pathogenesis and Its Implications for Disease Control. Cell 162, 488-492.

Dick, G.W., Kitchen, S.F., Haddow, A.J., 1952. Zika virus. I. Isolations and serological specificity. Trans R Soc Trop Med Hyg 46, 509-520.

Dreux, M., Gastaminza, P., Wieland, S.F., Chisari, F.V., 2009. The autophagy machinery is required to initiate hepatitis C virus replication. Proc Natl Acad Sci U S A 106, 14046-14051.

Driggers, R.W., Ho, C.Y., Korhonen, E.M., Kuivanen, S., Jaaskelainen, A.J., Smura, T., Rosenberg, A., Hill, D.A., DeBiasi, R.L., Vezina, G., Timofeev, J., Rodriguez, F.J., Levanov, L., Razak, J., Iyengar, P., Hennenfent, A., Kennedy, R., Lanciotti, R., du Plessis, A., Vapalahti, O., 2016. Zika Virus Infection with Prolonged Maternal Viremia and Fetal Brain Abnormalities. N Engl J Med 374, 2142-2151.

Dumont, F.J., Su, Q., 1996. Mechanism of action of the immunosuppressant rapamycin. Life Sci 58, 373-395.

Efeyan, A., Sabatini, D.M., 2010. mTOR and cancer: many loops in one pathway. Current opinion in cell biology 22, 169-176.

Elshahawi, H., Syed Hassan, S., Balasubramaniam, V., 2019. Importance of Zika Virus NS5 Protein for Viral Replication. Pathogens 8.

Faizan, M.I., Abdullah, M., Ali, S., Naqvi, I.H., Ahmed, A., Parveen, S., 2016. Zika Virus-Induced Microcephaly and Its Possible Molecular Mechanism. Intervirology 59, 152-158.

Feldman, M.E., Apsel, B., Uotila, A., Loewith, R., Knight, Z.A., Ruggero, D., Shokat, K.M., 2009. Active-site inhibitors of mTOR target rapamycin-resistant outputs of mTORC1 and mTORC2. PLoS Biol 7, e38.

Fernandez-Marcos, P.J., Nobrega-Pereira, S., 2016. NADPH: new oxygen for the ROS theory of aging. Oncotarget 7, 50814-50815.

Ferrari, M., Zevini, A., Palermo, E., Muscolini, M., Alexandridi, M., Etna, M.P., Coccia, E.M., Fernandez-Sesma, A., Coyne, C., Zhang, D.D., Marques, E.T.A., Olagnier, D., Hiscott, J.,

2020. Dengue Virus Targets Nrf2 for NS2B3-Mediated Degradation Leading to Enhanced Oxidative Stress and Viral Replication. J Virol 94.

Figueiredo, V.C., Markworth, J.F., Cameron-Smith, D., 2017. Considerations on mTOR regulation at serine 2448: implications for muscle metabolism studies. Cellular and molecular life sciences : CMLS 74, 2537-2545.

Fontaine, K.A., Sanchez, E.L., Camarda, R., Lagunoff, M., 2015. Dengue virus induces and requires glycolysis for optimal replication. J Virol 89, 2358-2366.

Fontes-Garfias, C.R., Shan, C., Luo, H., Muruato, A.E., Medeiros, D.B.A., Mays, E., Xie, X., Zou, J., Roundy, C.M., Wakamiya, M., Rossi, S.L., Wang, T., Weaver, S.C., Shi, P.Y., 2017. Functional Analysis of Glycosylation of Zika Virus Envelope Protein. Cell Rep 21, 1180-1190.

Foster, K.G., Fingar, D.C., 2010. Mammalian target of rapamycin (mTOR): conducting the cellular signaling symphony. J Biol Chem 285, 14071-14077.

Franco, R., Cidlowski, J.A., 2012. Glutathione efflux and cell death. Antioxid Redox Signal 17, 1694-1713.

Gabriel, E., Ramani, A., Karow, U., Gottardo, M., Natarajan, K., Gooi, L.M., Goranci-Buzhala, G., Krut, O., Peters, F., Nikolic, M., Kuivanen, S., Korhonen, E., Smura, T., Vapalahti, O., Papantonis, A., Schmidt-Chanasit, J., Riparbelli, M., Callaini, G., Kronke, M., Utermohlen, O., Gopalakrishnan, J., 2017. Recent Zika Virus Isolates Induce Premature Differentiation of Neural Progenitors in Human Brain Organoids. Cell Stem Cell 20, 397-406 e395.

Ganley, I.G., Lam du, H., Wang, J., Ding, X., Chen, S., Jiang, X., 2009. ULK1.ATG13.FIP200 complex mediates mTOR signaling and is essential for autophagy. J Biol Chem 284, 12297-12305.

Gannage, M., Dormann, D., Albrecht, R., Dengjel, J., Torossi, T., Ramer, P.C., Lee, M., Strowig, T., Arrey, F., Conenello, G., Pypaert, M., Andersen, J., Garcia-Sastre, A., Munz, C., 2009. Matrix protein 2 of influenza A virus blocks autophagosome fusion with lysosomes. Cell Host Microbe 6, 367-380.

Garcez, P.P., Loiola, E.C., Madeiro da Costa, R., Higa, L.M., Trindade, P., Delvecchio, R., Nascimento, J.M., Brindeiro, R., Tanuri, A., Rehen, S.K., 2016. Zika virus impairs growth in human neurospheres and brain organoids. Science 352, 816-818.

Garcez, P.P., Nascimento, J.M., de Vasconcelos, J.M., Madeiro da Costa, R., Delvecchio, R., Trindade, P., Loiola, E.C., Higa, L.M., Cassoli, J.S., Vitoria, G., Sequeira, P.C., Sochacki, J., Aguiar, R.S., Fuzii, H.T., de Filippis, A.M., da Silva Goncalves Vianez Junior, J.L., Tanuri, A., Martins-de-Souza, D., Rehen, S.K., 2017. Zika virus disrupts molecular fingerprinting of human neurospheres. Sci Rep 7, 40780.

Garcia-Garcia, A., Anandhan, A., Burns, M., Chen, H., Zhou, Y., Franco, R., 2013. Impairment of Atg5-dependent autophagic flux promotes paraquat- and MPP(+)-induced apoptosis but not rotenone or 6-hydroxydopamine toxicity. Toxicol Sci 136, 166-182.

Gebhard, L.G., Filomatori, C.V., Gamarnik, A.V., 2011. Functional RNA elements in the dengue virus genome. Viruses 3, 1739-1756.

George, A., Panda, S., Kudmulwar, D., Chhatbar, S.P., Nayak, S.C., Krishnan, H.H., 2012. Hepatitis C virus NS5A binds to the mRNA cap-binding eukaryotic translation initiation 4F (eIF4F) complex and up-regulates host translation initiation machinery through eIF4E-binding protein 1 inactivation. J Biol Chem 287, 5042-5058.

Gerold, G., Bruening, J., Weigel, B., Pietschmann, T., 2017. Protein Interactions during the Flavivirus and Hepacivirus Life Cycle. Mol Cell Proteomics 16, S75-S91.

Gil, L., Martinez, G., Tapanes, R., Castro, O., Gonzalez, D., Bernardo, L., Vazquez, S., Kouri, G., Guzman, M.G., 2004. Oxidative stress in adult dengue patients. Am J Trop Med Hyg 71, 652-657.

Gingras, A.C., Gygi, S.P., Raught, B., Polakiewicz, R.D., Abraham, R.T., Hoekstra, M.F., Aebersold, R., Sonenberg, N., 1999. Regulation of 4E-BP1 phosphorylation: a novel two-step mechanism. Genes Dev 13, 1422-1437.

Gingras, A.C., Kennedy, S.G., O'Leary, M.A., Sonenberg, N., Hay, N., 1998. 4E-BP1, a repressor of mRNA translation, is phosphorylated and inactivated by the Akt(PKB) signaling pathway. Genes Dev 12, 502-513.

Gkountakos, A., Pilotto, S., Mafficini, A., Vicentini, C., Simbolo, M., Milella, M., Tortora, G., Scarpa, A., Bria, E., Corbo, V., 2018. Unmasking the impact of Rictor in cancer: novel insights of mTORC2 complex. Carcinogenesis 39, 971-980.

Godoy, A.S., Lima, G.M., Oliveira, K.I., Torres, N.U., Maluf, F.V., Guido, R.V., Oliva, G., 2017. Crystal structure of Zika virus NS5 RNA-dependent RNA polymerase. Nat Commun 8, 14764.

Gorrini, C., Harris, I.S., Mak, T.W., 2013. Modulation of oxidative stress as an anticancer strategy. Nat Rev Drug Discov 12, 931-947.

Gullberg, R.C., Jordan Steel, J., Moon, S.L., Soltani, E., Geiss, B.J., 2015. Oxidative stress influences positive strand RNA virus genome synthesis and capping. Virology 475, 219-229.

Gupta, G., Lim, L., Song, J., 2015. NMR and MD Studies Reveal That the Isolated Dengue NS3 Protease Is an Intrinsically Disordered Chymotrypsin Fold Which Absolutely Requests NS2B for Correct Folding and Functional Dynamics. PLoS One 10, e0134823.

Hackett, B.A., Cherry, S., 2018. Flavivirus internalization is regulated by a size-dependent endocytic pathway. Proc Natl Acad Sci U S A 115, 4246-4251.

Halliwell, B., 2007. Biochemistry of oxidative stress. Biochem Soc Trans 35, 1147-1150.

Hamel, R., Dejarnac, O., Wichit, S., Ekchariyawat, P., Neyret, A., Luplertlop, N., Perera-Lecoin, M., Surasombatpattana, P., Talignani, L., Thomas, F., Cao-Lormeau, V.M., Choumet, V., Briant, L., Despres, P., Amara, A., Yssel, H., Misse, D., 2015. Biology of Zika Virus Infection in Human Skin Cells. J Virol 89, 8880-8896.

Hansen, I.A., Attardo, G.M., Park, J.H., Peng, Q., Raikhel, A.S., 2004. Target of rapamycin-mediated amino acid signaling in mosquito anautogeny. Proc Natl Acad Sci U S A 101, 10626-10631.

Hayes, J.D., Dinkova-Kostova, A.T., 2014. The Nrf2 regulatory network provides an interface between redox and intermediary metabolism. Trends Biochem Sci 39, 199-218.

Heaton, N.S., Perera, R., Berger, K.L., Khadka, S., Lacount, D.J., Kuhn, R.J., Randall, G., 2010. Dengue virus nonstructural protein 3 redistributes fatty acid synthase to sites of viral replication and increases cellular fatty acid synthesis. Proc Natl Acad Sci U S A 107, 17345-17350.

Heaton, N.S., Randall, G., 2010. Dengue virus-induced autophagy regulates lipid metabolism. Cell Host Microbe 8, 422-432.

Heukelbach, J., Alencar, C.H., Kelvin, A.A., de Oliveira, W.K., Pamplona de Goes Cavalcanti, L., 2016. Zika virus outbreak in Brazil. J Infect Dev Ctries 10, 116-120.

Ho, H.Y., Cheng, M.L., Weng, S.F., Chang, L., Yeh, T.T., Shih, S.R., Chiu, D.T., 2008. Glucose-6-phosphate dehydrogenase deficiency enhances enterovirus 71 infection. J Gen Virol 89, 2080-2089.

Hsieh, S.C., Zou, G., Tsai, W.Y., Qing, M., Chang, G.J., Shi, P.Y., Wang, W.K., 2011. The C-terminal helical domain of dengue virus precursor membrane protein is involved in virus assembly and entry. Virology 410, 170-180.

Huang, H., Falgout, B., Takeda, K., Yamada, K.M., Dhawan, S., 2017. Nrf2-dependent induction of innate host defense via heme oxygenase-1 inhibits Zika virus replication. Virology 503, 1-5.

Huang, J., Manning, B.D., 2009. A complex interplay between Akt, TSC2 and the two mTOR complexes. Biochem Soc Trans 37, 217-222.

Huang, W.C., Abraham, R., Shim, B.S., Choe, H., Page, D.T., 2016. Zika virus infection during the period of maximal brain growth causes microcephaly and corticospinal neuron apoptosis in wild type mice. Sci Rep 6, 34793.

Huang, Y., Wang, Y., Meng, S., Chen, Z., Kong, H., Pan, T., Lu, G., Li, X., 2020. Autophagy Contributes to Host Immunity and Protection against Zika Virus Infection via Type I IFN Signaling. Mediators Inflamm 2020, 9527147.

Inoki, K., Li, Y., Zhu, T., Wu, J., Guan, K.L., 2002. TSC2 is phosphorylated and inhibited by Akt and suppresses mTOR signalling. Nat Cell Biol 4, 648-657.

Itoh, K., Chiba, T., Takahashi, S., Ishii, T., Igarashi, K., Katoh, Y., Oyake, T., Hayashi, N., Satoh, K., Hatayama, I., Yamamoto, M., Nabeshima, Y., 1997. An Nrf2/small Maf heterodimer mediates the induction of phase II detoxifying enzyme genes through antioxidant response elements. Biochem Biophys Res Commun 236, 313-322.

Itoh, K., Wakabayashi, N., Katoh, Y., Ishii, T., Igarashi, K., Engel, J.D., Yamamoto, M., 1999. Keap1 represses nuclear activation of antioxidant responsive elements by Nrf2 through binding to the amino-terminal Neh2 domain. Genes Dev 13, 76-86.

Ivanov, A.V., Bartosch, B., Smirnova, O.A., Isaguliants, M.G., Kochetkov, S.N., 2013. HCV and oxidative stress in the liver. Viruses 5, 439-469.

Jan, E., Mohr, I., Walsh, D., 2016. A Cap-to-Tail Guide to mRNA Translation Strategies in Virus-Infected Cells. Annu Rev Virol 3, 283-307.

Johri, M.K., Lashkari, H.V., Gupta, D., Vedagiri, D., Harshan, K.H., 2019. mTORC1 restricts hepatitis C virus RNA replication through ULK1-mediated suppression of miR-122 and facilitates post-replication events. The Journal of general virology.

Jordan, T.X., Randall, G., 2016. Flavivirus modulation of cellular metabolism. Curr Opin Virol 19, 7-10.

Julien, L.A., Carriere, A., Moreau, J., Roux, P.P., 2010. mTORC1-activated S6K1 phosphorylates Rictor on threonine 1135 and regulates mTORC2 signaling. Molecular and cellular biology 30, 908-921.

Karimi, O., Goorhuis, A., Schinkel, J., Codrington, J., Vreden, S.G.S., Vermaat, J.S., Stijnis, C., Grobusch, M.P., 2016. Thrombocytopenia and subcutaneous bleedings in a patient with Zika virus infection. Lancet 387, 939-940.

Karuppan, M.K.M., Ojha, C.R., Rodriguez, M., Lapierre, J., Aman, M.J., Kashanchi, F., Toborek, M., Nair, M., El-Hage, N., 2020. Reduced-Beclin1-Expressing Mice Infected with Zika-R103451 and Viral-Associated Pathology during Pregnancy. Viruses 12.

Kassai, H., Sugaya, Y., Noda, S., Nakao, K., Maeda, T., Kano, M., Aiba, A., 2014. Selective activation of mTORC1 signaling recapitulates microcephaly, tuberous sclerosis, and neurodegenerative diseases. Cell Rep 7, 1626-1639.

Kazmi, S.S., Ali, W., Bibi, N., Nouroz, F., 2020. A review on Zika virus outbreak, epidemiology, transmission and infection dynamics. J Biol Res (Thessalon) 27, 5.

Ke, P.Y., 2018. The Multifaceted Roles of Autophagy in Flavivirus-Host Interactions. Int J Mol Sci 19.

Ke, P.Y., Chen, S.S., 2011. Activation of the unfolded protein response and autophagy after hepatitis C virus infection suppresses innate antiviral immunity in vitro. J Clin Invest 121, 37-56.

Khakpoor, A., Panyasrivanit, M., Wikan, N., Smith, D.R., 2009. A role for autophagolysosomes in dengue virus 3 production in HepG2 cells. J Gen Virol 90, 1093-1103.

Khandia, R., Dadar, M., Munjal, A., Dhama, K., Karthik, K., Tiwari, R., Yatoo, M.I., Iqbal, H.M.N., Singh, K.P., Joshi, S.K., Chaicumpa, W., 2019. A Comprehensive Review of Autophagy and Its Various Roles in Infectious, Non-Infectious, and Lifestyle Diseases: Current Knowledge and Prospects for Disease Prevention, Novel Drug Design, and Therapy. Cells 8.

Kim, J., Kundu, M., Viollet, B., Guan, K.L., 2011. AMPK and mTOR regulate autophagy through direct phosphorylation of Ulk1. Nat Cell Biol 13, 132-141.

Kim, K., Qiang, L., Hayden, M.S., Sparling, D.P., Purcell, N.H., Pajvani, U.B., 2016. mTORC1-independent Raptor prevents hepatic steatosis by stabilizing PHLPP2. Nature communications 7, 10255.

Kim, Y.C., Guan, K.L., 2015. mTOR: a pharmacologic target for autophagy regulation. J Clin Invest 125, 25-32.

Kindhauser, M.K., Allen, T., Frank, V., Santhana, R.S., Dye, C., 2016. Zika: the origin and spread of a mosquito-borne virus. Bull World Health Organ 94, 675-686C.

Kobayashi, A., Kang, M.I., Okawa, H., Ohtsuji, M., Zenke, Y., Chiba, T., Igarashi, K., Yamamoto, M., 2004. Oxidative stress sensor Keap1 functions as an adaptor for Cul3-based E3 ligase to regulate proteasomal degradation of Nrf2. Mol Cell Biol 24, 7130-7139.

Kobayashi, S., Orba, Y., Yamaguchi, H., Takahashi, K., Sasaki, M., Hasebe, R., Kimura, T., Sawa, H., 2014. Autophagy inhibits viral genome replication and gene expression stages in West Nile virus infection. Virus Res 191, 83-91.

Kong, E.Y., Cheng, S.H., Yu, K.N., 2018. Induction of autophagy and interleukin 6 secretion in bystander cells: metabolic cooperation for radiation-induced rescue effect? J Radiat Res 59, 129-140.

Korenaga, M., Wang, T., Li, Y., Showalter, L.A., Chan, T., Sun, J., Weinman, S.A., 2005. Hepatitis C virus core protein inhibits mitochondrial electron transport and increases reactive oxygen species (ROS) production. J Biol Chem 280, 37481-37488.

Kostyuchenko, V.A., Lim, E.X., Zhang, S., Fibriansah, G., Ng, T.S., Ooi, J.S., Shi, J., Lok, S.M., 2016. Structure of the thermally stable Zika virus. Nature 533, 425-428.

Kudchodkar, S.B., Yu, Y., Maguire, T.G., Alwine, J.C., 2006. Human cytomegalovirus infection alters the substrate specificities and rapamycin sensitivities of raptor- and rictor-containing complexes. Proc Natl Acad Sci U S A 103, 14182-14187.

Kumar, A., Hou, S., Airo, A.M., Limonta, D., Mancinelli, V., Branton, W., Power, C., Hobman, T.C., 2016. Zika virus inhibits type-I interferon production and downstream signaling. EMBO Rep 17, 1766-1775.

Kuno, G., Chang, G.J., 2007. Full-length sequencing and genomic characterization of Bagaza, Kedougou, and Zika viruses. Arch Virol 152, 687-696.

Kuss-Duerkop, S.K., Wang, J., Mena, I., White, K., Metreveli, G., Sakthivel, R., Mata, M.A., Munoz-Moreno, R., Chen, X., Krammer, F., Diamond, M.S., Chen, Z.J., Garcia-Sastre, A., Fontoura, B.M.A., 2017. Influenza virus differentially activates mTORC1 and mTORC2 signaling to maximize late stage replication. PLoS Pathog 13, e1006635.

Lamark, T., Svenning, S., Johansen, T., 2017. Regulation of selective autophagy: the p62/SQSTM1 paradigm. Essays Biochem 61, 609-624.

Lancaster, M.A., Renner, M., Martin, C.A., Wenzel, D., Bicknell, L.S., Hurles, M.E., Homfray, T., Penninger, J.M., Jackson, A.P., Knoblich, J.A., 2013. Cerebral organoids model human brain development and microcephaly. Nature 501, 373-379.

Lazear, H.M., Diamond, M.S., 2016. Zika Virus: New Clinical Syndromes and Its Emergence in the Western Hemisphere. J Virol 90, 4864-4875.

Le Sage, V., Cinti, A., Amorim, R., Mouland, A.J., 2016. Adapting the Stress Response: Viral Subversion of the mTOR Signaling Pathway. Viruses 8.

Ledur, P.F., Karmirian, K., Pedrosa, C., Souza, L.R.Q., Assis-de-Lemos, G., Martins, T.M., Ferreira, J., de Azevedo Reis, G.F., Silva, E.S., Silva, D., Salerno, J.A., Ornelas, I.M., Devalle, S., Madeiro da Costa, R.F., Goto-Silva, L., Higa, L.M., Melo, A., Tanuri, A., Chimelli, L., Murata, M.M., Garcez, P.P., Filippi-Chiela, E.C., Galina, A., Borges, H.L., Rehen, S.K., 2020. Zika virus infection leads to mitochondrial failure, oxidative stress and DNA damage in human iPSC-derived astrocytes. Sci Rep 10, 1218.

Lee, C.J., Liao, C.L., Lin, Y.L., 2005. Flavivirus activates phosphatidylinositol 3-kinase signaling to block caspase-dependent apoptotic cell death at the early stage of virus infection. J Virol 79, 8388-8399.

Lee, H.K., Iwasaki, A., 2008. Autophagy and antiviral immunity. Curr Opin Immunol 20, 23-29.

Lee, J.M., Calkins, M.J., Chan, K., Kan, Y.W., Johnson, J.A., 2003. Identification of the NF-E2-related factor-2-dependent genes conferring protection against oxidative stress in primary cortical astrocytes using oligonucleotide microarray analysis. J Biol Chem 278, 12029-12038.

Lee, Y.R., Hu, H.Y., Kuo, S.H., Lei, H.Y., Lin, Y.S., Yeh, T.M., Liu, C.C., Liu, H.S., 2013. Dengue virus infection induces autophagy: an in vivo study. J Biomed Sci 20, 65.

Lee, Y.R., Lei, H.Y., Liu, M.T., Wang, J.R., Chen, S.H., Jiang-Shieh, Y.F., Lin, Y.S., Yeh, T.M., Liu, C.C., Liu, H.S., 2008. Autophagic machinery activated by dengue virus enhances virus replication. Virology 374, 240-248.

Li, A., Wang, W., Wang, Y., Chen, K., Xiao, F., Hu, D., Hui, L., Liu, W., Feng, Y., Li, G., Tan, Q., Liu, Y., Wu, K., Wu, J., 2020. NS5 Conservative Site Is Required for Zika Virus to Restrict the RIG-I Signaling. Front Immunol 11, 51.

Li, C., Xu, D., Ye, Q., Hong, S., Jiang, Y., Liu, X., Zhang, N., Shi, L., Qin, C.F., Xu, Z., 2016a. Zika Virus Disrupts Neural Progenitor Development and Leads to Microcephaly in Mice. Cell Stem Cell 19, 120-126.

Li, G., Poulsen, M., Fenyvuesvolgyi, C., Yashiroda, Y., Yoshida, M., Simard, J.M., Gallo, R.C., Zhao, R.Y., 2017a. Characterization of cytopathic factors through genome-wide analysis of the Zika viral proteins in fission yeast. Proc Natl Acad Sci U S A 114, E376-E385.

Li, H., Clum, S., You, S., Ebner, K.E., Padmanabhan, R., 1999. The serine protease and RNA-stimulated nucleoside triphosphatase and RNA helicase functional domains of dengue virus type 2 NS3 converge within a region of 20 amino acids. J Virol 73, 3108-3116.

Li, H., Saucedo-Cuevas, L., Regla-Nava, J.A., Chai, G., Sheets, N., Tang, W., Terskikh, A.V., Shresta, S., Gleeson, J.G., 2016b. Zika Virus Infects Neural Progenitors in the Adult Mouse Brain and Alters Proliferation. Cell Stem Cell 19, 593-598.

Li, Z., Brecher, M., Deng, Y.Q., Zhang, J., Sakamuru, S., Liu, B., Huang, R., Koetzner, C.A., Allen, C.A., Jones, S.A., Chen, H., Zhang, N.N., Tian, M., Gao, F., Lin, Q., Banavali, N., Zhou, J., Boles, N., Xia, M., Kramer, L.D., Qin, C.F., Li, H., 2017b. Existing drugs as broad-spectrum and potent inhibitors for Zika virus by targeting NS2B-NS3 interaction. Cell Res 27, 1046-1064.

Li, Z., Sakamuru, S., Huang, R., Brecher, M., Koetzner, C.A., Zhang, J., Chen, H., Qin, C.F., Zhang, Q.Y., Zhou, J., Kramer, L.D., Xia, M., Li, H., 2018. Erythrosin B is a potent and broad-spectrum orthosteric inhibitor of the flavivirus NS2B-NS3 protease. Antiviral Res 150, 217-225.

Liang, Q., Luo, Z., Zeng, J., Chen, W., Foo, S.S., Lee, S.A., Ge, J., Wang, S., Goldman, S.A., Zlokovic, B.V., Zhao, Z., Jung, J.U., 2016. Zika Virus NS4A and NS4B Proteins Deregulate Akt-mTOR Signaling in Human Fetal Neural Stem Cells to Inhibit Neurogenesis and Induce Autophagy. Cell Stem Cell 19, 663-671.

Liao, S.L., Raung, S.L., Chen, C.J., 2002. Japanese encephalitis virus stimulates superoxide dismutase activity in rat glial cultures. Neurosci Lett 324, 133-136.

Lindenbach, B.D., Rice, C.M., 2003. Molecular biology of flaviviruses. Adv Virus Res 59, 23-61.

Lipton, J.O., Sahin, M., 2014. The neurology of mTOR. Neuron 84, 275-291.

Liu, Y., Gordesky-Gold, B., Leney-Greene, M., Weinbren, N.L., Tudor, M., Cherry, S., 2018. Inflammation-Induced, STING-Dependent Autophagy Restricts Zika Virus Infection in the Drosophila Brain. Cell Host Microbe 24, 57-68 e53.

Lorenz, I.C., Allison, S.L., Heinz, F.X., Helenius, A., 2002. Folding and dimerization of tick-borne encephalitis virus envelope proteins prM and E in the endoplasmic reticulum. J Virol 76, 5480-5491.

Lu, Y., Wambach, M., Katze, M.G., Krug, R.M., 1995. Binding of the influenza virus NS1 protein to double-stranded RNA inhibits the activation of the protein kinase that phosphorylates the elF-2 translation initiation factor. Virology 214, 222-228.

Lum, F.M., Low, D.K., Fan, Y., Tan, J.J., Lee, B., Chan, J.K., Renia, L., Ginhoux, F., Ng, L.F., 2017. Zika Virus Infects Human Fetal Brain Microglia and Induces Inflammation. Clin Infect Dis 64, 914-920.

Ma, J., Ketkar, H., Geng, T., Lo, E., Wang, L., Xi, J., Sun, Q., Zhu, Z., Cui, Y., Yang, L., Wang, P., 2018. Zika Virus Non-structural Protein 4A Blocks the RLR-MAVS Signaling. Front Microbiol 9, 1350.

Mackenzie, J.M., Jones, M.K., Young, P.R., 1996. Immunolocalization of the dengue virus nonstructural glycoprotein NS1 suggests a role in viral RNA replication. Virology 220, 232-240.

Mackenzie, J.M., Khromykh, A.A., Parton, R.G., 2007. Cholesterol manipulation by West Nile virus perturbs the cellular immune response. Cell Host Microbe 2, 229-239.

Macnamara, F.N., 1954. Zika virus: a report on three cases of human infection during an epidemic of jaundice in Nigeria. Trans R Soc Trop Med Hyg 48, 139-145.

Maslow, J.N., Roberts, C.C., 2020. Zika Virus: A Brief History and Review of Its Pathogenesis Rediscovered. Methods Mol Biol 2142, 1-8.

McDonald, P.C., Oloumi, A., Mills, J., Dobreva, I., Maidan, M., Gray, V., Wederell, E.D., Bally, M.B., Foster, L.J., Dedhar, S., 2008. Rictor and integrin-linked kinase interact and regulate Akt phosphorylation and cancer cell survival. Cancer research 68, 1618-1624.

McLean, J.E., Wudzinska, A., Datan, E., Quaglino, D., Zakeri, Z., 2011. Flavivirus NS4A-induced autophagy protects cells against death and enhances virus replication. J Biol Chem 286, 22147-22159.

McNulty, S., Flint, M., Nichol, S.T., Spiropoulou, C.F., 2013. Host mTORC1 signaling regulates andes virus replication. J Virol 87, 912-922.

Meade, N., Furey, C., Li, H., Verma, R., Chai, Q., Rollins, M.G., DiGiuseppe, S., Naghavi, M.H., Walsh, D., 2018. Poxviruses Evade Cytosolic Sensing through Disruption of an mTORC1-mTORC2 Regulatory Circuit. Cell 174, 1143-1157 e1117.

Meertens, L., Carnec, X., Lecoin, M.P., Ramdasi, R., Guivel-Benhassine, F., Lew, E., Lemke, G., Schwartz, O., Amara, A., 2012. The TIM and TAM families of phosphatidylserine receptors mediate dengue virus entry. Cell Host Microbe 12, 544-557.

Menon, S., Dibble, C.C., Talbott, G., Hoxhaj, G., Valvezan, A.J., Takahashi, H., Cantley, L.C., Manning, B.D., 2014. Spatial control of the TSC complex integrates insulin and nutrient regulation of mTORC1 at the lysosome. Cell 156, 771-785.

Merino-Ramos, T., Vazquez-Calvo, A., Casas, J., Sobrino, F., Saiz, J.C., Martin-Acebes, M.A., 2016. Modification of the Host Cell Lipid Metabolism Induced by Hypolipidemic Drugs Targeting the Acetyl Coenzyme A Carboxylase Impairs West Nile Virus Replication. Antimicrob Agents Chemother 60, 307-315.

Mesci, P., Macia, A., LaRock, C.N., Tejwani, L., Fernandes, I.R., Suarez, N.A., de, A.Z.P.M., Beltrao-Braga, P.C.B., Nizet, V., Muotri, A.R., 2018. Modeling neuro-immune interactions during Zika virus infection. Hum Mol Genet 27, 41-52.

Miller, S., Kastner, S., Krijnse-Locker, J., Buhler, S., Bartenschlager, R., 2007. The non-structural protein 4A of dengue virus is an integral membrane protein inducing membrane alterations in a 2K-regulated manner. J Biol Chem 282, 8873-8882.

Miner, J.J., Diamond, M.S., 2017. Zika Virus Pathogenesis and Tissue Tropism. Cell Host Microbe 21, 134-142.

Miner, J.J., Sene, A., Richner, J.M., Smith, A.M., Santeford, A., Ban, N., Weger-Lucarelli, J., Manzella, F., Ruckert, C., Govero, J., Noguchi, K.K., Ebel, G.D., Diamond, M.S., Apte, R.S., 2016. Zika Virus Infection in Mice Causes Panuveitis with Shedding of Virus in Tears. Cell Rep 16, 3208-3218.

Mitsuishi, Y., Taguchi, K., Kawatani, Y., Shibata, T., Nukiwa, T., Aburatani, H., Yamamoto, M., Motohashi, H., 2012. Nrf2 redirects glucose and glutamine into anabolic pathways in metabolic reprogramming. Cancer Cell 22, 66-79.

Mlakar, J., Korva, M., Tul, N., Popovic, M., Poljsak-Prijatelj, M., Mraz, J., Kolenc, M., Resman Rus, K., Vesnaver Vipotnik, T., Fabjan Vodusek, V., Vizjak, A., Pizem, J., Petrovec, M., Avsic Zupanc, T., 2016. Zika Virus Associated with Microcephaly. N Engl J Med 374, 951-958.

Moinova, H.R., Mulcahy, R.T., 1999. Up-regulation of the human gamma-glutamylcysteine synthetase regulatory subunit gene involves binding of Nrf-2 to an electrophile responsive element. Biochem Biophys Res Commun 261, 661-668.

Moorman, N.J., Shenk, T., 2010. Rapamycin-resistant mTORC1 kinase activity is required for herpesvirus replication. J Virol 84, 5260-5269.

Muffat, J., Li, Y., Omer, A., Durbin, A., Bosch, I., Bakiasi, G., Richards, E., Meyer, A., Gehrke, L., Jaenisch, R., 2018. Human induced pluripotent stem cell-derived glial cells and neural progenitors display divergent responses to Zika and dengue infections. Proc Natl Acad Sci U S A 115, 7117-7122.

Muller, D.A., Young, P.R., 2013. The flavivirus NS1 protein: molecular and structural biology, immunology, role in pathogenesis and application as a diagnostic biomarker. Antiviral Res 98, 192-208.

Munoz-Jordan, J.L., Laurent-Rolle, M., Ashour, J., Martinez-Sobrido, L., Ashok, M., Lipkin, W.I., Garcia-Sastre, A., 2005. Inhibition of alpha/beta interferon signaling by the NS4B protein of flaviviruses. J Virol 79, 8004-8013.

Musso, D., Bossin, H., Mallet, H.P., Besnard, M., Broult, J., Baudouin, L., Levi, J.E., Sabino, E.C., Ghawche, F., Lanteri, M.C., Baud, D., 2018. Zika virus in French Polynesia 2013-14: anatomy of a completed outbreak. Lancet Infect Dis 18, e172-e182.

Musso, D., Gubler, D.J., 2016. Zika Virus. Clin Microbiol Rev 29, 487-524.

Musso, D., Ko, A.I., Baud, D., 2019. Zika Virus Infection - After the Pandemic. N Engl J Med 381, 1444-1457.

Musso, D., Nilles, E.J., Cao-Lormeau, V.M., 2014. Rapid spread of emerging Zika virus in the Pacific area. Clin Microbiol Infect 20, O595-596.

Nambala, P., Su, W.C., 2018. Role of Zika Virus prM Protein in Viral Pathogenicity and Use in Vaccine Development. Front Microbiol 9, 1797.

Nambala, P., Yu, W.Y., Lo, Y.C., Lin, C.W., Su, W.C., 2020. Ubiquitination of Zika virus precursor membrane protein promotes the release of viral proteins. Virus Res 286, 198065.

Nazio, F., Strappazzon, F., Antonioli, M., Bielli, P., Cianfanelli, V., Bordi, M., Gretzmeier, C., Dengjel, J., Piacentini, M., Fimia, G.M., Cecconi, F., 2013. mTOR inhibits autophagy by controlling ULK1 ubiquitylation, self-association and function through AMBRA1 and TRAF6. Nat Cell Biol 15, 406-416.

Nguyen, T., Nioi, P., Pickett, C.B., 2009. The Nrf2-antioxidant response element signaling pathway and its activation by oxidative stress. J Biol Chem 284, 13291-13295.

O'Shea, C., Klupsch, K., Choi, S., Bagus, B., Soria, C., Shen, J., McCormick, F., Stokoe, D., 2005. Adenoviral proteins mimic nutrient/growth signals to activate the mTOR pathway for viral replication. EMBO J 24, 1211-1221.

Ojha, C.R., Rodriguez, M., Karuppan, M.K.M., Lapierre, J., Kashanchi, F., El-Hage, N., 2019. Toll-like receptor 3 regulates Zika virus infection and associated host inflammatory response in primary human astrocytes. PLoS One 14, e0208543.

Olagnier, D., Muscolini, M., Coyne, C.B., Diamond, M.S., Hiscott, J., 2016. Mechanisms of Zika Virus Infection and Neuropathogenesis. DNA Cell Biol 35, 367-372.

Oliveira, E.R.A., de Alencastro, R.B., Horta, B.A.C., 2017. New insights into flavivirus biology: the influence of pH over interactions between prM and E proteins. J Comput Aided Mol Des 31, 1009-1019.

Olmo, I.G., Carvalho, T.G., Costa, V.V., Alves-Silva, J., Ferrari, C.Z., Izidoro-Toledo, T.C., da Silva, J.F., Teixeira, A.L., Souza, D.G., Marques, J.T., Teixeira, M.M., Vieira, L.B., Ribeiro, F.M., 2017. Zika Virus Promotes Neuronal Cell Death in a Non-Cell Autonomous Manner by Triggering the Release of Neurotoxic Factors. Front Immunol 8, 1016.

Pajares, M., Jimenez-Moreno, N., Garcia-Yague, A.J., Escoll, M., de Ceballos, M.L., Van Leuven, F., Rabano, A., Yamamoto, M., Rojo, A.I., Cuadrado, A., 2016. Transcription factor NFE2L2/NRF2 is a regulator of macroautophagy genes. Autophagy 12, 1902-1916.

Pajares, M., Rojo, A.I., Arias, E., Diaz-Carretero, A., Cuervo, A.M., Cuadrado, A., 2018. Transcription factor NFE2L2/NRF2 modulates chaperone-mediated autophagy through the regulation of LAMP2A. Autophagy 14, 1310-1322.

Patra, K.C., Hay, N., 2014. The pentose phosphate pathway and cancer. Trends Biochem Sci 39, 347-354.

Pavlova, N.N., Thompson, C.B., 2016. The Emerging Hallmarks of Cancer Metabolism. Cell Metab 23, 27-47.

Peng, L., Liang, D., Tong, W., Li, J., Yuan, Z., 2010. Hepatitis C virus NS5A activates the mammalian target of rapamycin (mTOR) pathway, contributing to cell survival by disrupting the interaction between FK506-binding protein 38 (FKBP38) and mTOR. J Biol Chem 285, 20870-20881.

Perera-Lecoin, M., Meertens, L., Carnec, X., Amara, A., 2013. Flavivirus entry receptors: an update. Viruses 6, 69-88.

Petiot, A., Ogier-Denis, E., Blommaart, E.F., Meijer, A.J., Codogno, P., 2000. Distinct classes of phosphatidylinositol 3'-kinases are involved in signaling pathways that control macroautophagy in HT-29 cells. J Biol Chem 275, 992-998.

Pierson, T.C., Diamond, M.S., 2018. The emergence of Zika virus and its new clinical syndromes. Nature 560, 573-581.

Pierson, T.C., Diamond, M.S., 2020. The continued threat of emerging flaviviruses. Nat Microbiol 5, 796-812.

Pizzino, G., Irrera, N., Cucinotta, M., Pallio, G., Mannino, F., Arcoraci, V., Squadrito, F., Altavilla, D., Bitto, A., 2017. Oxidative Stress: Harms and Benefits for Human Health. Oxid Med Cell Longev 2017, 8416763.

Pletnev, A.G., Bray, M., Lai, C.J., 1993. Chimeric tick-borne encephalitis and dengue type 4 viruses: effects of mutations on neurovirulence in mice. J Virol 67, 4956-4963.

Poppers, J., Mulvey, M., Khoo, D., Mohr, I., 2000. Inhibition of PKR activation by the proline-rich RNA binding domain of the herpes simplex virus type 1 Us11 protein. J Virol 74, 11215-11221.

Prasad, V.M., Miller, A.S., Klose, T., Sirohi, D., Buda, G., Jiang, W., Kuhn, R.J., Rossmann, M.G., 2017. Structure of the immature Zika virus at 9 A resolution. Nat Struct Mol Biol 24, 184-186.

Pryor, M.J., Gualano, R.C., Lin, B., Davidson, A.D., Wright, P.J., 1998. Growth restriction of dengue virus type 2 by site-specific mutagenesis of virus-encoded glycoproteins. J Gen Virol 79 (Pt 11), 2631-2639.

Pryor, M.J., Wright, P.J., 1994. Glycosylation mutants of dengue virus NS1 protein. J Gen Virol 75 (Pt 5), 1183-1187.

Pullen, N., Thomas, G., 1997. The modular phosphorylation and activation of p70s6k. FEBS Lett 410, 78-82.

Qian, X., Nguyen, H.N., Jacob, F., Song, H., Ming, G.L., 2017. Using brain organoids to understand Zika virus-induced microcephaly. Development 144, 952-957.

Qian, X., Nguyen, H.N., Song, M.M., Hadiono, C., Ogden, S.C., Hammack, C., Yao, B., Hamersky, G.R., Jacob, F., Zhong, C., Yoon, K.J., Jeang, W., Lin, L., Li, Y., Thakor, J., Berg, D.A., Zhang, C., Kang, E., Chickering, M., Nauen, D., Ho, C.Y., Wen, Z., Christian, K.M., Shi, P.Y., Maher, B.J., Wu, H., Jin, P., Tang, H., Song, H., Ming, G.L., 2016. Brain-Region-Specific Organoids Using Mini-bioreactors for Modeling ZIKV Exposure. Cell 165, 1238-1254.

Quicke, K.M., Bowen, J.R., Johnson, E.L., McDonald, C.E., Ma, H., O'Neal, J.T., Rajakumar, A., Wrammert, J., Rimawi, B.H., Pulendran, B., Schinazi, R.F., Chakraborty, R., Suthar, M.S., 2016. Zika Virus Infects Human Placental Macrophages. Cell Host Microbe 20, 83-90.

Ramezani, A., Nahad, M.P., Faghihloo, E., 2018. The role of Nrf2 transcription factor in viral infection. J Cell Biochem 119, 6366-6382.

Rasmussen, S.A., Jamieson, D.J., Honein, M.A., Petersen, L.R., 2016. Zika Virus and Birth Defects--Reviewing the Evidence for Causality. N Engl J Med 374, 1981-1987.

Rastogi, M., Sharma, N., Singh, S.K., 2016. Flavivirus NS1: a multifaceted enigmatic viral protein. Virol J 13, 131.

Rawal, G., Yadav, S., Kumar, R., 2016. Zika virus: An overview. J Family Med Prim Care 5, 523-527.

Rebbani, K., Tsukiyama-Kohara, K., 2016. HCV-Induced Oxidative Stress: Battlefield-Winning Strategy. Oxid Med Cell Longev 2016, 7425628.

Reggiori, F., Monastyrska, I., Verheije, M.H., Cali, T., Ulasli, M., Bianchi, S., Bernasconi, R., de Haan, C.A., Molinari, M., 2010. Coronaviruses Hijack the LC3-I-positive EDEMosomes, ER-derived vesicles exporting short-lived ERAD regulators, for replication. Cell Host Microbe 7, 500-508.

Roosendaal, J., Westaway, E.G., Khromykh, A., Mackenzie, J.M., 2006. Regulated cleavages at the West Nile virus NS4A-2K-NS4B junctions play a major role in rearranging cytoplasmic membranes and Golgi trafficking of the NS4A protein. J Virol 80, 4623-4632.

Rothan, H.A., Fang, S., Mahesh, M., Byrareddy, S.N., 2019. Zika Virus and the Metabolism of Neuronal Cells. Mol Neurobiol 56, 2551-2557.

Routhu, N.K., Lehoux, S.D., Rouse, E.A., Bidokhti, M.R.M., Giron, L.B., Anzurez, A., Reid, S.P., Abdel-Mohsen, M., Cummings, R.D., Byrareddy, S.N., 2019. Glycosylation of Zika Virus is Important in Host-Virus Interaction and Pathogenic Potential. Int J Mol Sci 20.

Sager, G., Gabaglio, S., Sztul, E., Belov, G.A., 2018. Role of Host Cell Secretory Machinery in Zika Virus Life Cycle. Viruses 10.

Saisawang, C., Kuadkitkan, A., Auewarakul, P., Smith, D.R., Ketterman, A.J., 2018. Glutathionylation of dengue and Zika NS5 proteins affects guanylyltransferase and RNA dependent RNA polymerase activities. PLoS One 13, e0193133.

Sanchez, E.L., Lagunoff, M., 2015. Viral activation of cellular metabolism. Virology 479-480, 609-618.

Sarbassov, D.D., Ali, S.M., Sengupta, S., Sheen, J.H., Hsu, P.P., Bagley, A.F., Markhard, A.L., Sabatini, D.M., 2006. Prolonged rapamycin treatment inhibits mTORC2 assembly and Akt/PKB. Mol Cell 22, 159-168.

Sarbassov, D.D., Guertin, D.A., Ali, S.M., Sabatini, D.M., 2005. Phosphorylation and regulation of Akt/PKB by the rictor-mTOR complex. Science 307, 1098-1101.

Saxton, R.A., Sabatini, D.M., 2017a. mTOR Signaling in Growth, Metabolism, and Disease. Cell 168, 960-976.

Saxton, R.A., Sabatini, D.M., 2017b. mTOR Signaling in Growth, Metabolism, and Disease. Cell 169, 361-371.

Schjoldager, K.T., Narimatsu, Y., Joshi, H.J., Clausen, H., 2020. Global view of human protein glycosylation pathways and functions. Nat Rev Mol Cell Biol 21, 729-749.

Schmeisser, K., Parker, J.A., 2019. Pleiotropic Effects of mTOR and Autophagy During Development and Aging. Front Cell Dev Biol 7, 192.

Scholz, D., Poltl, D., Genewsky, A., Weng, M., Waldmann, T., Schildknecht, S., Leist, M., 2011. Rapid, complete and large-scale generation of post-mitotic neurons from the human LUHMES cell line. J Neurochem 119, 957-971.

Seet, R.C., Lee, C.Y., Lim, E.C., Quek, A.M., Yeo, L.L., Huang, S.H., Halliwell, B., 2009. Oxidative damage in dengue fever. Free Radic Biol Med 47, 375-380.

Seglen, P.O., Gordon, P.B., 1982. 3-Methyladenine: specific inhibitor of autophagic/lysosomal protein degradation in isolated rat hepatocytes. Proc Natl Acad Sci U S A 79, 1889-1892.

Shang, Z., Song, H., Shi, Y., Qi, J., Gao, G.F., 2018. Crystal Structure of the Capsid Protein from Zika Virus. J Mol Biol 430, 948-962.

Shao, R.X., Zhang, L., Peng, L.F., Sun, E., Chung, W.J., Jang, J.Y., Tsai, W.L., Hyppolite, G., Chung, R.T., 2010. Suppressor of cytokine signaling 3 suppresses hepatitis C virus replication in an mTOR-dependent manner. J Virol 84, 6060-6069.

Sharma, S., Tandel, K., Dash, P.K., Parida, M., 2017. Zika virus: A public health threat. J Med Virol 89, 1693-1699.

Shives, K.D., Beatman, E.L., Chamanian, M., O'Brien, C., Hobson-Peters, J., Beckham, J.D., 2014. West nile virus-induced activation of mammalian target of rapamycin complex 1 supports viral growth and viral protein expression. J Virol 88, 9458-9471.

Shrivastava, S., Bhanja Chowdhury, J., Steele, R., Ray, R., Ray, R.B., 2012. Hepatitis C virus upregulates Beclin1 for induction of autophagy and activates mTOR signaling. J Virol 86, 8705-8712.

Sies, H., 2015. Oxidative stress: a concept in redox biology and medicine. Redox Biol 4, 180-183.

Simanjuntak, Y., Liang, J.J., Chen, S.Y., Li, J.K., Lee, Y.L., Wu, H.C., Lin, Y.L., 2018. Ebselen alleviates testicular pathology in mice with Zika virus infection and prevents its sexual transmission. PLoS Pathog 14, e1006854.

Sir, D., Chen, W.L., Choi, J., Wakita, T., Yen, T.S., Ou, J.H., 2008. Induction of incomplete autophagic response by hepatitis C virus via the unfolded protein response. Hepatology 48, 1054-1061.

Sirohi, D., Chen, Z., Sun, L., Klose, T., Pierson, T.C., Rossmann, M.G., Kuhn, R.J., 2016. The 3.8 A resolution cryo-EM structure of Zika virus. Science 352, 467-470.

Sirohi, D., Kuhn, R.J., 2017. Zika Virus Structure, Maturation, and Receptors. J Infect Dis 216, S935-S944.

Siskos, N., Stylianopoulou, E., Skavdis, G., Grigoriou, M.E., 2021. Molecular Genetics of Microcephaly Primary Hereditary: An Overview. Brain Sci 11.

Song, W., Zhang, H., Zhang, Y., Chen, Y., Lin, Y., Han, Y., Jiang, J., 2021. Identification and Characterization of Zika Virus NS5 Methyltransferase Inhibitors. Front Cell Infect Microbiol 11, 665379.

Sotcheff, S., Routh, A., 2020. Understanding Flavivirus Capsid Protein Functions: The Tip of the Iceberg. Pathogens 9.

Stanton, R.C., 2012. Glucose-6-phosphate dehydrogenase, NADPH, and cell survival. IUBMB Life 64, 362-369.

Stewart, D., Killeen, E., Naquin, R., Alam, S., Alam, J., 2003. Degradation of transcription factor Nrf2 via the ubiquitin-proteasome pathway and stabilization by cadmium. J Biol Chem 278, 2396-2402.

Stohr, S., Costa, R., Sandmann, L., Westhaus, S., Pfaender, S., Anggakusuma, Dazert, E., Meuleman, P., Vondran, F.W., Manns, M.P., Steinmann, E., von Hahn, T., Ciesek, S., 2016. Host cell mTORC1 is required for HCV RNA replication. Gut 65, 2017-2028.

Sun, Z., Zhang, S., Chan, J.Y., Zhang, D.D., 2007. Keap1 controls postinduction repression of the Nrf2-mediated antioxidant response by escorting nuclear export of Nrf2. Mol Cell Biol 27, 6334-6349.

Swaminathan, S., Schlaberg, R., Lewis, J., Hanson, K.E., Couturier, M.R., 2016. Fatal Zika Virus Infection with Secondary Nonsexual Transmission. N Engl J Med 375, 1907-1909.

Taguchi, K., Motohashi, H., Yamamoto, M., 2011. Molecular mechanisms of the Keap1-Nrf2 pathway in stress response and cancer evolution. Genes Cells 16, 123-140.

Takei, N., Nawa, H., 2014. mTOR signaling and its roles in normal and abnormal brain development. Front Mol Neurosci 7, 28.

Tan, T.Y., Fibriansah, G., Kostyuchenko, V.A., Ng, T.S., Lim, X.X., Zhang, S., Lim, X.N., Wang, J., Shi, J., Morais, M.C., Corti, D., Lok, S.M., 2020. Capsid protein structure in Zika virus reveals the flavivirus assembly process. Nat Commun 11, 895.

Tang, H., Hammack, C., Ogden, S.C., Wen, Z., Qian, X., Li, Y., Yao, B., Shin, J., Zhang, F., Lee, E.M., Christian, K.M., Didier, R.A., Jin, P., Song, H., Ming, G.L., 2016. Zika Virus Infects Human Cortical Neural Progenitors and Attenuates Their Growth. Cell Stem Cell 18, 587-590.

Tassaneetrithep, B., Burgess, T.H., Granelli-Piperno, A., Trumpfheller, C., Finke, J., Sun, W., Eller, M.A., Pattanapanyasat, K., Sarasombath, S., Birx, D.L., Steinman, R.M., Schlesinger, S., Marovich, M.A., 2003. DC-SIGN (CD209) mediates dengue virus infection of human dendritic cells. J Exp Med 197, 823-829.

Thai, M., Thaker, S.K., Feng, J., Du, Y., Hu, H., Ting Wu, T., Graeber, T.G., Braas, D., Christofk, H.R., 2015. MYC-induced reprogramming of glutamine catabolism supports optimal virus replication. Nat Commun 6, 8873.

Thaker, S.K., Ch'ng, J., Christofk, H.R., 2019a. Viral hijacking of cellular metabolism. BMC Biol 17, 59.

Thaker, S.K., Chapa, T., Garcia, G., Jr., Gong, D., Schmid, E.W., Arumugaswami, V., Sun, R., Christofk, H.R., 2019b. Differential Metabolic Reprogramming by Zika Virus Promotes Cell Death in Human versus Mosquito Cells. Cell Metab 29, 1206-1216 e1204.

Thapa, R., Biswas, B., Mallick, D., Ghosh, A., 2009. Acute pancreatitis--complicating hepatitis E virus infection in a 7-year-old boy with glucose 6 phosphate dehydrogenase deficiency. Clin Pediatr (Phila) 48, 199-201.

Thomanetz, V., Angliker, N., Cloetta, D., Lustenberger, R.M., Schweighauser, M., Oliveri, F., Suzuki, N., Ruegg, M.A., 2013. Ablation of the mTORC2 component rictor in brain or Purkinje cells affects size and neuron morphology. J Cell Biol 201, 293-308.

Thoreen, C.C., Kang, S.A., Chang, J.W., Liu, Q., Zhang, J., Gao, Y., Reichling, L.J., Sim, T., Sabatini, D.M., Gray, N.S., 2009. An ATP-competitive mammalian target of rapamycin inhibitor reveals rapamycin-resistant functions of mTORC1. J Biol Chem 284, 8023-8032.

Tian, Y., Jiang, W., Gao, N., Zhang, J., Chen, W., Fan, D., Zhou, D., An, J., 2010. Inhibitory effects of glutathione on dengue virus production. Biochem Biophys Res Commun 397, 420-424.

Tomar, S., Mudgal, R., Fatma, B., 2017. Chapter 6 - Flavivirus Protease: An Antiviral Target, in: Gupta, S.P. (Ed.), Viral Proteases and Their Inhibitors. Academic Press, pp. 137-161.

Tonelli, C., Chio, I.I.C., Tuveson, D.A., 2018. Transcriptional Regulation by Nrf2. Antioxid Redox Signal 29, 1727-1745.

Valadao, A.L., Aguiar, R.S., de Arruda, L.B., 2016. Interplay between Inflammation and Cellular Stress Triggered by Flaviviridae Viruses. Front Microbiol 7, 1233.

Valente, A.P., Moraes, A.H., 2019. Zika virus proteins at an atomic scale: how does structural biology help us to understand and develop vaccines and drugs against Zika virus infection? J Venom Anim Toxins Incl Trop Dis 25, e20190013.

Van Grol, J., Subauste, C., Andrade, R.M., Fujinaga, K., Nelson, J., Subauste, C.S., 2010. HIV-1 inhibits autophagy in bystander macrophage/monocytic cells through Src-Akt and STAT3. PLoS One 5, e11733.

van Hemert, F., Berkhout, B., 2016. Nucleotide composition of the Zika virus RNA genome and its codon usage. Virol J 13, 95.

Vasallo, C., Gastaminza, P., 2015. Cellular stress responses in hepatitis C virus infection: Mastering a two-edged sword. Virus Res 209, 100-117.

Wang, A., Thurmond, S., Islas, L., Hui, K., Hai, R., 2017. Zika virus genome biology and molecular pathogenesis. Emerg Microbes Infect 6, e13.

Wang, J., Chen, Y., Gao, N., Wang, Y., Tian, Y., Wu, J., Zhang, J., Zhu, J., Fan, D., An, J., 2013. Inhibitory effect of glutathione on oxidative liver injury induced by dengue virus serotype 2 infections in mice. PLoS One 8, e55407.

Wang, J., Liu, J., Zhou, R., Ding, X., Zhang, Q., Zhang, C., Li, L., 2018. Zika virus infected primary microglia impairs NPCs proliferation and differentiation. Biochem Biophys Res Commun 497, 619-625.

Wang, X., Proud, C.G., 2011. mTORC1 signaling: what we still don't know. J Mol Cell Biol 3, 206-220.

Warrener, P., Tamura, J.K., Collett, M.S., 1993. RNA-stimulated NTPase activity associated with yellow fever virus NS3 protein expressed in bacteria. J Virol 67, 989-996.

Watanabe, Y., Bowden, T.A., Wilson, I.A., Crispin, M., 2019. Exploitation of glycosylation in enveloped virus pathobiology. Biochim Biophys Acta Gen Subj 1863, 1480-1497.

Welsch, S., Miller, S., Romero-Brey, I., Merz, A., Bleck, C.K., Walther, P., Fuller, S.D., Antony, C., Krijnse-Locker, J., Bartenschlager, R., 2009. Composition and three-dimensional architecture of the dengue virus replication and assembly sites. Cell Host Microbe 5, 365-375.

Wen, Z., Song, H., Ming, G.L., 2017. How does Zika virus cause microcephaly? Genes Dev 31, 849-861.

Wheeler, A.C., 2018. Development of Infants With Congenital Zika Syndrome: What Do We Know and What Can We Expect? Pediatrics 141, S154-S160.

Wild, A.C., Moinova, H.R., Mulcahy, R.T., 1999. Regulation of gamma-glutamylcysteine synthetase subunit gene expression by the transcription factor Nrf2. J Biol Chem 274, 33627-33636.

Winkler, G., Randolph, V.B., Cleaves, G.R., Ryan, T.E., Stollar, V., 1988. Evidence that the mature form of the flavivirus nonstructural protein NS1 is a dimer. Virology 162, 187-196.

Wong, J., Zhang, J., Si, X., Gao, G., Mao, I., McManus, B.M., Luo, H., 2008. Autophagosome supports coxsackievirus B3 replication in host cells. J Virol 82, 9143-9153.

Wu, K.C., Cui, J.Y., Klaassen, C.D., 2011. Beneficial role of Nrf2 in regulating NADPH generation and consumption. Toxicol Sci 123, 590-600.

Wu, T.T., Li, W.M., Yao, Y.M., 2016. Interactions between Autophagy and Inhibitory Cytokines. Int J Biol Sci 12, 884-897.

Wu, Y.H., Chiu, D.T., Lin, H.R., Tang, H.Y., Cheng, M.L., Ho, H.Y., 2015. Glucose-6-Phosphate Dehydrogenase Enhances Antiviral Response through Downregulation of NADPH Sensor HSCARG and Upregulation of NF-kappaB Signaling. Viruses 7, 6689-6706.

Wu, Y.H., Tseng, C.P., Cheng, M.L., Ho, H.Y., Shih, S.R., Chiu, D.T., 2008. Glucose-6-phosphate dehydrogenase deficiency enhances human coronavirus 229E infection. J Infect Dis 197, 812-816.

Xie, X., Gayen, S., Kang, C., Yuan, Z., Shi, P.Y., 2013. Membrane topology and function of dengue virus NS2A protein. J Virol 87, 4609-4622.

Xu, X., Song, H., Qi, J., Liu, Y., Wang, H., Su, C., Shi, Y., Gao, G.F., 2016. Contribution of intertwined loop to membrane association revealed by Zika virus full-length NS1 structure. EMBO J 35, 2170-2178.

Yang, H., Rudge, D.G., Koos, J.D., Vaidialingam, B., Yang, H.J., Pavletich, N.P., 2013. mTOR kinase structure, mechanism and regulation. Nature 497, 217-223.

Yip, J., Geng, X., Shen, J., Ding, Y., 2016. Cerebral Gluconeogenesis and Diseases. Front Pharmacol 7, 521.

Yu, Y., Maguire, T.G., Alwine, J.C., 2011. Human cytomegalovirus activates glucose transporter 4 expression to increase glucose uptake during infection. J Virol 85, 1573-1580.

Yuan, L., Huang, X.Y., Liu, Z.Y., Zhang, F., Zhu, X.L., Yu, J.Y., Ji, X., Xu, Y.P., Li, G., Li, C., Wang, H.J., Deng, Y.Q., Wu, M., Cheng, M.L., Ye, Q., Xie, D.Y., Li, X.F., Wang, X., Shi, W., Hu, B., Shi, P.Y., Xu, Z., Qin, C.F., 2017. A single mutation in the prM protein of Zika virus contributes to fetal microcephaly. Science 358, 933-936.

Zanluca, C., Melo, V.C., Mosimann, A.L., Santos, G.I., Santos, C.N., Luz, K., 2015. First report of autochthonous transmission of Zika virus in Brazil. Mem Inst Oswaldo Cruz 110, 569-572.

Zask, A., Verheijen, J.C., Curran, K., Kaplan, J., Richard, D.J., Nowak, P., Malwitz, D.J., Brooijmans, N., Bard, J., Svenson, K., Lucas, J., Toral-Barza, L., Zhang, W.G., Hollander, I., Gibbons, J.J., Abraham, R.T., Ayral-Kaloustian, S., Mansour, T.S., Yu, K., 2009. ATP-

competitive inhibitors of the mammalian target of rapamycin: design and synthesis of highly potent and selective pyrazolopyrimidines. J Med Chem 52, 5013-5016.

Zevini, A., Ferrari, M., Olagnier, D., Hiscott, J., 2020. Dengue virus infection and Nrf2 regulation of oxidative stress. Curr Opin Virol 43, 35-40.

Zhang, C., Feng, T., Cheng, J., Li, Y., Yin, X., Zeng, W., Jin, X., Li, Y., Guo, F., Jin, T., 2017. Structure of the NS5 methyltransferase from Zika virus and implications in inhibitor design. Biochem Biophys Res Commun 492, 624-630.

Zhang, Z., Rong, L., Li, Y.P., 2019. Flaviviridae Viruses and Oxidative Stress: Implications for Viral Pathogenesis. Oxid Med Cell Longev 2019, 1409582.

Zinzalla, V., Stracka, D., Oppliger, W., Hall, M.N., 2011. Activation of mTORC2 by association with the ribosome. Cell 144, 757-768.